



Escuela Técnica Superior de Ingeniería de Caminos, Canales y Puertos UNIVERSIDAD DE CANTABRIA

CURVED STEEL GIRDER BRIDGES: OVERVIEW OF TYPICAL ERECTION PROCEDURES AND ANALYSIS WORKFLOW IMPROVEMENTS

Trabajo realizado por: Alberto Arnedo Ruiz

Dirigido:

Pablo Pascual Muñoz.

Titulación:

Máster Universitario en Ingeniería de Caminos, Canales y Puertos

Santander, septiembre de 2025





Alberto Arnedo Ruiz

RESUMEN

Título: Puentes de vigas de acero curvos: Repaso de técnicas de montaje

típicas y mejoras en el proceso de análisis.

Autor: Alberto Arnedo Ruiz
Director: Pablo Pascual Muñoz
Fecha: 5 de septiembre 2025

Palabras clave: Ingeniería de construcción, vigas de acero curvas, análisis de

estabilidad, efectos de segundo orden, fases de construcción, cimbra temporal, diseño paramétrico, mallado en análisis de

elementos finitos.

Los puentes de vigas de acero son uno de los tipos de puentes más comunes debido a su eficiencia en luces cortas a medianas. Los puentes de vigas de acero curvas, en particular, tienen la ventaja de poder seguir una alineación de carretera específica en zonas con espacio limitado, como pueden ser las áreas urbanas de alta densidad.

Sin embargo, las vigas curvas tienen una desventaja en comparación con las vigas rectas durante la etapa de montaje. Su geometría en planta hace que, de forma natural, tiendan a volcarse debido a las cargas de gravedad. Las fuerzas de torsión también se magnifican y los efectos de segundo orden pueden causar el pandeo del alma.

Para capturar adecuadamente el comportamiento del puente durante el montaje, se debe desarrollar un modelo de análisis de elementos finitos 3D, que discretice la viga curva en una serie de elementos rectos. La práctica actual generalmente implica modelar el análisis en un software CAD para luego importarlo a un software de FEA, o el uso de un software de modelado de puentes especializado para modelar el puente paramétricamente. Cada uno de estos métodos tiene sus ventajas y desventajas inherentes, pero ambos son problemáticos cuando se requieren análisis de sensibilidad o modificaciones de la geometría, ya que a veces es más rápido empezar de cero que modificar los modelos existentes.

El propósito de esta tesis es proponer una metodología que pueda ser implementada fácilmente por cualquier oficina de ingeniería con software accesible, como hojas de cálculo y el software de cálculo de elección. Para lograrlo, después de analizar las limitaciones típicas que definen la construcción por fases de las vigas de acero curvas y su análisis, se propone una metodología de modelado basada en el número de identificación de los nodos, elementos de línea, y elementos de área, para acelerar la creación del modelo FEA y su modificación posterior con el propósito de realizar análisis de sensibilidad.

La metodología descrita se aplica luego a un caso específico y se comparan los resultados entre el mismo puente con dos tamaños de malla diferentes. Los resultados demuestran que la metodología propuesta es una alternativa adecuada a las prácticas de modelado actuales y se puede utilizar para realizar rápidamente análisis de sensibilidad con diferentes tamaños de malla sin tener que invertir grandes cantidades de tiempo en la modificación de los modelos existentes.





Alberto Arnedo Ruiz

ABSTRACT

Title: Curved steel girder bridges: Overview of typical erection procedure

and analysis workflow improvements.

Author: Alberto Arnedo Ruiz
Tutor: Pablo Pascual Muñoz
Date: September 5th, 2025

Key Words: Construction engineering, curved steel girders, stability analysis,

second-order effects, construction staging, temporary shoring,

parametric design, FEA meshing.

Steel girder bridges are one of the most common type of bridges due to the efficiency in short to medium span lengths. Curved steel girders bridges specifically have the advantage of being able to follow a specific road alignment along a site with limited space, such as high-density urban areas.

Curved girders, however, have a disadvantage compared to straight girders during the erection stage. Their shape makes them naturally want to overturn due to the gravity loads. Torsional forces are also magnified, second-order effects may cause web-buckling.

To adequately capture the behavior of the bridge during erection, a 3D FEA model needs to be developed, discretizing the curve girder in a series of straight elements. Current practice usually involves the modeling of the analysis model in a CAD software to then be imported into a FEA software, or the use of highly specialized bridge modeling software to parametrically model the bridge. Each of these methods have their inherent advantages and disadvantages, but both are problematic when sensitivity analysis or geometry modifications are required, since sometimes is faster to just start from scratch than to modify the existing models.

The purpose of this thesis is to propose a methodology to be easily implemented by any engineering office with easily accessible software, such as spreadsheets and their FEA software choice. To achieve that, after walking through the typical constraints that define the staged construction of the curved steel girders and its analysis, a modeling methodology based on the element IDs of joints, frames and plate elements is proposed to speed up the creation of the FEA model and its modification for sensitivity analysis purposes.

The methodology described is then applied to a specific case scenario, and results between the same bridge with two different mesh sizes are compared. The results prove that the methodology proposed is an appropriate alternative to the current modeling practices, and can be used to quickly perform sensitivity analysis with different mesh sizes without having to invest large amounts of time in modifying existing models.





Alberto Arnedo Ruiz

Index

1.	INTRODUCTION				
	1.1.	MOTIVATION AND PURPOSE	2		
2.		GROUND			
	2.1. 2.1.1.	STABILITY ANALYSIS			
	2.1.1. 2.1.2.	,			
	2.1.2.	•			
	2.1.3. 2.1.4.	-			
	2.1.4. 2.1.5.				
		TEMPORARY SUPPORTS			
	2.2. 2.2.1.				
	2.2.1.				
		ADDITIONAL ITEMS RELEVANT TO THE STAGED CONSTRUCTION			
	2.3.1.				
	_	3.1.1. Rigging components			
	_	3.1.2. Strength requirements			
	_	3.1.3. Stability during lifting			
		Cranes			
		3.2.1. Lifting capacity			
	2.3	3.2.2. Support reactions			
	2.3.	3.2.3. Barges	21		
	2.3.	3.2.4. Surcharge loading	22		
3.	METH	HODOLOGY	26		
	3.1.	ELEMENT IDS.	26		
		LAYOUT LINE			
	_	GIRDER WORK POINT GEOMETRY			
		MESH POINTS			
		FRAME AND PLATE ELEMENTS			
		Boundary conditions			
		STAGED ANALYSIS			
	3.7.1.				
	3.7.2.				
	_	STUDY			
4.					
		GEOMETRY DEFINITION			
		SECTION PROPERTIES ASSIGNMENT			
	_	LOAD ASSIGNMENT			
	4.4.	CONSTRUCTION STAGES	56		
5.	RESUL	LTS	67		
	5.1.	COARSER MESH MODEL	67		
		FINER MESH MODEL			
	_	COMPARISON			
6.	CONC	CLUSION AND FUTURE DEVELOPMENT	71		
7.	RIBLIC	OGRAPHY			





Alberto Arnedo Ruiz

List of figures

FIGURE 1. BREAKDOWN OF BRIDGE TYPES ON THE NHS	1
Figure 2. Collapse of State Route 69 Bridge over the Tennessee River at Clifton, Tennessee	2
FIGURE 3. TYPICAL FIXED BEARING AS PER NYSDOT STANDARD SHEETS [5]	θ
FIGURE 4. OVERHANG BRACKET FORMWORK AT STEEL GIRDER	
FIGURE 5. TYPICAL GIRDER TIE-DOWN DETAIL AT ABUTMENT/PIER SUPPORTS [7]	g
Figure 6. Skewed bridge load path diagram [8]	
FIGURE 7. ACROW BRIDGE SUPPORT SYSTEM IN ATLANTA'S NORTHWEST CORRIDOR PROJECT [9]	
Figure 8. Temporary shoring bracket at Harrod's Creek KY Project [10]\	
Figure 9. Typical single girder rigging scheme [7]	
FIGURE 10. TYPICAL DOUBLE GIRDER RIGGING SCHEME [7]	
FIGURE 11. GROUND PRESSURE DIAGRAM FROM THE LIEBHERR CRANE PLANNER 2.0 SOFTWARE	
FIGURE 12. CRANE ON TIMBER MATS	
FIGURE 13. CRAWLER CRANE OVER STEEL MAT	
FIGURE 14. CRANE OVER BARGE AT BIG BOX BRIDGE IN BOSTON	
FIGURE 15. HORIZONTAL PRESSURE ON WALL CAUSED BY A UNIFORMLY LOADED STRIP	
FIGURE 16. HORIZONTAL PRESSURE ON A WALL CAUSED BY A POINT LOAD	
FIGURE 17. OFFSET TANGENT METHOD SKETCH	
FIGURE 18. JOINT NUMBER DEFINITION	
FIGURE 19. FRAME DEFINITION FROM JOINT LIST	
FIGURE 20. PLATE DEFINITION FROM JOINT LIST	
FIGURE 21. FRAME ELEMENTS SECTION PROPERTIES ASSIGNMENT WORKFLOW	
Figure 22. Typical Bridge Cross-Section [15]	
FIGURE 23. FRAMING PLAN [15]	
FIGURE 24. GIRDER ELEVATION [15]	
FIGURE 25. ISOMETRIC VIEW OF GIRDER WORK POINTS.	
FIGURE 26. ISOMETRIC VIEW OF GIRDER AND CROSS FRAMES WORK POINTS	
FIGURE 27. ISOMETRIC VIEW WITH CROSS FRAMES AND PERMANENT VERTICAL SUPPORTS	
FIGURE 28. ERROR DUE TO LACK OF SIGNIFICANT FIGURES IN PLANS	
FIGURE 29. ISOMETRIC VIEW WITH MESH POINTS	
FIGURE 30. ISOMETRIC VIEW WITH WEB PLATES AND FLANGES	
FIGURE 31. ZOMMED IN MODEL WITH AREA LABELS	
FIGURE 32. FRAME SECTION LABELS ON 1ST SPAN	
FIGURE 33. EXTRUDED REPRESENTATION OF GIRDER WEB AND TOP FLANGE	
FIGURE 34. MODEL GROUPS AND SUPPORT DEFINITIONS	
FIGURE 35. STAGE 1.1 MODEL	
FIGURE 36. STAGE 1.2 MODEL	
FIGURE 37. STAGE 1.3 MODEL	
FIGURE 38. STAGE 2.1 MODEL	
FIGURE 39. STAGE 2.2 MODEL	
FIGURE 40. STAGE 2.3 MODEL	
FIGURE 41. STAGE 3.1 MODEL	
FIGURE 42. STAGE 3.2 MODEL	
FIGURE 43. STAGE 3.3 MODEL	
FIGURE 44. STAGE 4.1 MODEL	
Figure 45. Stage 4.2 model	
Figure 46. Stage 4.3 model	
FIGURE 47. STAGE 5.1 MODEL	
Figure 48. Stage 5.2 model	
FIGURE 49. STAGE 5.3 MODEL	
FIGURE 50. MESH AT FINER MODEL	
FIGURE 51. JOINT REACTIONS IN FINAL CONDITION - COARSER MODEL	
Figure 52. Joint reactions in final condition – finer model	





Alberto Arnedo Ruiz

List of tables

Table 1. Summary of rigging elements selection based on pick weight	15
TABLE 2. SUMMARY OF UPPER WIRE ROPE SIZE SELECTION FOR DOUBLE GIRDERS PICK BASED ON PICK WEIGHT	16
Table 3. Maximum load rating based on type of crane mounting [11]	18
TABLE 4. MEMBER SIZES [15]	34
Table 5. Relevant dimensions [15]	34
Table 6. Layout definition table	34
Table 7. Girder work points definition (1 of 4)	35
Table 8. Girder work points definition (2 of 4)	36
Table 9. Girder work points definition (3 of 4)	
Table 10. Girder work points definition (4 of 4)	38
Table 11. Diaphragm work points geometry (1 of 3)	40
Table 12. Diaphragm work points geometry (2 of 3)	41
Table 13. Diaphragm work points geometry (3 of 3)	42
TABLE 14. GIRDER SECTION CHANGES WORK POINTS (1 OF 3)	44
TABLE 15. GIRDER SECTION CHANGES WORK POINTS (2 OF 3)	45
Table 16. Girder section changes work points (3 od 3)	
TABLE 17. MESH WORK POINTS (1 OF 3)	47
TABLE 18. MESH WORK POINTS (2 OF 3)	48
TABLE 19. MESH WORK POINTS (3 OF 3)	49
Table 20. Frame elements definition table	51
Table 21. Area elements definition	52
TABLE 22. WEB SECTION DEFINITION	53
TABLE 23. SECTION PROPERTIES AT GIRDER AND SECTION CHANGE WORK POINTS (TOP FLANGE)	54
Table 24. Section properties at girder and section change work points (bottom flange)	54
Table 25. Frame section properties assignment	55
Table 26. Group assignments	56
Table 27. Joint reactions table in final condition – coarser model	68
Table 28. Maximum longitudinal joint deflection (coarse model)	68
Table 29. Maximum transverse joint deflection (coarse model)	68
Table 30. Maximum vertical joint deflection (coarse model)	68
Table 31. Joint reactions table in final condition — finer model	69
Table 32. Maximum longitudinal joint deflection (fine model)	70
Table 33. Maximum transverse joint deflection (fine model)	70
Table 34. Maximum vertical joint deflection (fine model)	70





Alberto Arnedo Ruiz

1. INTRODUCTION

Steel girder bridges are among the most common type of bridges in the world. According to a 2015 study by the U.S. Department of Transportation Federal Highway Administration titled "Comprehensive Truck Size and Weight Limits Study - Bridge Structure Comparative Analysis Technical Report", a total of 34,334 bridges in the United States National Highway System are classified as steel girder bridges, representing a 38.5%.

Brio	lge Type	IS		Other NHS		TOTAL	
		# of Bridges	Frequency (%)	# of Bridges	Frequency (%)	# of Bridges	Frequency (%)
1	Reinforced Concrete Slab	5101	11.2%	4903	11.2%	10004	11.2%
2	Pre-stressed Concrete Beam/Girder Simple Span	9382	20.6%	11079	25.4%	20461	23.0%
3	Pre-stressed Concrete Beam/Girder Continuous Span	2131	4.7%	3817	8.8%	5948	6.8%
4	Steel Beam/Girder Simple Span (L < 100 ft.)	6183	13.6%	5195	11.9%	11378	12.8%
5	Steel Beam/Girder, Simple Span (L > = 100 ft.)	2847	6.3%	1983	4.6%	4830	5.4%
6	Steel Beam/Girder, Continuous Spans (L < 100 ft.)	6755	14.9%	3958	9.1%	10713	12.0%
7	Steel Beam/Girder, Continuous Spans (L > = 100 ft.)	4255	9.4%	3158	7.3%	7413	8.3%
8	Girder Floor-beam Systems	774	1.7%	553	1.3%	1327	1.5%
9	Reinforced Concrete Tee Beam	2639	5.8%	3499	8.0%	6138	6.9%
10	Box Beams	5248	11.6%	5094	11.7%	10342	11.6%
11	Through Truss	102	0.2%	289	0.7%	391	0.5%
TOTAL		45,417	100%	43,528	100%	88,945	100%

Figure 1. Breakdown of bridge types on the NHS

One of main advantages of steel girder bridges compared to concrete girder bridges is the lower weight of the bridge. The lighter weight of the bridge provides a series of benefits to its use in high congested urban areas:

- Steel girder bridges become significantly more efficient than concrete bridges the longer the span is. With longer spans, the depth of the concrete girder increases more rapidly than with steel girders, increasing the difference in total weight of the superstructure. The longer spans allow bridges in urban areas to have fewer piers and foundations, reducing the total space that they take.
- The reduced girder depth is very useful in intersections where vertical clearance is of special importance, as over railroad tracks.
- The reduced weight allows for an easier erection process, with smaller cranes required to erect the same length girders. The smaller cranes not only provide significant savings, but also have smaller footprints in construction areas where the jobsite size is be very limited.
- The easier erection process allows to speed up the construction process and cost, reducing the total time that traffic needs to be stopped or rerouted.

Curved girder bridges are increasingly common in urban areas due to the limited right of way, and allow the construction of longer continuous span bridges with large curvatures. Compared to straight girders, however, curved girders have higher torsional stresses. Since the center of gravity of a simple span curve girder is not aligned with the bearings (if they are at located at the girder ends), the self-weight only causes these stresses.





Alberto Arnedo Ruiz

In the partially built structure, where all the steel has been erected but the concrete deck has not been poured yet, the cross frames transfer the torsional stresses to the adjacent girders. Cross frames from curve girder bridges are usually larger than from straight girder bridges to account for these additional loads.

The inherent instability of curved girders is however even more noticeable during the erection sequence. If not properly braced, a single curved girder will easily overturn right after being set. In addition to the stability issues, the torsional stresses can buckle the girder webs, causing the collapse of the structure.

In May 16, 1995, the State Route 69 Bridge over the Tennessee River collapsed during construction. According to the investigation, "the collapse of the SR 69 bridge resulted from a lateral instability in one of the three primary plate girders. The instability was precipitated by the removal of a critical cross frame that had been partially installed for bracing purposes."



Figure 2. Collapse of State Route 69 Bridge over the Tennessee River at Clifton, Tennessee

1.1. Motivation and purpose

Due to the stability singularities of curved steel girder bridges previously discussed, a careful study of the staged erection of all components is necessary. In large infrastructure projects, like airports infrastructure retrofitting, coordination of different construction tasks is complex and can alter field conditions, such as available work zone areas for crane placements, equipment availability, workforce, etc., altering the staged construction





Alberto Arnedo Ruiz

erection of the steel girders erection. These types of projects usually incur financial penalties if the construction timeline is extended, and equipment costs will increase significantly with delays. To keep with schedule, alternative staging options can be provided to the contractor to adapt to different conditions, but not all conditions can be forecasted. Since the exact project progress will not be known until the date of erection gets closer, a significant portion of the staged construction analysis might end up being reviewed weeks before the actual erection.

Current structural analysis software specialized in bridge design, such as CSI Bridge is focused only on overall construction stages, bundling all steel erection in one single stage, followed up by the concrete deck pours. The "piece by piece" steel staging involves a more hands-on approach that can become cumbersome.

In addition to the staging itself, curved girders add a complexity level to the geometry of the model. The curve is modelled as a series of straight frame elements. The length of each segment needs to be short enough to adequately represent the curve. Although some guidelines are given by existing literature [1], grid coarseness needs to be studied on a case-by-case approach to understand the sensitivity of the model. It is typical to start with coarser grids, since finer grid models can take several hours to solve, to obtain preliminary results, and just then increase the number of mesh points for more accurate results. The additional meshing is easier to perform in straight girders, but significantly more complicated in curved girders.

A large development in visual programing tools, such as Dynamo or Grasshopper has occurred in the last decade. These tools help users with limited programing knowledge to build parametric models with a large library of built in geometric tools. The use of these programs can help speed up the process of updating geometric models that are then synced with a variety of finite element method software, but have a steep learning curve, and are difficult to implement in smaller design firms due to the added software cost and initial time investment.

The purpose of this thesis is to:

- Provide an overview of the typical construction means and methods to erect curved steel girder bridges. This is developed in chapter 2.
- Provide a methodology, with the aid of a series of workflows as a reference, to speed up the creation and modification of a FEA model oriented towards the stability analysis of a curved steel girder bridge. This is described in chapter 3.
- Apply the working methodology to one case study. This is described in chapter 4.
- Validate the model by checking the results from the staged analysis. This is described in chapter 0.
- Summarize and compare the proposed methodology with the current practice methods, and propose improvements for future research. This is described in chapter 6.





Alberto Arnedo Ruiz

2. BACKGROUND

2.1. Stability analysis

The study of the erection procedure requires to perform a staged construction analysis through a refined analysis method [1].

2.1.1. Geometry

Commonly, generic structural FEM software is used to perform the staged analysis. The geometry of the bridge can be imported from a CAD drawing, and then the frame and plate elements can be created inside the FEM software. In the case of straight girders, this is a straightforward method since only points where section properties, boundary conditions, or diaphragms need to be initially defined, and then subdivisions are easily done with the edit tools within the FEM software. In curved girders, however, the girders must be divided in enough straight segments to accurate represent the curve. The process can be quite tedious, time consuming, and prone to making input errors. Additionally, if changes to the geometry occur during the design process, it is often easier to create a new bridge model from scratch than to modify the cad file and import the file again [2].

A series of bridge specific FEM software packages like Midas Civil or CSiBridge include geometric modules or tools to model a wide variety of bridge shapes. Additionally, they usually include some level of staged analysis input, although it is more focused towards the changes in behavior during the concrete deck pouring, facilitating the analysis of the bridge at non-composite and composite stages. The advantages of this method over importing CAD files into a generic FEM software are the built-in parametric tools that reduce the total time required to model the bridge, and facilitate changes in design midanalysis. On the other hand, the price for the software significantly more expensive, the programs can have a steeper learning curve, and the engineer needs to have a deep understanding of all the automatic modeling elements and boundary conditions that are generated within the program.

An alternative approach is to develop a spreadsheet to parametrically define the girders just like the geometric modules of bridge specific software does. This approach allows the designer more versatility in the modeling, and a higher integration with all the elements of the stability analysis, including the staging analysis and loading conditions. This alternative will be the topic of discussion in chapter 3.

The refinement in the modeling of the bridge is a common topic of discussion. A more refined model will typically yield more accurate results, but also require larger computational power. Less refined models will give less accurate results, but are faster to create and run. The amount of refinement required depends on the behavior of the structure to the loads analyzed, and the elements that want to be analyzed. For a stability analysis, a 3D model where the webs are modeled as plate elements and the flanges as beam elements is common practice. Using beam elements for the flange reduce the size of the problem, but captures the St. Venant and warping stiffness of the beam [3]. The beam elements also make it easier to input linear loads into the model, since a plate only model would require all loads to be transformed to surface loads based on the flange width.





Alberto Arnedo Ruiz

An additional advantage of a 3D model is the ability to model the constrains at their actual location. This is very critical for the lateral loads analysis.

AASHTO provides some general guidelines on article 4.6.3.3 regarding the minimum recommended meshing required for a refined analysis [1]:

- Aspect ratio of shells elements (ratio between long to short side dimension of shell element) not to exceed five
- A minimum of five, and preferably nine, nodes per beam span

It does not, however give additional recommendations for curved girders. The Federal Highway Administration [4] recommends a shell element aspect ratio close to unity, although aspect ratios of three or more is often good enough. No guidance other than performing a sensitivity is given.

Regarding the meshing of the girder web, the Federal Highway Administration guidance suggest using between one and twelve elements, and recommends a minimum of four elements to capture the parabolic shear behavior.

Assuming a span-to-depth ratio of 25 for curved girders, as recommended by AASHTO article 2.5.2.6.3 [1], we can calculate a range of typical number of nodes per span.

Number of nodes per span
$$= \frac{Span \text{ to depth ratio}}{Maximum \text{ shell aspect ratio}} x \text{ (No. of shell elements along girder depth)}$$

Minimum number of nodes =
$$\frac{25}{5}$$
 x 2 = 10

Average number of nodes =
$$\frac{25}{3}$$
 x 5 = 41.66 ~ 42

Maximum number of nodes =
$$\frac{25}{1}$$
 x 13 = 325

As observed, the maximum number of nodes can vary within an order of magnitude depending on the desired meshed size, which is directly proportional to the computational time required to solve the problem.

2.1.2. Boundary conditions

Boundary conditions during the different stages might be different than in the final location for the same elements. For example, bearings will displace outwards at the end abutments during steel erection and concrete deck pouring to accommodate for the rotation at the girder ends. Jacking is required to reset the bearings to its centered position (at a specific design temperature) if the elongation is over the tolerance limits for bridge construction.





Alberto Arnedo Ruiz

Fixed bearings typically have a welded connection between the girder bottom flange and the bearing sole plate. Since the bridge will not be able to be jacked if it is welded to the bearing pads, this operation is usually performed after all the steel has been erected and the concrete has been poured.

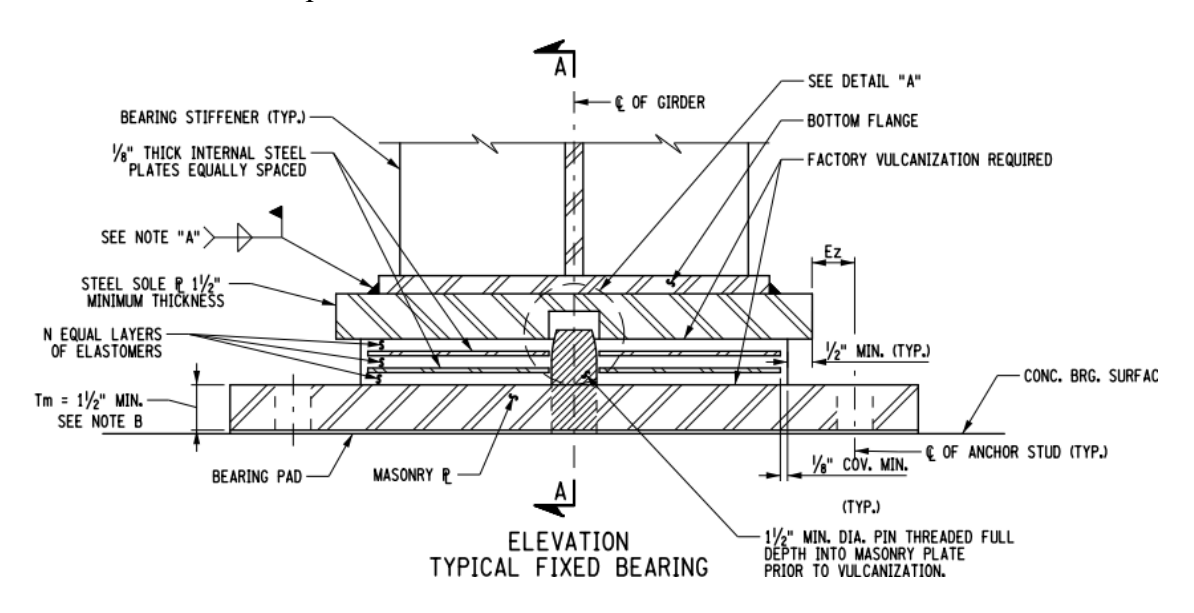


Figure 3. Typical fixed bearing as per NYSDOT Standard Sheets [5]

Therefore, during the staged construction analysis, the bearings will be modeled as fixed in the vertical direction only. If uplift at the girder bearings is a concern, the bearing may be modeled as a compression only spring, allowing the girder to lift from the bearing. Temporary tie-downs can be used to restrain the girders from uplift. In the horizontal degrees of freedom, tiebacks and timber blocking are frequently used to restrain the bridge transversally and longitudinally. The temporary bracing elements may only be present in certain stages of erection, and needs to be appropriately reflected in the staged analysis. For more detail information about temporary bracing see section 2.2.1 Bracing below.

2.1.3. Loading conditions

Loading specifications will vary based on the local governing design specifications. The engineering fundamentals in which the different design standards are based on are generally the same. For stability analysis of the steel girders the only loads present on the structure are the steel self-weight, the possible construction loads due to workers or attached temporary platform to the girders, and the wind loads during construction. Since uplift and overturning is a possible issue during erection, using a dead load factor over 1 can be unconservative. As a reference, ASSHTO LRFD [1] applies a maximum dead load factor of 1.25, and a minimum of 0.9. Uncertainty in the total weight of the steel structure from the shop drawings is not as high as with the poured deck, due to the variable haunch and deck thickness.

2.1.4. Dead load





Alberto Arnedo Ruiz

The weight of the structure can be obtained from the shop drawings if available. The reactions from the modeled geometry are factored to account for the extra weight not modeled, such as bolt connections, connecting plates, and paint. If shop drawings are not available, a 1.1 factor can be used for a preliminary design, with a unit steel weight of 490 pcf, but should be verified and revised with the final shop takeoffs.

Splice plates are added to the model as point loads where required, and do not need to me explicitly modeled. To save time during erection, the splices are usually lifted with whichever girder section connected to it is erected first. The extra weight from the splice plates is quite significant compared to the linear weight of the girder section, and will cantilever off from the previous pier location. If the cantilever distance is too long, a temporary shoring will be needed to reduce the overhang.

Finally, overhang brackets for the exterior girder's formwork are preferably installed on ground prior to lifting. The vertical load can be divided equally between the top flange and bottom flange beam elements. A force couple is also added to the top and bottom flange to account for the torsional force on the girder.



Figure 4. Overhang bracket formwork at steel girder

2.1.5. Wind load

Wind loads in the structure are also different for final condition than during steel erection. Since the deck is not present during steel erection, the air flow around the girders is higher during erection, translating into a larger drag coefficient [6].

The most critical load case scenario occurs when the wind direction is perpendicular to the girder web angle, towards the concave side of the web, due to the limited torsional





Alberto Arnedo Ruiz

stiffness during erection. In this direction, the torsional forces due to dead load will add up to the wind load effects.

2.2. Temporary supports

2.2.1. Bracing

Temporary lateral bracing is required during erection stages. As discussed in section 2.1.2 Boundary conditions above, the fixed bearings may not be restraining the girder in the horizontal degrees of freedom due to the constructability requirements. If no bracing is used, the steel girders would be fully relying in friction to not be "floating" over the bearings. There are three main types of bracing details, depending on the direction in which they are acting:

- Transverse bracing restrains the girder in the direction perpendicular to the girder web. It provides a load path for the wind loads into the abutments, piers, or temporary shoring towers. If attached to the top flange of the girders, it will also provide some additional rotational restrain. Typical details of transverse bracing are:
 - Timber blocking beams between the girder, and the adjacent girders bearing pedestals.
 - O Lever hoists, or wire rope with a turnbuckle and end shackles or eye hook ends at the bearing locations. The proposed bearing anchors can be used during the construction stages to attach the end of a lever hoist, while the other end is attached to the adjacent girder end stiffener.
 - Keeper angles, at each side of the girder, anchored to the abutments and piers with temporary anchor rods, or using the proposed bearing anchors.
 The keepers are installed leaving a small gap to be fitted tight with shims.
 - A combination of lever hoists from adjacent top and bottom girder flanges, and a set of two timber beams going diagonally from top to bottom of adjacent girders, forming a temporary intermediate diaphragm. Provides additional rotational stiffness to the girders, useful during stages in which long cantilevers occur.
- Longitudinal bracing restrains the girder in the direction parallel to the girders.
 - Wire rope with a lever hoist for pre-tensioning, from the girder bottom flange to a temporary anchor rod into the existing abutments and piers.
 - Keeper angle at the end of the girder, anchored to the abutments with temporary anchor rods.
- Diagonal bracing, transferring both longitudinal and transverse forces.





Alberto Arnedo Ruiz

- O Wire rope with lever hoist from the intermediate stiffener of one girder to the intermediate stiffener of another girder. Helps reduce stresses in the girder by creating a kind of truss in the transverse direction.
- Wire rope with level hoist from the intermediate stiffener of one girder to a temporary anchor into an abutment or pier. Reduces the span in the transverse direction in which the girders are spanning to transfer the wind loads

• Tie-downs

O Lever hoist or wire rope with a turnbuckle and end shackle or eye hook ends from the girder to a lower element, such as the abutment face, or a counterweight on grade. Prevent uplift of the girder, common in bridges with a high degree of curvature, or skewed abutments.

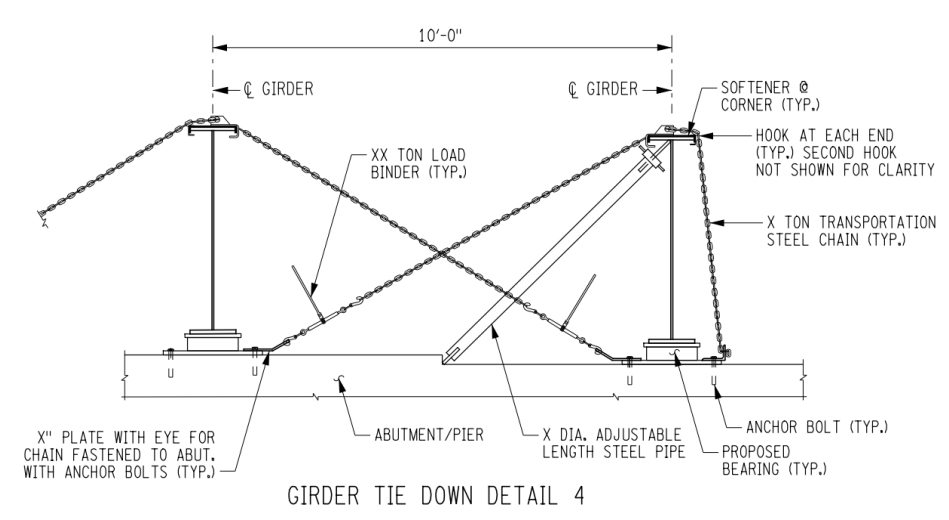


Figure 5. Typical girder tie-down detail at abutment/pier supports [7]

It is important not to over constrain the bridge, since a certain flexibility is required during erection to fit all the different pieces together. In addition to adding temporary bracing, it can also be considered as an option not adding certain proposed diaphragms until all the girders of that span have been erected. This is common in highly skewed abutments, where the intermediate diaphragms are perpendicular to the girders. Since the first intermediate diaphragms will brace one girder at a spot much closer to the support with respect to the span length than to the adjacent girders, the diaphragm will act as a main member, and will transfer the vertical loads to the closest bearing point, trying to uplift the girder with the further bearing. See Figure 6 below for a typical skewed bridge load path. Consideration can be given to not include the diaphragm until most of the bridge was been erected to avoid the possible uplift forces.





Alberto Arnedo Ruiz

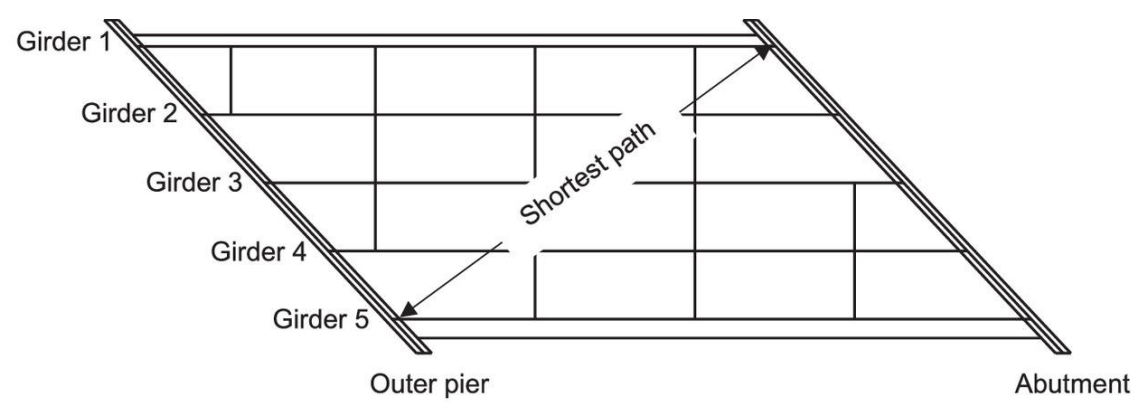


Figure 6. Skewed bridge load path diagram [8]

The maximum loads that typical lateral bracing details can transfer is limited by concentrated local stresses. If a bracing connection is done to the intermediate stiffener bolts, the maximum allowed load might be limited, for example, by the maximum weak axis moment that the stiffeners can take before failure. If using a hook connection to the top flange, the vertical force component will bend the flange plate if not distributed through a wide enough length.

2.2.2. Vertical shoring

Vertical shoring systems give temporary vertical and transverse support to girders during erection. Long girder cantilevers due to splice locations present two main issues:

- The stresses in the girders due to vertical loads may be larger than during other stages where the steel has been complete erected. The reduced stiffness also translates into large vertical displacements that can complicate bolting operations for ironworkers during the fitting of the following sections. A shoring vertical system provides an additional vertical support during construction to reduce the stresses at the girders, and provide geometrical control options to move the splices vertically into the optimal vertical fit condition.
- The stresses in the girders due to lateral loads can cause web buckling issues during high wind event due to the lack of transverse stiffness. When diagonal bracing, as discussed in section 2.2.1 above, cannot provide an adequate load path to transfer the lateral loads, vertical shoring system are used.

For bridges where the vertical clearance to the existing grade is under 20 feet, shoring posts braced in one direction only may be used. Each girder lands directly above one shoring post.

In bridges where shoring towers may rise over 20 feet, buckling will reduce significantly the capacity of a single line of shoring posts due to the large unbraced length. In such cases, a shoring tower. Usually, a set of two shoring towers formed by 4 post each, forming a square shape is placed at each side of the centerline of the bridge. A cap beam or truss then spans between the two shoring towers, just below the proposed girders bottom flanges. The girders then land on the cap beam.





Alberto Arnedo Ruiz



Figure 7. Acrow bridge support system in Atlanta's Northwest Corridor Project [9]

For the same reasons explained in section 2.1.2 Boundary conditions above, longitudinal movement needs to be allowed at the top of the shoring systems. Adjustability to the vertical elevation of the shoring system with jack-up systems is vital for the geometric control of the bridge during erection.

A different option to temporary support a girder can be the use of a holding crane, and requires to have at least two different cranes in the field. In bridges high above the ground with large spans, instead of using a shoring tower system, a crane will "hold" one girder in place, until the next girder section, which reaches the following pier, is installed with a separate crane. Once the second girder section has been installed, the holding crane can release the girder.



Figure 8. Temporary shoring bracket at Harrod's Creek KY Project [10]\

2.3. Additional items relevant to the staged construction

This section will give an overview of two items that can influence the staged construction but will not be part of the methodology described in chapter 3.





Alberto Arnedo Ruiz

In section 2.3.1, the typical rigging configurations, strength and stability requirements are discussed. Rigging assemblies can become a significant portion of the total pick weight for very long girders, reducing the effective weight that the crane can pick.

In section 2.3.2, the typical types of cranes used and the surcharge loads into the existing structures are discussed. In addition to the extra cost of using larger cranes, crane size might be limited by the specific job site conditions, such as subsurface elements or available space. These limitations will then affect the maximum weight that can be picked at a time, forcing the use of temporary shoring towers are discussed in section 2.2.2.

2.3.1. Rigging

Rigging design is an important part in the planning of curved steel girders erection. Compared to straight girders, curved girders have a much stricter limitation in the length of the spreader beam required. Curved girders are subject to non-negligible torsional forces that may distort the section.

Girders may be picked in pairs to reduce stability issues during girder setting.

2.3.1.1. Rigging components

Girders will typically be erected by one or two cranes at the same time. Double crane picks may be used for especially large girders due to the heavier weights, or at construction sites with access problems or space limitations that would require a large pick radius with a single crane.

The spreader beam is connected to the crane hook through a pair of wire rope or synthetic nylon slings. Wire rope slings have higher capacity, but can also be much heavier for the same capacity requirements, reducing the effective lifting capacity. For example, a 2 in diameter 6x36 XIP wire rope with a Flemish eye splice has a rated capacity of 37 US tons [11] with a weight of 7.39 lb/ft. A EE900 Tuflex® Eye and Eye polyester roundsling has a rated capacity of 77,000 lbs. [12] with a unit weight of 3.95 lb/ft, resulting in the synthetic sling having twice the strength to weight ratio. The slings angle with the horizontal is usually kept at a minimum of 45 degrees to limit the compressive reaction in the spreader beam. Larger angles may increase the overall capacity of the lifting device, but will require a higher vertical reach of the crane boom.

Multispan steel curved girder bridges will typically require a variety of lengths of spreader beams due to the difference in length between the splice locations along the girders. To reduce cost and increase reusability, modular or adjustable spreader beams are used. Adjustable spreader beams consist of telescopic pipe or hollow tube shapes that allow the user to adjust the length of the spreader beams at specific intervals with the use of adjustment pins. Modular spreader beams on the other hand, forms a single spreader beam with multiple intermediate pipe sections, and two end sections where the top and bottom shackles connect to the top and bottom slings.

In the case of single girder picks, another set of slings will drop from the spreader beam to the beam clamps vertically. In some occasions, another smaller spreader beam level





Alberto Arnedo Ruiz

parallel to the top one is used to double the amount of beam clamps due to concerns with the beam clamp capacity or local bending at the beam clamp location.

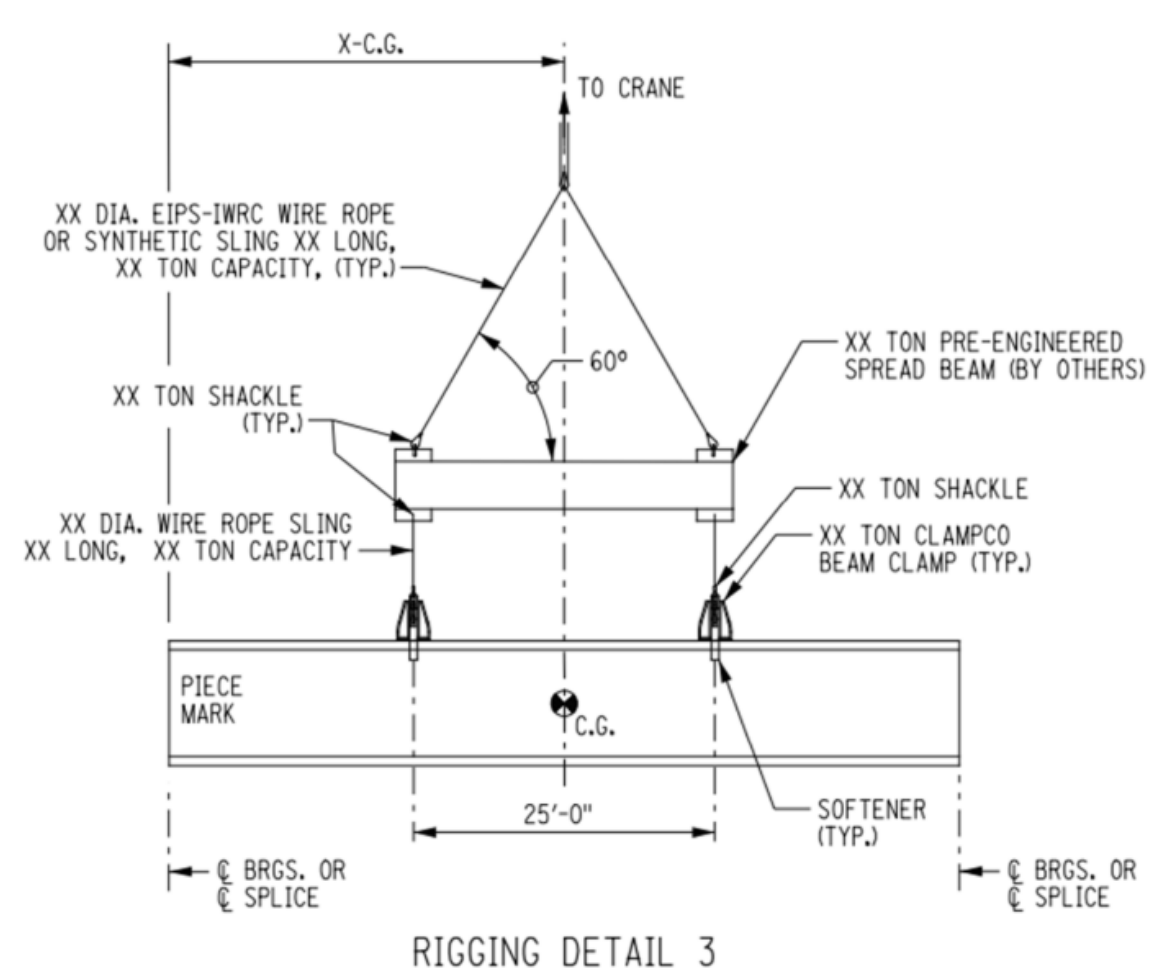


Figure 9. Typical single girder rigging scheme [7]

While the slings over the spreader beam are usually of the same length and symmetrical, the lower-level sling lengths need to be adjusted accordingly to accommodate the vertical slope of the girder in its final location. That means that one sling may be shorter than the other. Often, lever hoists are used to adjust the lengths in the field prior to picking the girders from the staging area. If this adjustability is not provided, one end of the girder may start transferring the vertical load from the crane to the proposed structure, loading the spreader beam asymmetrically, and inducing a lateral load in the crane which may reduce the crane capacity dramatically. For heavier picks, a double crane pick may be used, where two rigging assemblies are used near each end for the girder, with the cranes placed in opposite sides of the girder. A typical example is a single span over an inaccessible area, such as a railroad right of way, with a crane plate on each abutment end.

In double girder picks, a pair of spreader or equalizer beams perpendicular to the top-level spreader beam is used to drop a minimum of four slings into four different pick points, two per girder. Double girder picks are required during the erection of curved steel girder bridges due to the added stability, and are usually the first set of girders that is lifted at





Alberto Arnedo Ruiz

each span. Once a pair of girders is erected, single girders can be lifted and braced to the previously erected girder pair.

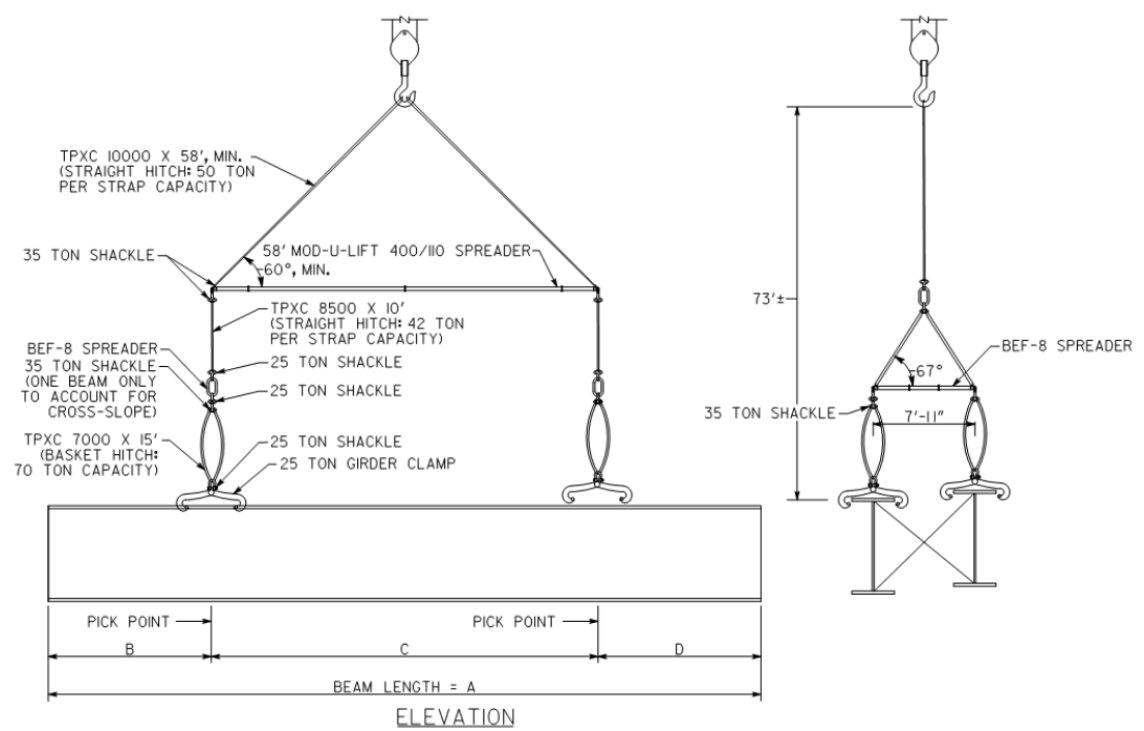


Figure 10. Typical double girder rigging scheme [7]

2.3.1.2. Strength requirements

As specified in OSHA 1926.753(e)(2) [11], "Components of the multiple lift rigging assembly shall be specifically designed and assembled with a maximum capacity for total assembly and for each individual attachment point. This capacity, certified by the manufacturer or a qualified rigger, shall be based on the manufacturer's specifications with a 5 to 1 safety factor for all components".

Additionally, on top of the 5 on 1 safety factor, many railroad agencies require that all the components of the lift rigging assembly are designed for 150% of the calculated pick weight when the lifting operations are near train tracks, when the failure of the crane or lifting components may damage or interrupt the normal service of the trains.

Design of rigging components is based on the weight of the heaviest pick throughout the project. A spreader beam size is selected for the combination of span distance and capacity required. Since the spreader beams are usually pre-engineered products, the capacity of the spreader beam is often significantly heavier than required. With the objective of reducing the total weight of the rigging assembly, the rest of the components are to be designed to the actual pick load they experience rather than the spreader beam capacity.

Required rigging components size have been tabulated in Table 1 based on the rigging scheme shown in Figure 9. Typical single girder rigging scheme Figure 9. Typical





Alberto Arnedo Ruiz

manufacturer products have been used. Maximum lifting capacity limited by largest beam clamp capacity. For higher loads, a different rigging arrangement is required.

Table 1. Summary of rigging elements selection based on pick weight

Lifting capacity	Beam	Shackle nominal	Bottom wire rope	rope Spreader		Upper wire rope diameter ⁴ (in)			
(Kips) ¹	clamp ²	size ³ (in)	diameter ⁴ (in)	beam	45	60	70		
140			(111)		deg.	deg.	deg. 2-1/4		
135	CCBC F-					2-1/4	2-1/4		
130	35				2-1/2	2-1/4			
125			2						
120		2					2		
115	IPBCNS								
110	32t			2-1/4	2				
105			1-3/4	Lightest spreader					
100	CCBC F-		1-5/4	beam with			1-3/4		
95	25			enough			1-3/4		
90	25		1-5/8	capacity at	2	1-3/4			
85	IPBCNS 22.5t		1-3/4	1-5/6	the desired	2	1-3/4	1-5/8	
80			span length			1-5/6			
75				1-1/2	– span length to be		1-5/8		
70			22.00	22.00			determined	1-3/4	
65			1-3/8	per rigging		1-1/2			
60	CCBC F-	1-1/2	1-1/4	stability analysis –	1-5/8		1-3/8		
55	15	1 1/2				1-3/8			
50		1-3/8	, .	shackles on			1-1/4		
45			=	top and bottom of	1-3/8	1-1/4			
40	IPBCNS	1-1/4	1-1/8	spreader		4 4 / 0	1-1/8		
35	13.5t	1-1/8	1	beam per	1-1/4	1-1/8	4		
30		1		manufacturer	1-1/8	1	1		
25			7/8		1		7/8		
20	CCBC F- 5	7/8	3/4		7/8	7/8	3/4		
15	IDDCE	3/4	5/8		3/4	3/4			
10	IPBCF 4.5t	5/8	1/2		5/8	9/16	9/16		
5	7.50	7/16	3/8		7/16	7/16	3/8		

¹ Lifting capacity = beam pick weight + self-weight of rigging elements below design element

15

² Per TheCrosbyGroup product catalog [22] ³ Crosby 209 Carbon Screw Pin Anchor Shackle [22]

⁴ 115 IWRC [19]





Alberto Arnedo Ruiz

In a double girder pick arrangement as shown in Figure 10, the rigging assembly is composed of (2) single girder picks assemblies in a lower level, and another one in an upper level. Table 1 can be used to design the lower-level assemblies, by diving the total pick load by 2. For the upper label design, additional lifting capacity range is provided in Table 2 since the total capacity of the assembly doubles.

Table 2. Summary of upper wire rope size selection for double girders pick based on pick weight

Lifting	Upper wire rope diameter ² (in)					
capacity (KIPS) ¹	45 deg.	60 deg.	70 deg.			
280						
275		3-1/2				
270						
265			3			
260			3			
255						
250	3-1/2	3				
245		3				
240						
235						
230						
225			2-3/4			
220			2-5/4			
215						
210		2-3/4				
205		2-0/4				
200	3					
195						
190						
185			2-1/2			
180						
175	2-3/4					
170		2-1/2				
165						
160						
155			2-1/4			
150	2-1/2	2-1/4				
145	Z-1/Z	2-1/4				

16

¹ Lifting capacity = beam pick weight + self-weight of rigging elements below design element

² 115 IWRC [19]





Alberto Arnedo Ruiz

2.3.1.3. Stability during lifting

Buckling of the girder also needs to be studied during erection due to the dead load only torsional forces. If a 2-pick point rigging assembly is used, there is as single solution where the center of gravity aligns with the pick points at an equidistant position [12].

The University of Texas at Austin developed a spreadsheet to calculate the stresses and deformations during lifting of a steel curved girder with a variable dimensions and diaphragms attached, and the location of the 2 pick points along the girder flange [13] [14]. The stresses are then compared to the critical buckling moment.

2.3.2. Cranes

Crane costs increase with their capacity. Ideally, the crane used has just enough capacity to lift the heaviest pick in the planned staged construction. Depending on the site conditions, some crane types may be preferable to others. There are two main features that classify the cranes mostly used in steel girders erection.

- Mobile or crawler
- Telescopic or lattice boom

Mobile cranes have regular axles and can travel on public roads. The larger the crane, the more axles it must be able to distribute all the load throughout the road infrastructure. During travel, they can usually carry all parts but the counterweight, which will be placed on the construction site. To distribute the load to the ground, a set of outriggers is extended from the crane body outwards. Modern mobile cranes can extend the outriggers anywhere between 0% and 100% of the allowed length to fit in tight spaces. Although they can move through rough terrain, they have more difficulties than crawler cranes when moving in uneven, soft, or very steep sections. Outriggers are set on timber or steel mats to distribute the load further down into the soil or other existing structure. Mobile cranes tend to have a telescopic boom, although options with lattice booms are also available in the market

Crawler cranes on the other hand move on continuous tracks. Their slower speed makes them unusable for public road use, and must be fully transported in parts to the construction site. The tracks, also known as crawlers, makes them much more versatile moving around a diverse terrain. No outriggers are required since the load is distributed through the same crawlers that are used to move the cranes. Timber mats are placed under the crane, from crawler to crawler to distribute the loads to the ground. Crawler cranes on timber mats are also commonly used over barges when the bridge spans over a large mass of water. Additional analysis is required to check the stability of the crane over the barge, and a reduced capacity of the crane needs to be calculated to account for the barge tilt. Crawler cranes tend to have a lattice boom, although options with telescopic booms are also available.

Telescopic booms allow the operator to adjust the boom length prior to every pick without having to mount new pieces. The quick adjustment is also beneficial when moving the crane through a crowded construction site with many obstacles. If a large pick radius is





Alberto Arnedo Ruiz

not required, a shorter boom length usually provides a higher lifting capacity than a longer boom at an almost vertical angle.

Lattice booms generally provide a higher capacity than telescopic booms at the same length. A long footprint of the worksite is necessary to attach the lattice boom to the crane.

2.3.2.1. Lifting capacity

Type of crane mounting	Maximum load ratings (percent of tipping loads)
Locomotive, without outriggers:	
Booms 60 feet or less	¹ 85
Booms over 60 feet	¹ 85
Locomotive, using outriggers fully extended	80
Crawler, without outriggers	75
Crawler, using outriggers fully extended	85
Truck and wheel mounted without outriggers or using outriggers fully extended	85

Table 3. Maximum load rating based on type of crane mounting [11]

In the U.S., OSHA provides a maximum load rating depending on the type of crane mounting (see Table 3). Crane manufacturers provide load chart tables with the capacity already reduced to account for the maximum allowable tipping load.

Lifting capacity may not be always limited by the crane itself, but by the capacity of the rigging assembly, including the crane hook block and rigging lines. It may be of interest to use a rigging assembly that does not have the full capacity of the crane, since the largest hook blocks and spreader beams can account for a significant portion of the total pick weights, especially for the ones that require a large pick radius.

2.3.2.2. Support reactions

Cranes need to be able to transfer the reactions in the outrigger or crawlers into the ground and/or existing structure below. Reactions can be estimated using simple equilibrium equations, but finding the center of gravity of all the crane components may be tricky. Some manufactures provide openly available software to calculate such reactions based on certain crane configurations, pick radius and pick weight.

In addition to the load cases from each pick, it is also important to consider the unloaded condition of the crane with the boom in the shortest and highest position, which may govern over the loaded case conditions.





Alberto Arnedo Ruiz

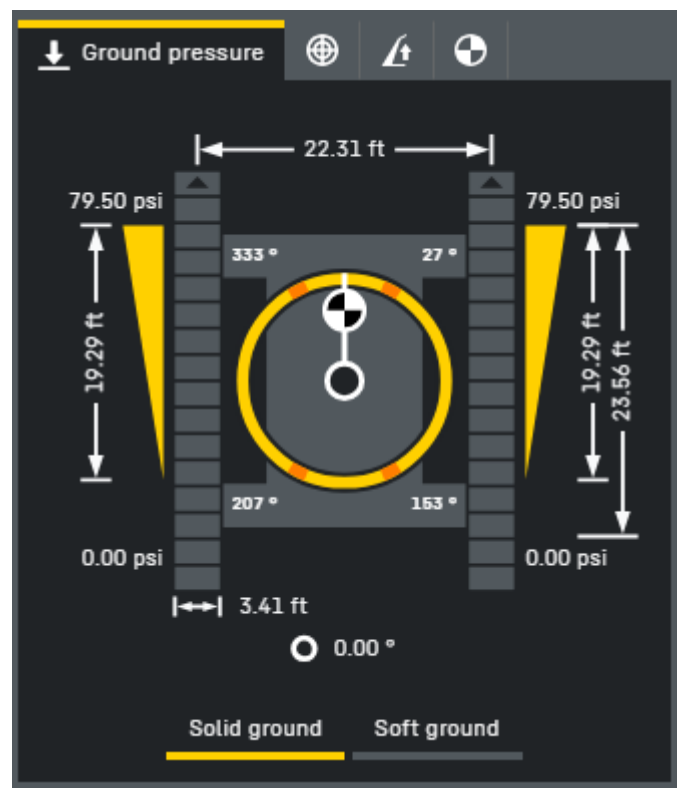


Figure 11. Ground pressure diagram from the Liebherr Crane Planner 2.0 software

The crane mats need to be stiff enough to distribute the loads in a wide enough area to avoid large settlement of the ground while picking, and to reduce the bearing pressure under the maximum allowed over the existing underground utilities.

Timber mats are they most common way to distribute the crane loads to the surface. One or two layers of timber beams perpendicular to each other are typical configurations. A steel plate can be used under the outrigger, on the top timber layer to distribute the load even more. Steel plates are not recommended under crawler cranes due to the possibility of skidding.





Alberto Arnedo Ruiz



Figure 12. Crane on timber mats

When the outrigger reactions are very high, and therefore large bearing areas are required, timber mats of reasonable dimensions lack the sufficient stiffness to distribute the loads. In this case, steel mats, formed by a series of beams welded together with a top and bottom cover plate are used.





Alberto Arnedo Ruiz



Figure 13. Crawler crane over steel mat

2.3.2.3. Barges

When a crane cannot get close enough to all the sections of a bridge from land, a barge is used to transport the crane. A loading plan is developed to move the crane from land to the barge. The crane is then lashed down to the barge to secure it in place. Once the barge reaches the desired location, a set of spud poles is lowered and driven into the seabed to secure the barge in place.

When loading the crane, the barge will rotate with respect to an axis perpendicular to the boom. The rotation of the barge will then rotate the whole crane forward, increasing the pick radius, and therefore reducing the capacity of the crane. This second order effect are especially noticeable in heavy, close-range picks, since the percentual increase in the radius is much larger.





Alberto Arnedo Ruiz

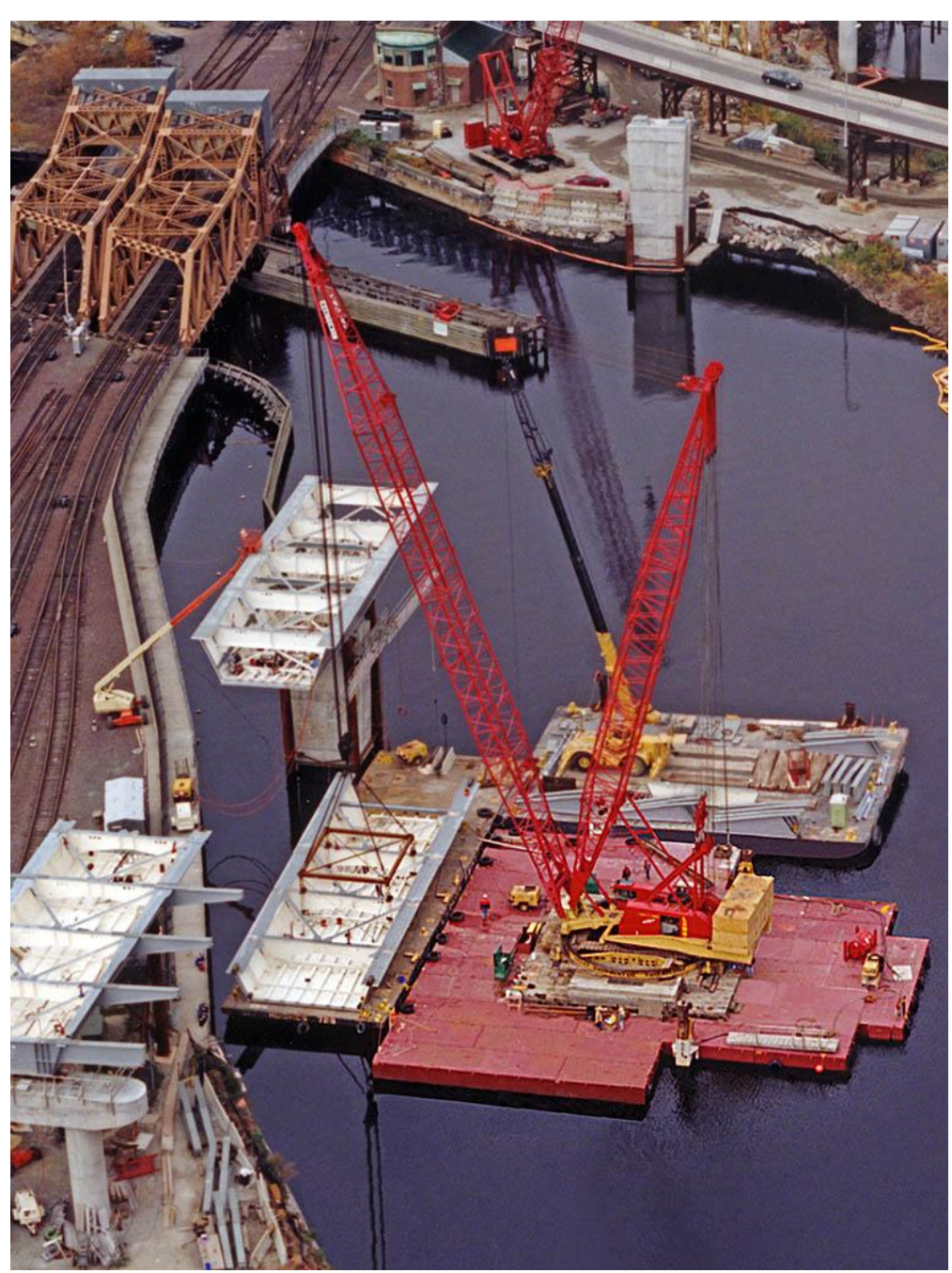


Figure 14. Crane over barge at Big Box Bridge in Boston

2.3.2.4. Surcharge loading

On occasion, the cranes will be placed near abutments, retaining walls, or existing underground buildings like pump stations or drain basins. (DOUBLE CHECK). In addition to the vertical bearing pressure previously discussed, a horizontal surcharge pressure will load these walls laterally. The existing structures are to be checked for additional surcharge loads. If the surcharge loads are too high for the existing structures, and no other logical crane placement is feasible, a grillage structure supported by





Alberto Arnedo Ruiz

micropiles may be studied to transfer the vertical loads under the zone of influence of the existing structures.

To calculate the lateral surcharge loads, the formulas given by AASHTO LRFD 9th Edition, article 3.11.6.2 may be used. All the equations provided in this section assume that the wall does not yield, which would provide conservative results in the case of a flexible wall. In most cases, the surcharge load is calculated using the equation provided for a uniformly strip parallel to the wall:

$$\Delta_{ph} = \frac{2p}{\pi} [\delta - \sin \delta \cos \cos (\delta + 2\alpha)]$$

where:

p = uniform load on strip parallel to wall (ksf).

 δ = angle between the point of interest along the wall and the edge points of the strip load (rad).

 α = angle between the wall and the line between the point of interest in the wall and the edge of the strip load at the closest side (rad).

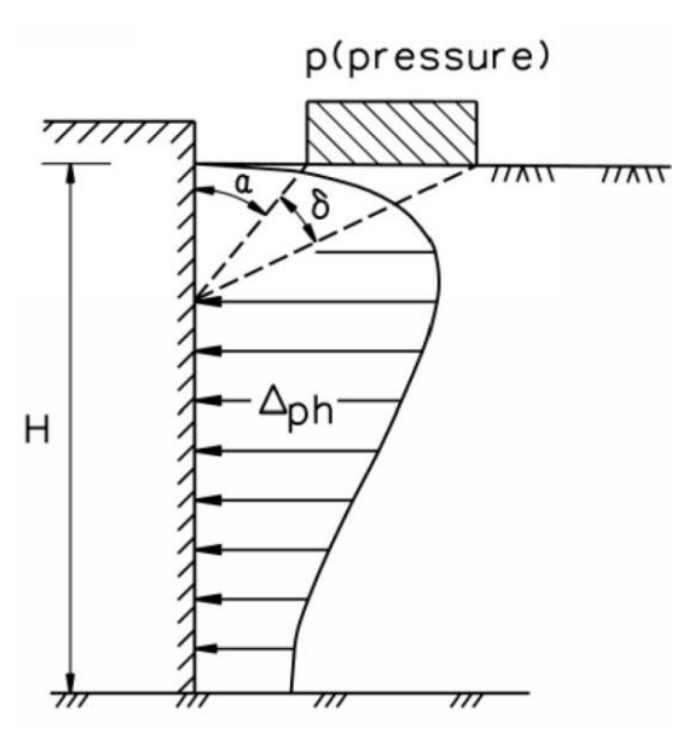


Figure 15. Horizontal Pressure on Wall Caused by a Uniformly Loaded Strip

The formula provides a two-dimensional solution, since it assumes an infinitely long strip load. A typical load case scenario for this application is the presence of an open lane of traffic near a retaining wall. In the case of the surcharge load due to the crane timber mat bearing pressures, it can be conservatively assumed that the rectangular load infinitely extends parallel to the wall.





Alberto Arnedo Ruiz

A more appropriate equation to be used for the typical crane surcharge loading condition is the one provided for a point load:

$$\Delta_{ph} = \frac{P}{\pi R^2} \left[\frac{3ZX^2}{R^3} - \frac{R(1 - 2v)}{R + Z} \right]$$

where:

P = point load (kip)

R = distance between the point load and point of interest in the wall (ft)

X = horizontal distance from back of wall to point of load application (ft)

Y = horizontal distance from point of wall under consideration to the plane perpendicular to the wall that passes through the point of load application (ft)

Z = vertical distance between the point of load application to the point on the wall under consideration

v = Poisson's ratio

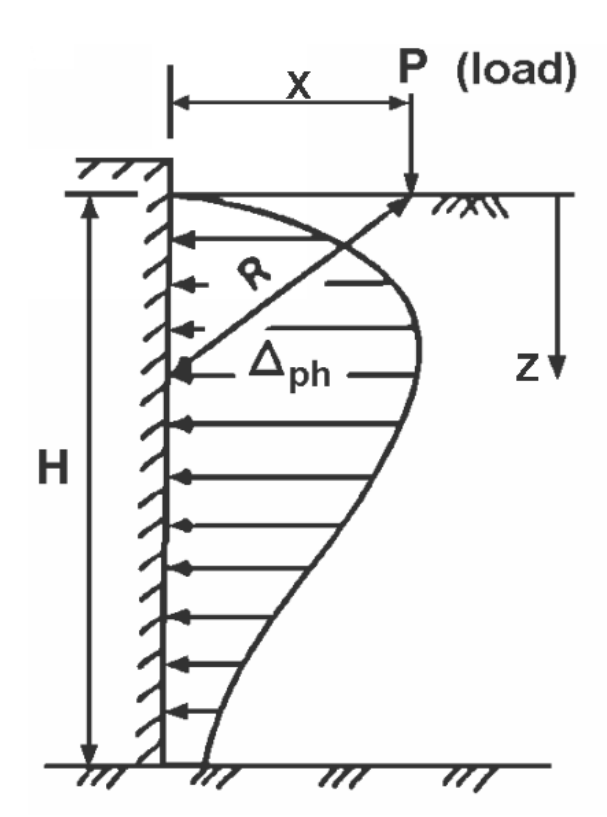


Figure 16. Horizontal pressure on a wall caused by a point load

The point load solution provides a three-dimension solution, since the horizontal pressure can be calculated for a point along the wall that is not in the wall section closest to the point load. The surcharge pressures from a resultant crane timber mat force are smaller than the ones assuming an infinitely strip load, providing more accurate results.

The maximum surcharge pressure is highly sensitive to the horizontal distance from the back of the wall to the point of load application, X. The large sensitivity can result in underestimations of the total surcharge in situations in which the timber mat dimension perpendicular to the wall is equal or larger than X, where the closest point of the timber





Alberto Arnedo Ruiz

mat to the wall would be at X/2 or less from the wall. For improved accuracy the surface load into the timber mat can be divided into a larger number of point loads equally spaced along the timber mat, and the results of all of them sum to obtain the full surcharge pressure.

A different, more simplified approach is used to calculate the surcharge pressures due to highway loading. As per article 3.11.6.4, the increase in horizontal pressure due to live load surcharge may be estimated as:

$$\Delta_p = k \gamma_s h_{eq}$$

where:

 Δ_p = constant horizontal earth pressure due to live load surcharge (ksf)

k = coefficient of lateral earth pressure

 γ_s = total unit weight of soil (kcf)

 h_{eq} = equivalent height of soil for vehicular load

AASHTO gives guidance on the equivalent height of soil for vehicular load to be used in certain cases. Equivalent height of soil for highway loadings on abutment perpendicular to traffic shall be:

- 4 feet for abutments of 5 feet in height
- 3 feet for abutments of 10 feet in height
- 2 feet for abutments of 20 feet or more in height

Equivalent height of soil for highway loadings on retaining walls parallel to traffic shall be:

- 5 feet for abutments of 5 feet in height
- 3.5 feet for abutments of 10 feet in height
- 2 feet for abutments of 20 feet or more in height
- 2 feet for any height if the distance between wall back face and the edge of traffic is over 1 foot

Value for intermediate wall heights may be interpolated in both cases.





Alberto Arnedo Ruiz

3. METHODOLOGY

To speed up the typical modeling process, a workflow to be easily implemented with spreadsheets is developed to quickly model the plate and frame FEM. The spreadsheet will allow the user to quickly perform changes to the model for a sensitivity analysis and automatic assignment of loads for stability analysis as well as the staged construction analysis.

3.1. Element IDs

To facilitate the manipulation of all the joints created for the FEA model, a 7-digit nomenclature is defined depending on the location of the point with respect to the girder elements. The nomenclature is defined as follows:

- First digit: Top flange (0) or bottom flange (1) location
- Second digit: Girder number
- Third digit: Girder piece
- Fourth digit: Cross frame section along the girder piece section
- Fifth digit: Section type within cross frames
- Sixth, seventh and eighth digits: Joint number between cross frames or section type

For example, joint number 11232031 refers to the thirty-first joint along the second girder section type after the third cross frame in the second girder piece of the first girder at the bottom flange location. The proper definition of the joint will facilitate the rearrangement, creation of frame and plate elements, and construction stage definitions.

3.2. Layout line

To define geometry of the girder we first need to add a layout line. 9 different input variables are required:

- Element number: Order in which the curves are being placed along the alignment.
- Element: Type of "curve" being used. Can be "Straight" or "Curve". A "Curve element follows a circular curve.
- Station Start: Begin station of the curve, in feet.
- Station End: End station of the curve, in feet.
- Curve Direction: Can be defined as "Right (Clockwise)" or "Left (Counterclockwise)" for the circular curves, or "-" for a straight line.
- Radius: Curve radius in feet. Set as "Infinite" for straight lines.
- Bearing: Direction of the tangent of the curve at the "Start Station" in radians. 0 radians indicate an east direction.
- Northing: Y coordinate of the curve at the "Station Start" in feet.
- Easting: X coordinate on the curve at the "Station Start" in feet.





Alberto Arnedo Ruiz

3.3. Girder work point geometry

The work points define the horizontal geometry of the girders. Since each girder piece is a straight lines or circular curves, the girder work points define the location of the splices, and the ends of the girders. To define the geometry of the girder, 8 different input variables per work point are required:

- WP: Work point number.
- Girder: Number of girders across the bridge section being defined
- Station: Work point station, based on the previously input layout line, in feet
- Offset: Distance between the girder work point and the perpendicular to the layout line, in feet
- Curve Type: Type of "curve" being used. Can be "Straight" or "Curve". A "Curve element follows a circular curve.
- Curve Direction: Can be defined as "Right (Clockwise)" or "Left (Counterclockwise)" for the circular curves, or "-" for a straight line.
- Radius Before: Radius of the girder at the section before the work point
- Radius after: Radius of the girder at the section after the work point

The coordinate of each work point is then calculated using the following sequence:

- 1. Obtain curve data from the layout curve at the work point
- 2. Calculate θ , angle between the bearing angle of the layout line at the work point station and the bearing angle of the layout line at the start station.

$$\theta_{i+1} = \theta_i \pm \frac{L_{i+1} - L_i}{R}$$

where:

 θ_{i+1} = Bearing angle at work point station θ_{i} = Bearing angle at start of layout curve

 L_{i+1} = Station at work point

L_i = Station at beginning of reference layout curve

R = Radius of curve

3. Calculate the coordinates of the work points along the layout line using the tangent offset method (See Figure 17 for graphical solution)

$$X_{i+1} = X_i + \sqrt{X^2 + O_x^2} \cos(\beta)$$
$$Y_{i+1} = Y_i + \sqrt{X^2 + O_x^2} \sin(\beta)$$

where:

 X_{i+1} = Easting coordinate at layout line at work point

X_i = Easting coordinate at start of layout curve

 Y_{i+1} = Northing coordinate at layout line at work point





Alberto Arnedo Ruiz

Y_i = Easting coordinate at start of layout curve

and:

$$X = Rsin(\alpha)$$

$$O_x = R - \sqrt{R^2 - X^2}$$

$$\beta = \theta_i \pm atan \left[\frac{O_x}{X}\right]$$

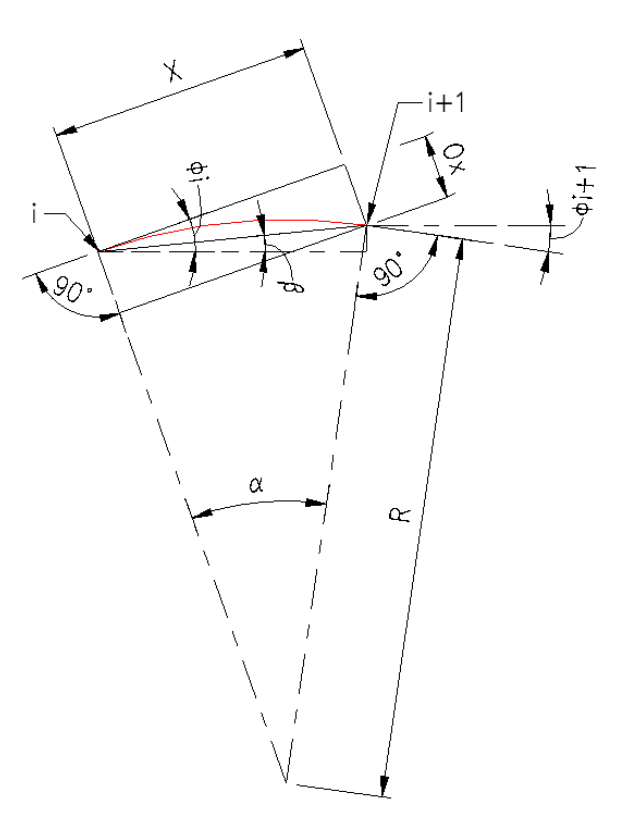


Figure 17. Offset tangent method sketch

4. Calculate the coordinates at the work points using the offset input

$$X_{Gi} = X_i \pm offset * cos \left(\theta_i + \frac{\pi}{2}\right)$$

where:

X_{Gi} = Work point coordinate at girder
 X_i = Work point coordinate at layout line

The joint number is then automatically defined for the work points that define the girder since only the first 2 digits need to be defined.





Alberto Arnedo Ruiz

In regards to the vertical elevation of the girder, it is generally acceptable to model the bridge as if it was flat, as long as the stiffness of the supports is properly accounted for. In bridges with large slopes, it may be preferred to model the girder at its actual elevation. For the purpose of this thesis, the bridge is model in the same elevation across the length of the bridge. Work points at the top flange are given an elevation equal to the girder depth. Work points at the bottom flange are given a "0" elevation.

Additionally, the work point coordinates for the cross frames and section change are defined with the same equations. The joint number for the cross frames is then automatically defined based on the location of the work point with respect to the girder work points (see Figure 18). The joint number for the section changes is defined based on the location of the work point with respect to the girder work point and diaphragm work point (see Figure 18).

3.4. Mesh points

To define all the required points, a maximum mesh size is chosen. Based on the maximum mesh size, the maximum segment length for each girder is defined. The length is then rounded down to create an equal spacing of the mesh points along the girder length. The definition of the mesh points is therefore independent of the work points previously defined.

Using the same geometric solution shown in the previous section, the mesh points coordinates are found. Mess points joint numbers are automatically defined based on its location with respect to the girder, cross frames, and section properties changes work points (see Figure 18).

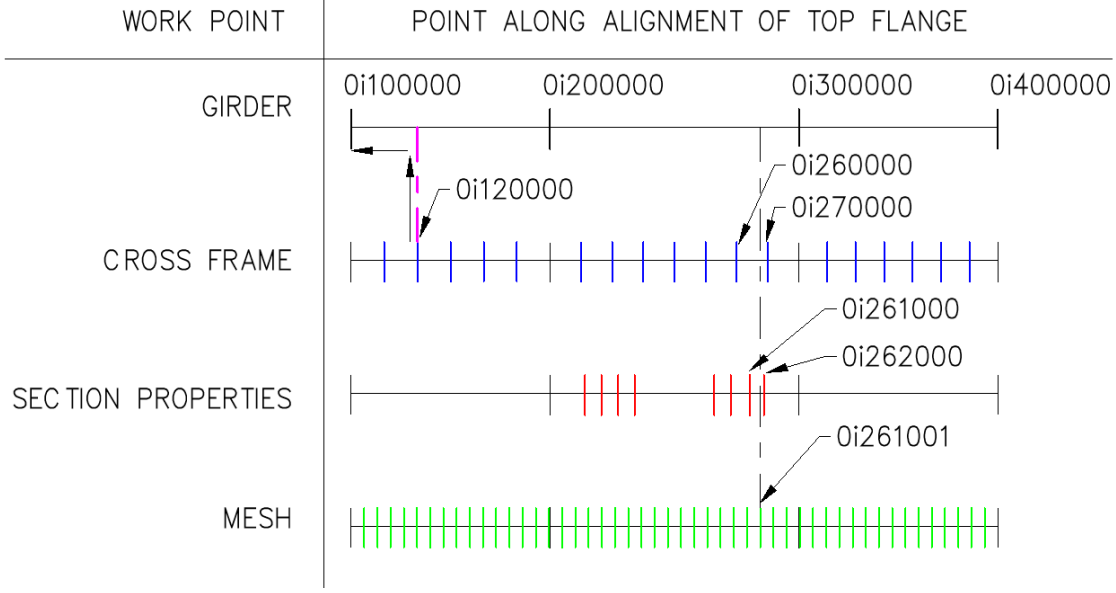


Figure 18. Joint number definition





Alberto Arnedo Ruiz

3.5. Frame and plate elements

The nomenclature used for the joints definition now facilitates the definition of the rest of the model elements. Since all the joints are numbered in sequence for the position along the girders in which they are located, the frames can be defined assembling together a list of joints starting from the first join to a list of joints starting from the second joint.

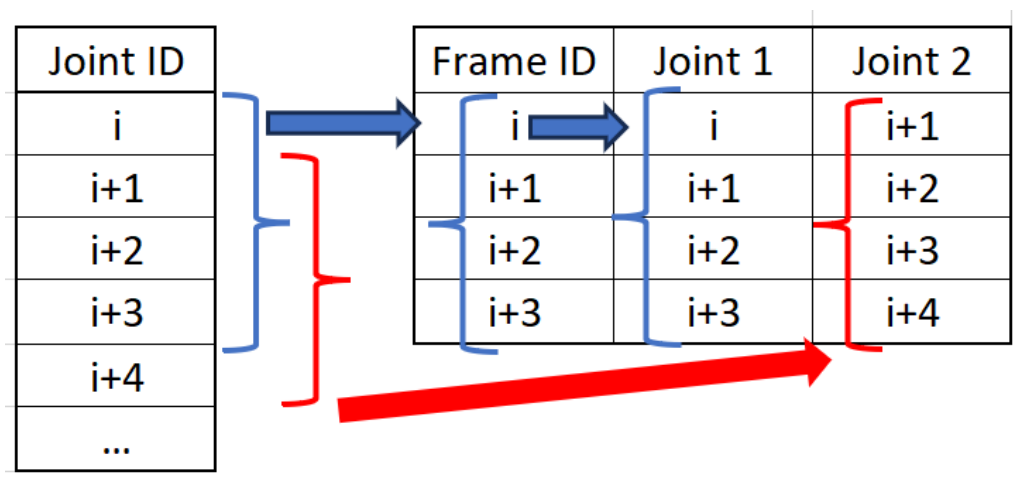


Figure 19. Frame definition from joint list

The same can be done for the definition of the plate elements. The bottom flange joints have the same definition as the top flange, with the additional first digit.

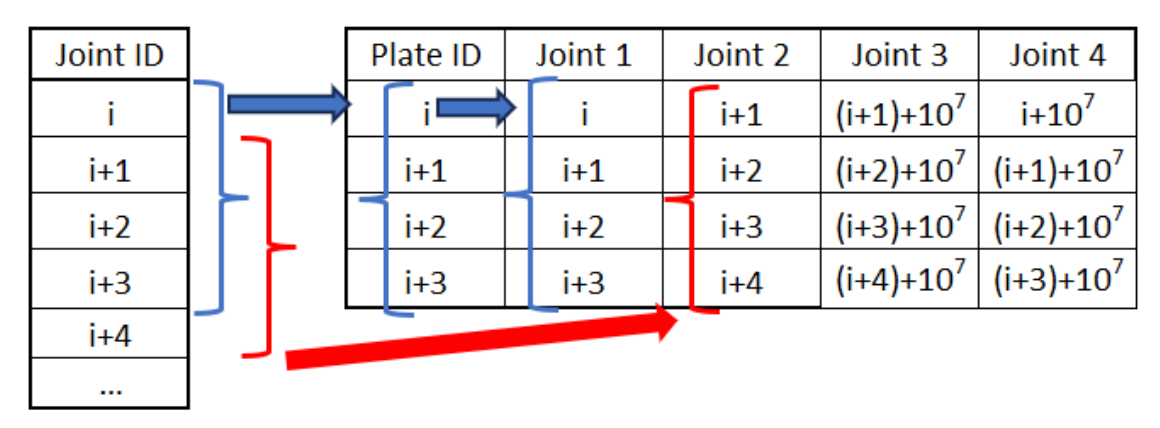


Figure 20. Plate definition from joint list

Once the frame and plate elements are created, section properties need to be assigned.

In the case of the plate elements, the girder web is many times of constant dimensions throughout the length of the beam. For cases in which the web thickness change between each girder piece, the section can be defined based on the value of the third digit of the plate ID. Since plates are defined from the coordinates from the top flange joints, in which the first digit has a value of 0, the digit to be extracted becomes the second digit in the way FEA software handles plate elements IDs. To extract the number, excel has the built in "MID", which returns the characters from the middle of a text string for a specific starting position and length. Since "MID" function returns a string value,





Alberto Arnedo Ruiz

"NUMBERVALUE" function can be used to convert the value back to a number. The following formula is shown as a valid option to use:

 $Girder\ section = NUMBERVALUE(MID(Plate\ ID, 2,1))$

Alternatively, a series of rounding operations to specific significant figures can be used to obtain the girder section value.

To assign the section properties of the flange elements, the joints that define the girder pieces and the section changes are tabulated. Since the frame elements share the same ID number as the first joints of each element, their ID can be compared with the list of relevant work points for section changes, and assign each frame element to the respective section properties. Figure 21 shows the workflow used which can be easily implemented in a spreadsheet format.

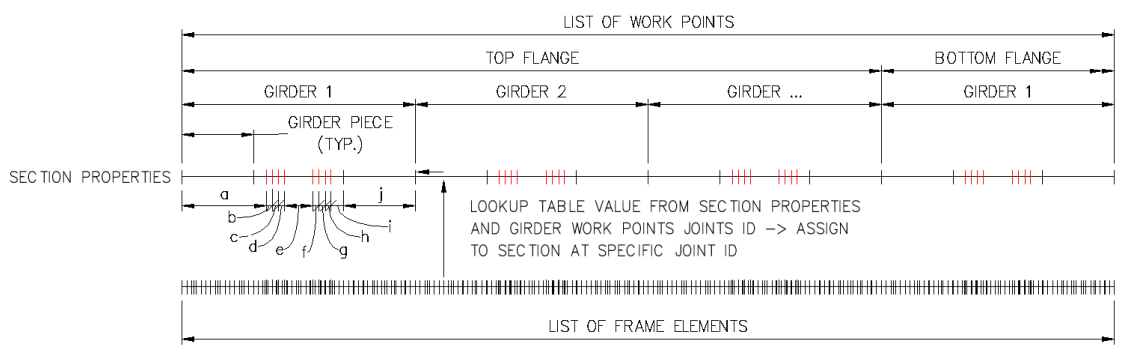


Figure 21. Frame elements section properties assignment workflow

Regarding the cross frames, the geometry and section properties are input manually based on the cross frames work points.

3.6. Boundary conditions

Vertical supports are individually assigned at the girder bearing locations and temporary shoring towers. While in a straight bridge, the global axis will generally coincide with the local axis of the girders, the bearings have to be individually rotated to the direction tangent to the girder at each bearing, which will coincide with the bearing angle at the work point station as defined in section 3.3.

3.7. Staged analysis

3.7.1. Group definition

To create a staged analysis, all programs usually require the creation of "groups" that are added to each stage. The nomenclature defined in section 3.1 comes handy once again. Joints belonging to a frame element that is added to a group, is automatically included in the specific construction stage even if it is not included in the same group, so only frame and plate elements are necessary to be added to the groups.





Alberto Arnedo Ruiz

To facilitate the understanding of each group, the naming is done based on their location in the bridge rather than the construction stage that they are intended to be erected. For girder, groups are defined as "GAB" where:

- G = Girder element
- A = Digit referring to the girder number
- B = Digit referring to the girder piece

Frame elements and plate elements are then tabulated and assigned a group based on the digits referring to their girder number and girder piece. For the top flange frame elements and plate elements, the first digit is 0, therefore the elements with IDs "ABXXXXXX" are assigned to group "GAB". For the bottom flame elements with IDs "1ABXXXXXX", the same group assignment is performed.

In the case of the cross frames, groups defined as "DABCE" are defined, where:

- D = Cross frame element (diaphragm)
- A = Digit referring to lower number girder that it connects
- B = Digit referring to higher number girder that it connects
- CD = Digits referring to number of cross frames along girder length

For example, D2305 refers to the 5th cross frame from the bridge start between girders 2 and 3.

3.7.2. Loading stages

Once the groups are defined, the construction stages are easy to define. On one level, the stages that account for the inclusion of each new bridge section and temporary bridge support are added. For each stage, a load case including the wind load in each direction perpendicular to the bridge layout line is analyzed. To include the possible second-order effects due to the lateral loads, a non-linear large displacement analysis is performed.





Alberto Arnedo Ruiz

4. CASE STUDY

A curved bridge is modeled using the methodology described in chapter 3 to show as example. For the purpose of this study, the software SAP2000 will be used, although tables can be modified to adapt to the preferred software. The bridge is based on a design example provided by AISC [15].

The bridge is a 3 span continuous curved bridge, 530 feet long, and 40.5ft wide. The cross section consists of 4 I-girders with 11 feet spacing in between them. The bridge is symmetrical with respect to the mis-span of span 2. Each girder has a total of 4 field splices, resulting in 5 separate sections per girder, and 20 for the whole bridge. The cross frames are equally spaced between bearing supports.

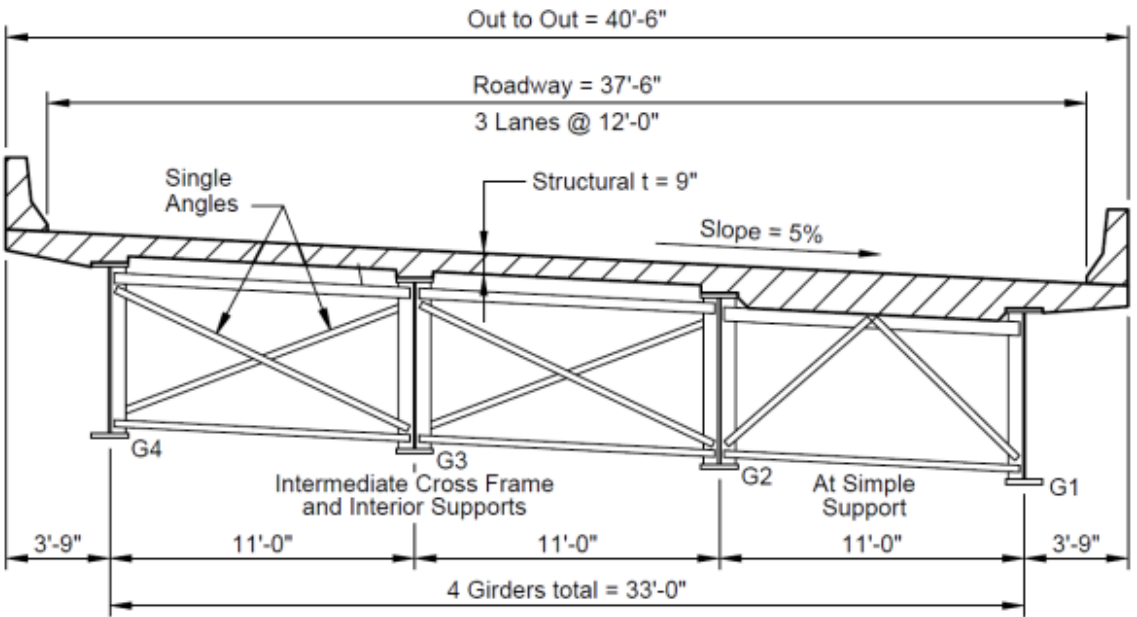


Figure 22. Typical Bridge Cross-Section [15]

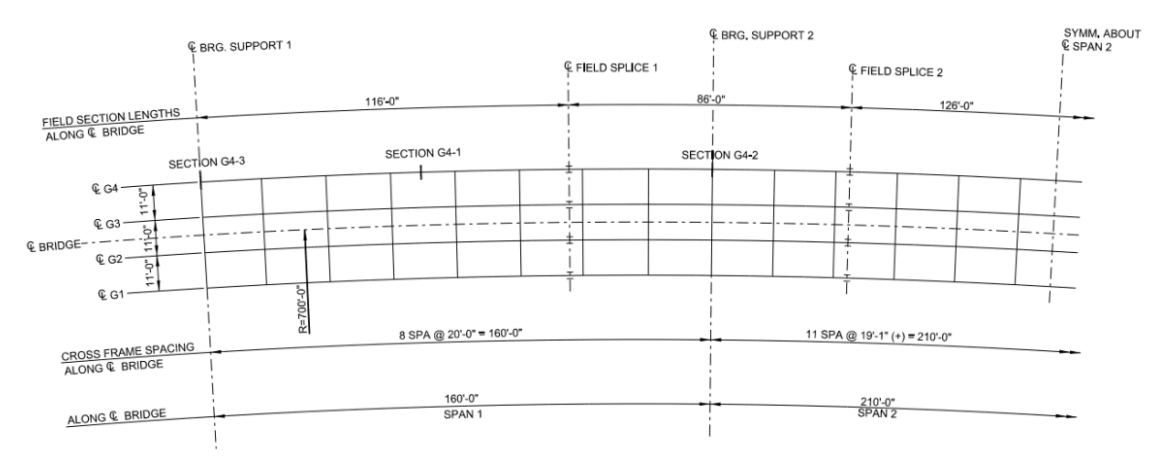


Figure 23. Framing plan [15]





Alberto Arnedo Ruiz

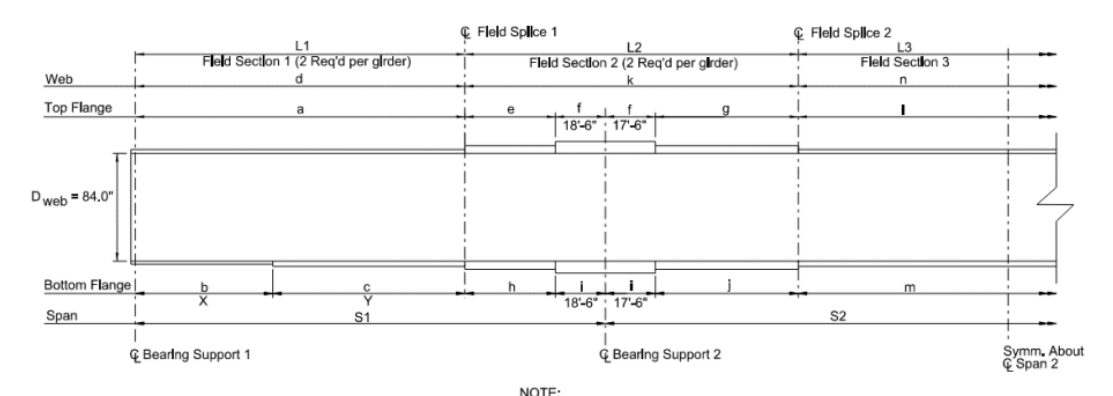


Figure 24. Girder elevation [15]

Member Sizes (Shown in Inches)

	а	b	С	d	е	f	g	h		j	k		m	n
G1	16X1	n/a	16X1	84x9/16	21x1.25	21x2.5	21x1.25	21x1.50	21x3	21x1.50	84x5/8	18X1	18X1	84x9/16
G2	18X1	n/a	18X1	84x9/16	18x1.25	18x2.5	18x1.25	19x1.50	19x3	19x1.50	84x5/8	18X1	18X1	84x9/16
G3	18X1	n/a	18X1	84x9/16	20x1.25	20x2.5	20x1.25	21x1.50	21x3	21x1.50	84x5/8	18X1	20X1	84x9/16
G4	20X1	21X1	21X1,625	84x9/16	28x1.25	28x2.5	28x1.25	27x1.50	27x3	27x1.50	84x5/8	20X1	21X1.5	84x9/16

Table 4. Member sizes [15]

Dimensions (Shown in feet)

	L1	L2	L3	S1	S2	X	Υ
G1	113.0	84.0	123.0	156.2	205.1	0	113.3
G2	115.1	85.3	125.0	158.7	208.4	0	115.1
G3	116.9	86.7	127.0	161.3	211.7	0	116.9
G4	118.7	88.0	129.0	163.8	215.0	33.0	85.7

Table 5. Relevant dimensions [15]

The end spans have 4 different section properties, while the interior span has 3. Relevant dimensions and member sizes are shown in Figure 24, Table 4 and Table 5.

4.1. Geometry definition

First the layout line is defined:

	Element number	Element	Station Start (ft)		Curve Direction	Radius (ft)	Bearing	Northing	Easting
ſ	1	Curve	0	530	Right (Clockwise)	700	0.379	0	0

Table 6. Layout definition table

The yellow cells refer to input values by the user.

Then we define the girder work point points, which separate each individual piece. For a continuous girder, it will define the location of the bearings at the end abutments and all the splice plates. See Table 7, Table 8, Table 9, and Table 10 for definition. Joint coordinates with their ID numbers are uploaded to the FEA software. See Figure 25 for isometric representation.

Girder work points definition (2 of 4)





Alberto Arnedo Ruiz

	Location	Station along alignment	Station Definition (Girder n x 10000) + station	Offset	Curve Type	Curve Direction	Radius Before	Radius After
WP	Girder	Static				O		
		ft		ft			ft	ft
1	1	0.00	10000.00	16.5	Curve	Right (Clockwise)	-	683.50
2	1	116.00	10113.27	16.5	Curve	Right (Clockwise)	683.50	683.50
3	1	202.00	10197.24	16.5	Curve	Right (Clockwise)	683.50	683.50
4	1	328.00	10320.27	16.5	Curve	Right (Clockwise)	683.50	683.50
5	1	414.00	10404.24	16.5	Curve	Right (Clockwise)	683.50	683.50
6	1	530.00	10517.51	16.5	Straight	-	683.50	683.50
1	2	0.00	20000.00	5.5	Curve	Right (Clockwise)	-	694.50
2	2	116.00	20115.09	5.5	Curve	Right (Clockwise)	694.50	694.50
3	2	202.00	20200.41	5.5	Curve	Right (Clockwise)	694.50	694.50
4	2	328.00	20325.42	5.5	Curve	Right (Clockwise)	694.50	694.50
5	2	414.00	20410.75	5.5	Curve	Right (Clockwise)	694.50	694.50
6	2	530.00	20525.84	5.5	Straight	-	694.50	694.50
1	3	0.00	30000.00	-5.5	Curve	Right (Clockwise)	-	705.50
2	3	116.00	30116.91	-5.5	Curve	Right (Clockwise)	705.50	705.50
3	3	202.00	30203.59	-5.5	Curve	Right (Clockwise)	705.50	705.50
4	3	328.00	30330.58	-5.5	Curve	Right (Clockwise)	705.50	705.50
5	3	414.00	30417.25	-5.5	Curve	Right (Clockwise)	705.50	705.50
6	3	530.00	30534.16	-5.5	Straight	-	705.50	705.50
1	4	0.00	40000.00	-16.5	Curve	Right (Clockwise)	-	716.50
2	4	116.00	40118.73	-16.5	Curve	Right (Clockwise)	716.50	716.50
3	4	202.00	40206.76	-16.5	Curve	Right (Clockwise)	716.50	716.50
4	4	328.00	40335.73	-16.5	Curve	Right (Clockwise)	716.50	716.50
5	4	414.00	40423.76	-16.5	Curve	Right (Clockwise)	716.50	716.50
6	4	530.00	40542.49	-16.5	Straight	-	716.50	716.50

Table 7. Girder work points definition (1 of 4)

The grey values refer to automatically calculated values depending on the inputs based on the methodology explained in section 3.3.





	Location	Layout element number	Element type	Station start	Curve Direction	Radius	Bearing (Start curve)	Bearing (WP)	Bearing (WP)
WP	Girder	Layout	П	S	Cul		Beari	B	B
						ft	radians	radians	degrees
1	1	1	Curve	0	Right (Clockwise)	700	0.379	0.3786	21.69
2	1	1	Curve	0	Right (Clockwise)	700	0.379	0.213	12.20
3	1	1	Curve	0	Right (Clockwise)	700	0.379	0.090	5.16
4	1	1	Curve	0	Right (Clockwise)	700	0.379	-0.090	-5.16
5	1	1	Curve	0	Right (Clockwise)	700	0.379	-0.213	-12.20
6	1	2	Straight	530	-	Infinite	-0.379	-0.3786	-21.69
1	2	1	Curve	0	Right (Clockwise)	700	0.379	0.379	21.69
2	2	1	Curve	0	Right (Clockwise)	700	0.379	0.213	12.20
3	2	1	Curve	0	Right (Clockwise)	700	0.379	0.090	5.16
4	2	1	Curve	0	Right (Clockwise)	700	0.379	-0.090	-5.16
5	2	1	Curve	0	Right (Clockwise)	700	0.379	-0.213	-12.20
6	2	2	Straight	530	•	Infinite	-0.379	-0.379	-21.69
1	3	1	Curve	0	Right (Clockwise)	700	0.379	0.379	21.69
2	3	1	Curve	0	Right (Clockwise)	700	0.379	0.213	12.20
3	3	1	Curve	0	Right (Clockwise)	700	0.379	0.090	5.16
4	3	1	Curve	0	Right (Clockwise)	700	0.379	-0.090	-5.16
5	3	1	Curve	0	Right (Clockwise)	700	0.379	-0.213	-12.20
6	3	2	Straight	530	-	Infinite	-0.379	-0.379	-21.69
1	4	1	Curve	0	Right (Clockwise)	700	0.379	0.379	21.69
2	4	1	Curve	0	Right (Clockwise)	700	0.379	0.213	12.20
3	4	1	Curve	0	Right (Clockwise)	700	0.379	0.090	5.16
4	4	1	Curve	0	Right (Clockwise)	700	0.379	-0.090	-5.16
5	4	1	Curve	0	Right (Clockwise)	700	0.379	-0.213	-12.20
6	4	2	Straight	530	-	Infinite	-0.379	-0.379	-21.69

Table 8. Girder work points definition (2 of 4)





	Location	Start curve	coordinate	Theta (Angle to layout element start) - radians	Increment in tangent direction	Increment in perpendicular to tangent	alpha (angle with tangent) - radians	Angle to layout element start point (radians)	Layout	coordinate
WP	Girder	x	Υ	Theta elemer	Х	ОХ	alpł tang	Angle t	Х	Y
		ft	ft	radians	ft	ft	radians	radians	ft	ft
1	1	0.0000	0.0000	0.00	0.00	0.00	0.00	0.38	0.00	0.00
2	1	0.0000	0.0000	0.17	115.47	9.59	0.08	0.30	110.84	33.77
3	1	0.0000	0.0000	0.29	199.21	28.94	0.14	0.23	195.80	46.73
4	1	0.0000	0.0000	0.47	316.13	75.45	0.23	0.14	321.63	46.73
5	1	0.0000	0.0000	0.59	390.28	118.90	0.30	0.08	406.59	33.77
6	1	517.4308	0.0000	0.00	0.00	0.00	0.00	-0.38	517.43	0.00
1	2	0.0000	0.0000	0.00	0.00	0.00	0.00	0.38	0.00	0.00
2	2	0.0000	0.0000	0.17	115.47	9.59	0.08	0.30	110.84	33.77
3	2	0.0000	0.0000	0.29	199.21	28.94	0.14	0.23	195.80	46.73
4	2	0.0000	0.0000	0.47	316.13	75.45	0.23	0.14	321.63	46.73
5	2	0.0000	0.0000	0.59	390.28	118.90	0.30	0.08	406.59	33.77
6	2	517.4308	0.0000	0.00	0.00	0.00	0.00	-0.38	517.43	0.00
1	3	0.0000	0.0000	0.00	0.00	0.00	0.00	0.38	0.00	0.00
2	3	0.0000	0.0000	0.17	115.47	9.59	0.08	0.30	110.84	33.77
3	3	0.0000	0.0000	0.29	199.21	28.94	0.14	0.23	195.80	46.73
4	3	0.0000	0.0000	0.47	316.13	75.45	0.23	0.14	321.63	46.73
5	3	0.0000	0.0000	0.59	390.28	118.90	0.30	0.08	406.59	33.77
6	3	517.4308	0.0000	0.00	0.00	0.00	0.00	-0.38	517.43	0.00
1	4	0.0000	0.0000	0.00	0.00	0.00	0.00	0.38	0.00	0.00
2	4	0.0000	0.0000	0.17	115.47	9.59	0.08	0.30	110.84	33.77
3	4	0.0000	0.0000	0.29	199.21	28.94	0.14	0.23	195.80	46.73
4	4	0.0000	0.0000	0.47	316.13	75.45	0.23	0.14	321.63	46.73
5	4	0.0000	0.0000	0.59	390.28	118.90	0.30	0.08	406.59	33.77
6	4	517.4308	0.0000	0.00	0.00	0.00	0.00	-0.3786	517.43	0.00

Table 9. Girder work points definition (3 of 4)





Alberto Arnedo Ruiz

	Location	Coordinates at	girder	Joint Number (Bottom Flange)	Joint number (Top Flange)	
WP	Girder	X	Y			
		ft	ft			
1	1	6.10	-15.33	1100000	11100000	
2	1	114.32	17.64	1200000	11200000	
3	1	197.28	30.30	1300000	11300000	
4	1	320.15	30.30	1400000	11400000	
5	1	403.11	17.64	1500000	11500000	
6	1	511.33	-15.33	1600000	11600000	
1	2	2.03	-5.11	2100000	12100000	
2	2	112.00	28.39	2200000	12200000	
3	2	196.29	41.25	2300000	12300000	
4	2	321.14	41.25	2400000	12400000	
5	2	405.43	28.39	2500000	12500000	
6	2	515.40	-5.11	2600000	12600000	
1	3	-2.03	5.11	3100000	13100000	
2	3	109.68	39.14	3200000	13200000	
3	3	195.31	52.21	3300000	13300000	
4	3	322.12	52.21	3400000	13400000	
5	3	407.75	39.14	3500000	13500000	
6	3	519.46	5.11	3600000	13600000	
1	4	-6.10	15.33	4100000	14100000	
2	4 107.35		49.89	4200000	14200000	
3	4 194.32		63.16	4300000	14300000	
4	4	323.11	63.16	4400000	14400000	
5	4	410.08	49.89	4500000	14500000	
6	4	523.53	15.33	4600000	14600000	

Table 10. Girder work points definition (4 of 4)

The columns highlighted in green provide the calculated plan view coordinates of the points as well as the joint numbers based on the nomenclature explained in section 3.1.

To facilitate the visualization, we assign the girder work points to one visualization group and assign them a color. This feature is typical across all FEA software.

The following points to represent are the diaphragms. See Table 11, Table 12, and Table 13 for definition. Only the coordinates for girder 1 are shown for clarity. See Figure 26 for graphical representation. Now that the cross frames work points are in the model, the cross frames can be easily manually added. See Figure 27 for graphical representation.





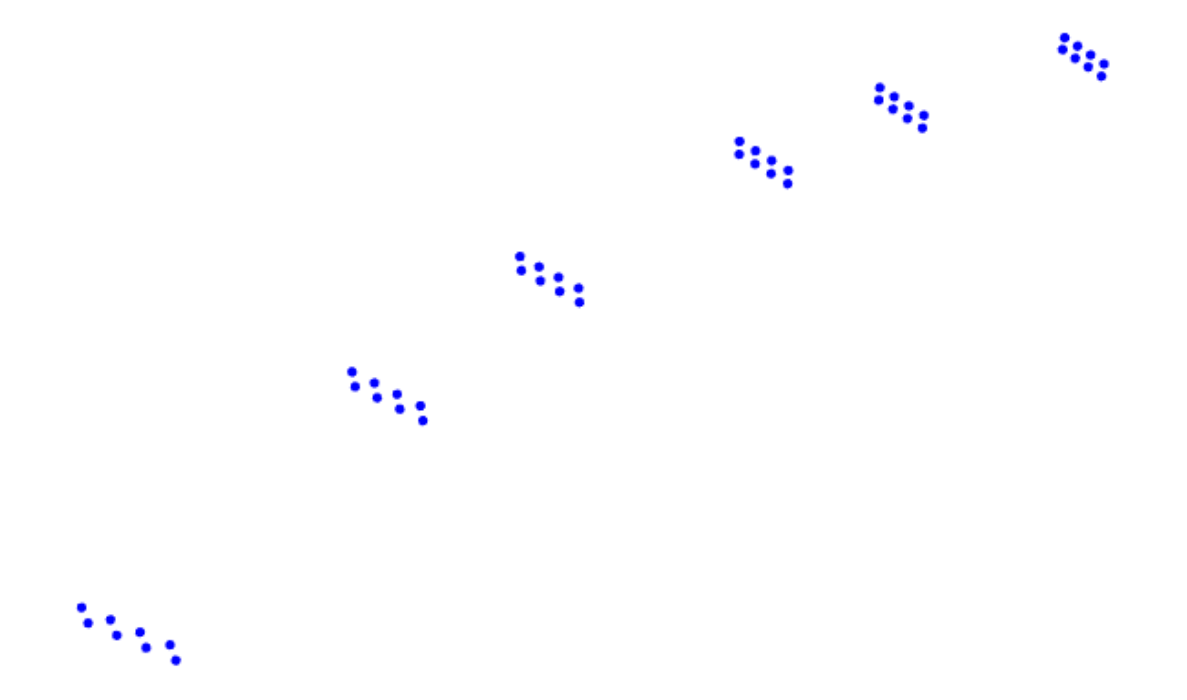


Figure 25. Isometric view of girder work points.

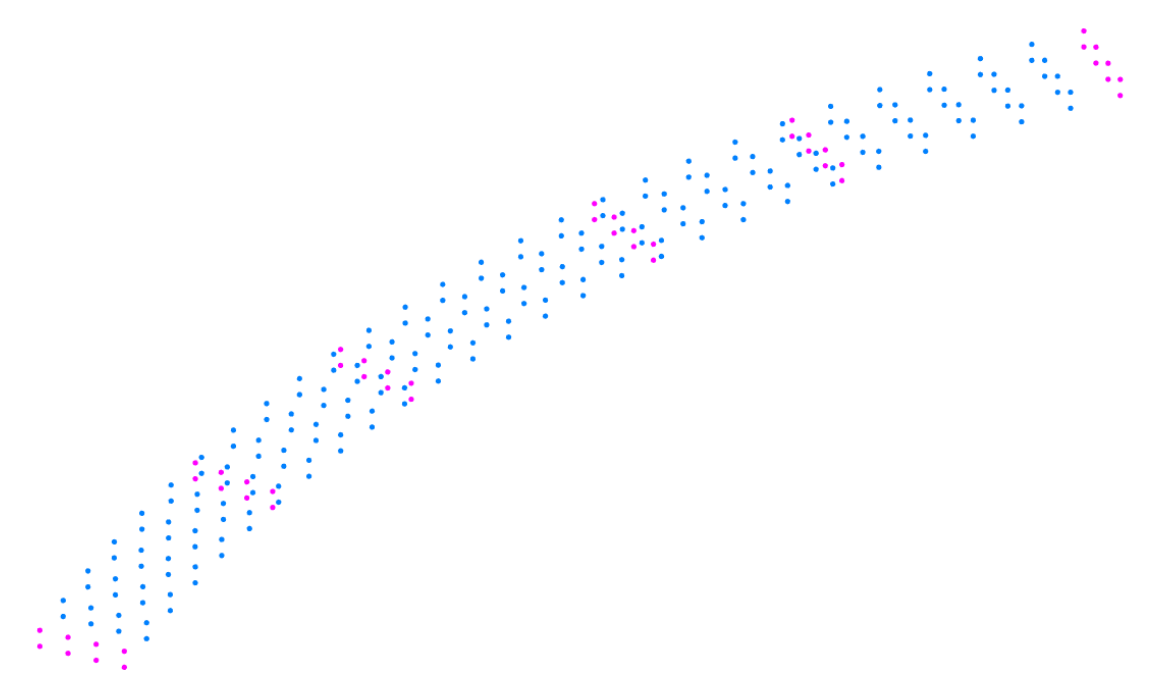


Figure 26. Isometric view of girder and cross frames work points





Girder	ft Station	: Offset	Diaphragm number along girder	Layout element number	Element type	Station start	Curve Direction	Radius	Bearing (Start curve)	Bering (WP)	Bering (WP)
1		#	1	1	Comme		Dialat (Claralussian)	ft	rad	rad	deg
1	0.00	16.50	1	1	Curve	0	Right (Clockwise)	700	0.38	0.379	21.69
1	20.00	16.50	2	1	Curve	0	Right (Clockwise)	700	0.38	0.350	20.05
1	40.00	16.50	3	1	Curve	0	Right (Clockwise)	700	0.38	0.321	18.42
1	60.00	16.50	4 5	1	Curve	0	Right (Clockwise)	700	0.38	0.293	16.78
1	80.00	16.50		1	Curve	0	Right (Clockwise)	700	0.38	0.264	15.14
1	100.00	16.50	6	1	Curve	0	Right (Clockwise)	700	0.38	0.236	13.51 11.87
1	140.00	16.50 16.50	2	1 1	Curve	0	Right (Clockwise)	700	0.38	0.207	10.23
1	160.00	16.50	3	1	Curve Curve	0	Right (Clockwise) Right (Clockwise)	700	0.38	0.179	8.59
1	179.09	16.50	4	1	Curve	0		700	0.38	0.130	7.03
1	198.18	16.50	1	1	Curve	0	Right (Clockwise) Right (Clockwise)	700	0.38	0.123	5.47
1	217.27	16.50	2	1	Curve	0	Right (Clockwise)	700	0.38	0.068	3.91
1	236.36	16.50	3	1	Curve	0	Right (Clockwise)	700	0.38	0.041	2.34
1	255.45	16.50	4	1	Curve	0	Right (Clockwise)	700	0.38	0.014	0.78
1	274.55	16.50	5	1	Curve	0	Right (Clockwise)	700	0.38	-0.014	-0.78
1	293.64	16.50	6	1	Curve	0	Right (Clockwise)	700	0.38	-0.041	-2.34
1	312.73	16.50	7	1	Curve	0	Right (Clockwise)	700	0.38	-0.068	-3.91
1	331.82	16.50	1	1	Curve	0	Right (Clockwise)	700	0.38	-0.095	-5.47
1	350.91	16.50	2	1	Curve	0	Right (Clockwise)	700	0.38	-0.123	-7.03
1	370.00	16.50	3	1	Curve	0	Right (Clockwise)	700	0.38	-0.150	-8.59
1	390.00	16.50	4	1	Curve	0	Right (Clockwise)	700	0.38	-0.179	-10.23
1	410.00	16.50	1	1	Curve	0	Right (Clockwise)	700	0.38	-0.207	-11.87
1	430.00	16.50	2	1	Curve	0	Right (Clockwise)	700	0.38	-0.236	-13.51
1	450.00	16.50	3	1	Curve	0	Right (Clockwise)	700	0.38	-0.264	-15.14
1	470.00	16.50	4	1	Curve	0	Right (Clockwise)	700	0.38	-0.293	-16.78
1	490.00	16.50	5	1	Curve	0	Right (Clockwise)	700	0.38	-0.321	-18.42
1	510.00	16.50	6	1	Curve	0	Right (Clockwise)	700	0.38	-0.350	-20.05
	530.00	16.50	1	1	Curve	0	Right (Clockwise)	700	0.38	-0.379	-21.69

Table 11. Diaphragm work points geometry (1 of 3)





Girder	Station	Station		Theta (Angle to layout element start) - radians	Increment in tangent direction	Increment in perpendicular to tangent	alpha (angle with tangent) - radians	Angle to layout element start point (radians)	l avout coordinate	
			Υ	e	X	OX	alp	Ā	Х	Υ
	ft	ft	ft	radians	ft	ft	radians	radians	ft	ft
1	0.00	0.0000	0.0000	0.00	0.00	0.00	0.00	0.38	0.00	0.00
1	20.00	0.0000	0.0000	0.03	20.00	0.29	0.01	0.36	18.69	7.13
1	40.00	0.0000	0.0000	0.06	39.98	1.14	0.03	0.35	37.57	13.71
1	60.00	0.0000	0.0000	0.09	59.93	2.57	0.04	0.34	56.63	19.76
1	80.00	0.0000	0.0000	0.11	79.83	4.57	0.06	0.32	75.86	25.26
1	100.00	0.0000	0.0000	0.14	99.66	7.13	0.07	0.31	95.24	30.21
1	120.00	0.0000	0.0000	0.17	119.41	10.26	0.09	0.29	114.75	34.60
1	140.00	0.0000	0.0000	0.20	139.07	13.95	0.10	0.28	134.38	38.43
1	160.00	0.0000	0.0000	0.23	158.61	18.21	0.11	0.26	154.11	41.70
1	179.09	0.0000	0.0000	0.26	177.14	22.78	0.13	0.25	173.02	44.30
1	198.18	0.0000	0.0000	0.28	195.54	27.87	0.14	0.24	192.00	46.38
1	217.27	0.0000	0.0000	0.31	213.80	33.45	0.16	0.22	211.03	47.94
1	236.36	0.0000	0.0000	0.34	231.90	39.53	0.17	0.21	230.09	48.98
1	255.45	0.0000	0.0000	0.36	249.82	46.10	0.18	0.20	249.17	49.50
1	274.55	0.0000	0.0000	0.39	267.56	53.15	0.20	0.18	268.26	49.50
1	293.64	0.0000	0.0000	0.42	285.10	60.69	0.21	0.17	287.34	48.98
1	312.73	0.0000	0.0000	0.45	302.43	68.70	0.22	0.16	306.41	47.94
1	331.82	0.0000	0.0000	0.47	319.53	77.18	0.24	0.14	325.43	46.38
1	350.91	0.0000	0.0000	0.50	336.40	86.13	0.25	0.13	344.41	44.30
1	370.00	0.0000	0.0000	0.53	353.01	95.53	0.26	0.11	363.32	41.70
1	390.00	0.0000	0.0000	0.56	370.13	105.86	0.28	0.10	383.05	38.43
1	410.00	0.0000	0.0000	0.59	386.96	116.68	0.29	0.09	402.68	34.60
1	430.00	0.0000	0.0000	0.61	403.46	127.97	0.31	0.07	422.19	30.21
1	450.00	0.0000	0.0000	0.64	419.64	139.73	0.32	0.06	441.57	25.26
1	470.00	0.0000	0.0000	0.67	435.47	151.95	0.34	0.04	460.80	19.76
1	490.00	0.0000	0.0000	0.70	450.95	164.61	0.35	0.03	479.86	13.71
1	510.00	0.0000	0.0000	0.73	466.06	177.71	0.36	0.01	498.74	7.13
1	530.00	0.0000	0.0000	0.76	480.79	191.24	0.38	0.00	517.43	0.00

Table 12. Diaphragm work points geometry (2 of 3)





Girder	Station	th x Coordinates at girder		Key Name	Girder segment location	Section definition	Joint Number (Top Flange)	Joint Number (Bottom Flange)
	ft		ft		9		Joi	ſ
1	0.00	6.10	-15.33	G1D0	1	10000.00	1110000	11110000
1	20.00	24.34	-8.37	G1D1	1	10020.00	1120000	11120000
1	40.00	42.78	-1.94	G1D2	1	10040.00	1130000	11130000
1	60.00	61.40	3.96	G1D3	1	10060.00	1140000	11140000
1	80.00	80.17	9.33	G1D4	1	10080.00	1150000	11150000
1	100.00	99.09	14.16	G1D5	1	10100.00	1160000	11160000
1	120.00	118.14	18.45	G1D0	2	10120.00	1210000	11210000
1	140.00	137.31	22.20	G1D1	2	10140.00	1220000	11220000
1	160.00	156.57	25.39	G1D2	2	10160.00	1230000	11230000
1	179.09	175.04	27.92	G1D3	2	10179.09	1240000	11240000
1	198.18	193.57	29.95	G1D0	3	10198.18	1310000	11250000
1	217.27	212.15	31.48	G1D1	3	10217.27	1320000	11310000
1	236.36	230.76	32.49	G1D2	3	10236.36	1330000	11320000
1	255.45	249.40	33.00	G1D3	3	10255.45	1340000	11330000
1	274.55	268.04	33.00	G1D4	3	10274.55	1350000	11340000
1	293.64	286.67	32.49	G1D5	3	10293.64	1360000	11350000
1	312.73	305.28	31.48	G1D6	3	10312.73	1370000	11360000
1	331.82	323.86	29.95	G1D0	4	10331.82	1410000	11410000
1	350.91	342.39	27.92	G1D1	4	10350.91	1420000	11420000
1	370.00	360.86	25.39	G1D2	4	10370.00	1430000	11430000
1	390.00	380.12	22.20	G1D3	4	10390.00	1440000	11440000
1	410.00	399.29	18.45	G1D0	5	10410.00	1510000	11450000
1	430.00		14.16	G1D1	5	10430.00	1520000	11510000
1	450.00		9.33	G1D2	5	10450.00	1530000	11520000
1	470.00	456.03	3.96	G1D3	5	10470.00	1540000	11530000
1	490.00	474.65	-1.94	G1D4	5	10490.00	1550000	11540000
1	510.00	493.09	-8.37	G1D5	5	10510.00	1560000	11550000
1	530.00	511.33	-15.33	G1D0	6	10530.00	1610000	11610000

Table 13. Diaphragm work points geometry (3 of 3)





Alberto Arnedo Ruiz

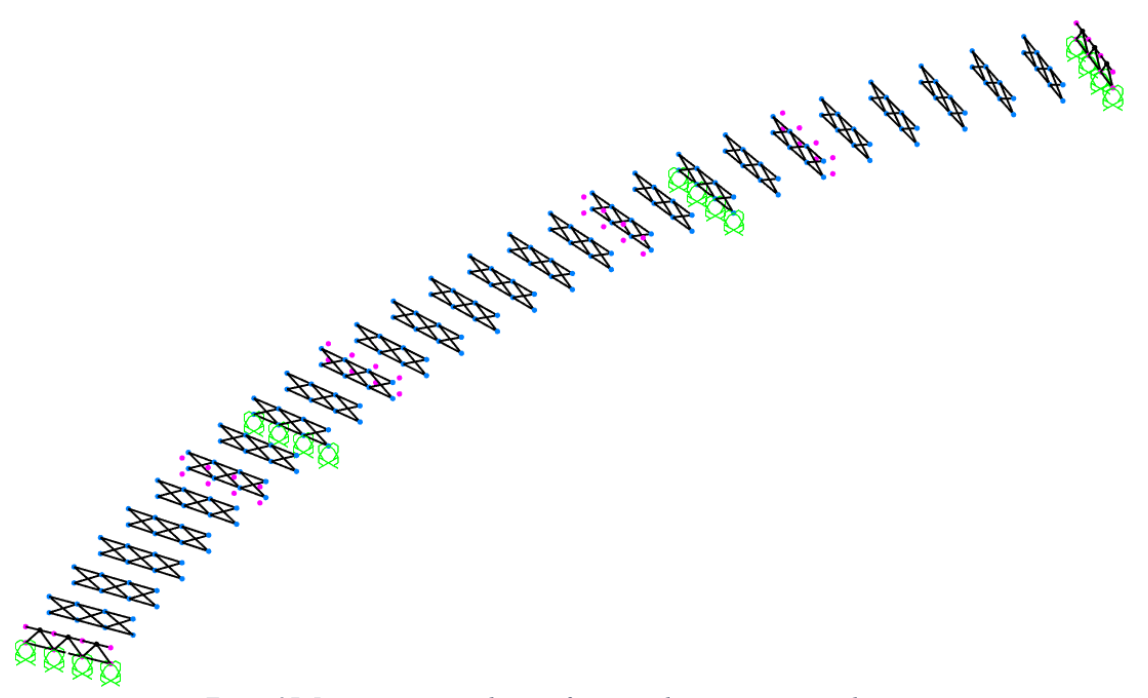


Figure 27. Isometric view with cross frames and permanent vertical supports

In addition to the cross frames, the vertical boundary conditions from the piers and abutments can be defined. Only the vertical direction is fixed since the longitudinal and transversal direction will be restrained through temporary structures. See Figure 27 for permanent vertical restrains. In a final stability analysis study, the supports from the shoring towers needs to studied and verified to confirm the assumption of an absolute pin is acceptable, especially in the transverse direction. A spring with the lateral stiffness of the shoring tower may be used, or the actual shoring tower elements can be included in the FEA model.

The next step is loading the joints where the section properties of the girder change. See Table 14, Table 15, and Table 16 for work points. Only the coordinates for girders 1 and 2 are shown. Due to insufficient significant figures in the dimensions provided in Table 5, some joints need to be removed due to misplacement along the girder. In Figure 28, the pink joints represent the end of one girder section, or the location of the field splice. The section changes coincide with the end of the girder, but due to the insufficient number of significant figures provided, the joint for the section change appears slightly moved. Delete prior to continuing with the model.





Alberto Arnedo Ruiz



Figure 28. Error due to lack of significant figures in plans

Section	Girder	Length along girder (WP)	Length along layout line	Station Definition	Layout element number	Element type	Length along girder (start point)	Curve Direction	Radius	Bearing (Start curve)
		ft					ft		ft	radians
1	1	0.0	0.0	10000	1	Curve	0.00	Right (Clockwise)	683.5	0.379
2	1	113.0	115.7	10113	1	Curve	0.00	Right (Clockwise)	683.5	0.379
3	1	137.7	141.0	10137.7	1	Curve	113.27	Right (Clockwise)	683.5	0.213
4	1	173.7	177.9	10173.7	1	Curve	113.27	Right (Clockwise)	683.5	0.213
5	1	197.0	201.8	10197	1	Curve	113.27	Right (Clockwise)	683.5	0.213
6	1	320.0	327.7	10320	1	Curve	197.24	Right (Clockwise)	683.5	0.090
7	1	343.3	351.6	10343.3	1	Curve	320.27	Right (Clockwise)	683.5	-0.090
8	1	379.3	388.5	10379.3	1	Curve	320.27	Right (Clockwise)	683.5	-0.090
9	1	404.0	413.8	10404	1	Curve	320.27	Right (Clockwise)	683.5	-0.090
10	1	517.0	529.5	10517	1	Curve	404.24	Right (Clockwise)	683.5	-0.213
1	2	0.0	0.0	20000	1	Curve	0.00	Right (Clockwise)	694.5	0.379
2	2	115.1	116.0	20115.1	1	Curve	115.09	Right (Clockwise)	694.5	0.213
3	2	140.2	141.3	20140.2	1	Curve	115.09	Right (Clockwise)	694.5	0.213
4	2	176.2	177.6	20176.2	1	Curve	115.09	Right (Clockwise)	694.5	0.213
5	2	200.4	202.0	20200.4	1	Curve	115.09	Right (Clockwise)	694.5	0.213
6	2	325.4	328.0	20325.4	1	Curve	200.41	Right (Clockwise)	694.5	0.090
7	2	349.6	352.4	20349.6	1	Curve	325.42	Right (Clockwise)	694.5	-0.090
8	2	385.6	388.7	20385.6	1	Curve	325.42	Right (Clockwise)	694.5	-0.090
9	2	410.7	414.0	20410.7	1	Curve	325.42	Right (Clockwise)	694.5	-0.090
10	2	525.8	530.0	20525.8	1	Curve	410.75	Right (Clockwise)	694.5	-0.213

Table 14. Girder section changes work points (1 of 3)





Section	Girder	Length along girder (WP)	Bering (WP)	Bering (WP)	Start curve	coordinate	Theta (Angle to layout element start - radians	Increment in tangent direction	n be
				4	X	Y		X	OX
	_	ft	radians	degrees	ft	ft	radians	ft	ft
1	1	0.0	0.38	21.69	6.10	-15.33	0.00	0.00	0.00
2	1	113.0	0.21	12.22	6.10	-15.33	0.17	112.49	9.32
3	1	137.7	0.18	10.15	114.32	17.64	0.04	24.43	0.44
4	1	173.7	0.12	7.13	114.32	17.64	0.09	60.36	2.67
5	1	197.0	0.09	5.18	114.32	17.64	0.12	83.52	5.12
6	1	320.0	-0.09	-5.13	197.28	30.30	0.18	122.10	10.99
7	1	343.3	-0.12	-7.09	320.15	30.30	0.03	23.03	0.39
8	1	379.3	-0.18	-10.11	320.15	30.30	0.09	58.96	2.55
9	1	404.0	-0.21	-12.18	320.15	30.30	0.12	83.52	5.12
10	1	517.0	-0.38	-21.65	403.11	17.64	0.16	112.25	9.28
1	2	0.0	0.38	21.69	2.03	-5.11	0.00	0.00	0.00
2	2	115.1	0.21	12.19	112.00	28.39	0.00	0.01	0.00
3	2	140.2	0.18	10.12	112.00	28.39	0.04	25.11	0.45
4	2	176.2	0.12	7.15	112.00	28.39	0.09	61.03	2.69
5	2	200.4	0.09	5.16	112.00	28.39	0.12	85.10	5.23
6	2	325.4	-0.09	-5.15	196.29	41.25	0.18	124.31	11.22
7	2	349.6	-0.12	-7.15	321.14	41.25	0.03	24.17	0.42
8	2	385.6	-0.18	-10.12	321.14	41.25	0.09	60.10	2.61
9	2	410.7	-0.21	-12.19	321.14	41.25	0.12	85.06	5.23
10	2	525.8	-0.38	-21.69	405.43	28.39	0.17	114.53	9.51

Table 15. Girder section changes work points (2 of 3)





Alberto Arnedo Ruiz

Section	Girder	Length along girder (WP)	alpha (angle with tangent) - radians	Angle to layout element start point (radians)	Coordinate at girder		Joint Number (Top flange)	Joint number (Bottom flange)
		ft	radians	ਾadians	ft	ft	γ	
		11	Taulalis	Taulalis	11	11		
1	1	0.0	0.00	0.38	6.10	- 15.33	1111000	11111000
2	1	113.0	0.08	0.30	114.06	17.58	1161000	11161000
3	1	137.7	0.02	0.19	138.29	22.37	1221000	11221000
4	1	173.7	0.04	0.17	173.88	27.78	1231000	11231000
5	1	197.0	0.06	0.15	197.05	30.28	1251000	11251000
6	1	320.0	0.09	0.00	319.88	30.32	1361000	11361000
7	1	343.3	0.02	-0.11	343.05	27.84	1421000	11421000
8	1	379.3	0.04	-0.13	378.64	22.46	1431000	11431000
9	1	404.0	0.06	-0.15	402.87	17.69	1451000	11451000
10	1	517.0	0.08	-0.30	510.86	- 15.14	1551000	11551000
1	2	0.0	0.00	0.38	2.03	-5.11	2111000	12111000
2	2	115.1	0.00	0.21	112.01	28.39	2161000	12161000
3	2	140.2	0.02	0.19	136.64	33.25	2221000	12221000
4	2	176.2	0.04	0.17	172.22	38.66	2231000	12231000
5	2	200.4	0.06	0.15	196.28	41.25	2251000	12251000
6	2	325.4	0.09	0.00	321.11	41.26	2361000	12361000
7	2	349.6	0.02	-0.11	345.17	38.66	2421000	12421000
8	2	385.6	0.04	-0.13	380.76	33.26	2431000	12431000
9	2	410.7	0.06	-0.15	405.38	28.40	2451000	12451000
10	2	525.8	0.08	-0.30	515.36	-5.10	2551000	12551000

Table 16. Girder section changes work points (3 od 3)

Finally, the mesh that defines all the joints is defined. For this example, the maximum mesh size has been selected for a plate aspect ratio of 5 to 1 with a total of 4 vertical subdivisions. Since the vertical subdivisions are done in already existing straight plate elements, these can be done in the post-process model creation built in SAP2000. See Table 17, Table 18, and Table 19, for work points. Only the first portion of mesh points of girder 1 is shown. See Figure 29. Isometric view with mesh points Figure 29 for graphical representation.





Alberto Arnedo Ruiz

Girder	Length along girder (WP)	Station Definition	Layout element number	Element type	Length along girder (start point)	Curve Direction	Radius	Bearing (Start curve)	Bering (WP)
	ft				ft		ft	radians	radians
1	0.0	10000.00	1	Curve	0.00	Right (Clockwise)	683.5	0.38	0.38
1	8.6	10008.62	1	Curve	0.00	Right (Clockwise)	683.5	0.38	0.37
1	17.2	10017.23	1	Curve	0.00	Right (Clockwise)	683.5	0.38	0.35
1	25.9	10025.85	1	Curve	0.00	Right (Clockwise)	683.5	0.38	0.34
1	34.5	10034.47	1	Curve	0.00	Right (Clockwise)	683.5	0.38	0.33
1	43.1	10043.08	1	Curve	0.00	Right (Clockwise)	683.5	0.38	0.32
1	51.7	10051.70	1	Curve	0.00	Right (Clockwise)	683.5	0.38	0.30
1	60.3	10060.32	1	Curve	0.00	Right (Clockwise)	683.5	0.38	0.29
1	68.9	10068.93	1	Curve	0.00	Right (Clockwise)	683.5	0.38	0.28
1	77.6	10077.55	1	Curve	0.00	Right (Clockwise)	683.5	0.38	0.27
1	86.2	10086.17	1	Curve	0.00	Right (Clockwise)	683.5	0.38	0.25
1	94.8	10094.78	1	Curve	0.00	Right (Clockwise)	683.5	0.38	0.24
1	103.4	10103.40	1	Curve	0.00	Right (Clockwise)	683.5	0.38	0.23
1	112.0	10112.02	1	Curve	0.00	Right (Clockwise)	683.5	0.38	0.21
1	120.6	10120.63	1	Curve	113.27	Right (Clockwise)	683.5	0.21	0.20
1	129.3	10129.25	1	Curve	113.27	Right (Clockwise)	683.5	0.21	0.19
1	137.9	10137.87	1	Curve	113.27	Right (Clockwise)	683.5	0.21	0.18
1	146.5	10146.48	1	Curve	113.27	Right (Clockwise)	683.5	0.21	0.16
1	155.1	10155.10	1	Curve	113.27	Right (Clockwise)	683.5	0.21	0.15
1	163.7	10163.72	1	Curve	113.27	Right (Clockwise)	683.5	0.21	0.14
1	172.3	10172.33	1	Curve	113.27	Right (Clockwise)	683.5	0.21	0.13
1	181.0	10180.95	1	Curve	113.27	Right (Clockwise)	683.5	0.21	0.11
1	189.6	10189.57	1	Curve	113.27	Right (Clockwise)	683.5	0.21	0.10
1	198.2	10198.18	1	Curve	197.24	Right (Clockwise)	683.5	0.09	0.09
1	206.8	10206.80	1	Curve	197.24	Right (Clockwise)	683.5	0.09	0.08
1	215.4	10215.42	1	Curve	197.24	Right (Clockwise)	683.5	0.09	0.06
1	224.0	10224.03	1	Curve	197.24	Right (Clockwise)	683.5	0.09	0.05

Table 17. Mesh work points (1 of 3)





Alberto Arnedo Ruiz

Girder	Length along girder (WP)	Bering (WP)	× Start curve	coordinate <	Theta (Angle to layout element start - radians	Increment in tangent direction	Increment in perpendicular to tangent	alpha (angle with tangent) - radians	Angle to layout element start point (radians)
	ft	degrees	ft	ft	radians	ft	ft	radians	radians
1	0.0	21.69	6.10	-15.33	0.00	0.00	0.00	0.00	0.38
1	8.6	20.97	6.10	-15.33	0.01	8.62	0.05	0.01	0.37
1	17.2	20.25	6.10	-15.33	0.03	17.23	0.22	0.01	0.37
1	25.9	19.52	6.10	-15.33	0.04	25.84	0.49	0.02	0.36
1	34.5	18.80	6.10	-15.33	0.05	34.45	0.87	0.03	0.35
1	43.1	18.08	6.10	-15.33	0.06	43.05	1.36	0.03	0.35
1	51.7	17.36	6.10	-15.33	0.08	51.65	1.95	0.04	0.34
1	60.3	16.63	6.10	-15.33	0.09	60.24	2.66	0.04	0.33
1	68.9	15.91	6.10	-15.33	0.10	68.82	3.47	0.05	0.33
1	77.6	15.19	6.10	-15.33	0.11	77.38	4.39	0.06	0.32
1	86.2	14.47	6.10	-15.33	0.13	85.94	5.42	0.06	0.32
1	94.8	13.75	6.10	-15.33	0.14	94.48	6.56	0.07	0.31
1	103.4	13.02	6.10	-15.33	0.15	103.01	7.81	0.08	0.30
1	112.0	12.30	6.10	-15.33	0.16	111.52	9.16	0.08	0.30
1	120.6	11.58	114.32	17.64	0.01	7.37	0.04	0.01	0.21
1	129.3	10.86	114.32	17.64	0.02	15.98	0.19	0.01	0.20
1	137.9	10.13	114.32	17.64	0.04	24.60	0.44	0.02	0.19
1	146.5	9.41	114.32	17.64	0.05	33.20	0.81	0.02	0.19
1	155.1	8.69	114.32	17.64	0.06	41.81	1.28	0.03	0.18
1	163.7	7.97	114.32	17.64	0.07	50.41	1.86	0.04	0.18
1	172.3	7.24	114.32	17.64	0.09	58.99	2.55	0.04	0.17
1	181.0	6.52	114.32	17.64	0.10	67.57	3.35	0.05	0.16
1	189.6	5.80	114.32	17.64	0.11	76.14	4.25	0.06	0.16
1	198.2	5.08	197.28	30.30	0.00	0.94	0.00	0.00	0.09
1	206.8	4.36	197.28	30.30	0.01	9.56	0.07	0.01	0.08
1	215.4	3.63	197.28	30.30	0.03	18.18	0.24	0.01	0.08
1	224.0	2.91	197.28	30.30	0.04	26.79	0.53	0.02	0.07

Table 18. Mesh work points (2 of 3)





Girder	Length along girder (WP)	× Coordinate at	girder	Joint number (top flange)	Joint number (bottom flange)
	ft)r	
1		ft	ft	1111001	11111001
1	0.0	6.10	-15.33	1111001	11111001
1	8.6	14.12	-12.20	1111002	11111002
1	17.2	22.19	-9.16	1111003	11111003
1	25.9	30.29	-6.23	1120001	11120001
1	34.5	38.43	-3.41	1120002	11120002
1	43.1	46.61	-0.68	1130001	11130001
1	51.7	54.81	1.94	1130002	11130002
1	60.3	63.05	4.46	1140001	11140001
1	68.9	71.33	6.88	1140002	11140002
1	77.6	79.63	9.19	1140003	11140003
1	86.2	87.96	11.39	1150001	11150001
1	94.8	96.31	13.49	1150002	11150002
1	103.4	104.70	15.49	1161001	11161001
1	112.0	113.10	17.37	1161002	11161002
1	120.6	121.53	19.16	1210001	11210001
1	129.3	129.99	20.83	1210002	11210002
1	137.9	138.46	22.40	1221001	11221001
1	146.5	146.95	23.86	1221002	11221002
1	155.1	155.46	25.22	1221003	11221003
1	163.7	163.98	26.47	1231001	11231001
1	172.3	172.53	27.61	1231002	11231002
1	181.0	181.08	28.64	1240001	11240001
1	189.6	189.65	29.57	1240002	11240002
1	198.2	198.22	30.38	1251001	11251001
1	206.8	206.81	31.09	1251002	11251002
1	215.4	215.41	31.69	1310001	11310001
1	224.0	224.01	32.18	1310002	11310002

Table 19. Mesh work points (3 of 3)





Alberto Arnedo Ruiz

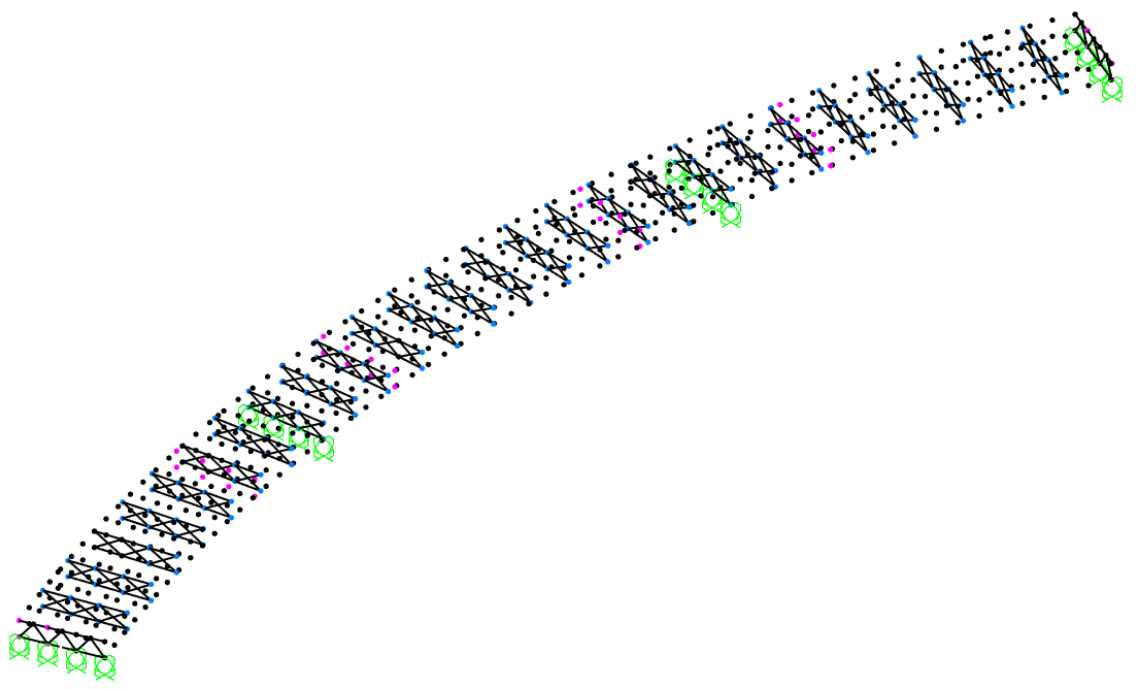


Figure 29. Isometric view with mesh points

With this section, all the joints of the model have now been added. The next step is to add the flange and web members. The joints are selected from the model and reorganized. See Figure 30 for isometric view, Table 20 for partial view of frame elements definition table, and Table 21 for partial view of the area elements definition table

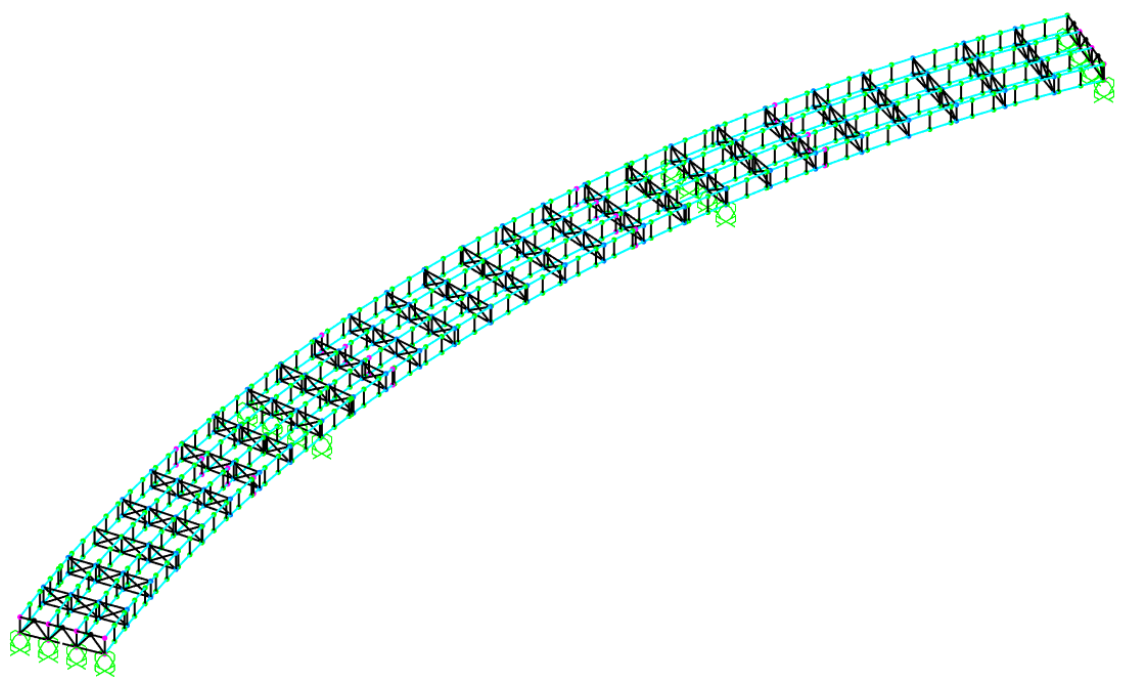


Figure 30. Isometric view with web plates and flanges





Alberto Arnedo Ruiz

Frame	Jointl	JointJ
1100000	1100000	1111002
1111002	1111002	1111003
1111003	1111003	1120000
1120000	1120000	1120001
1120001	1120001	1120002
1120002	1120002	1130000
1130000	1130000	1130001
1130001	1130001	1130002
1130002	1130002	1140000
1140000	1140000	1140001
1140001	1140001	1140002
1140002	1140002	1140003
1140003	1140003	1150000
1150000	1150000	1150001
1150001	1150001	1150002
1150002	1150002	1160000
1160000	1160000	1161001
1161001	1161001	1161002
1161002	1161002	1200000
1200000	1200000	1210000
1210000	1210000	1210001
1210001	1210001	1210002
1210002	1210002	1220000

Table 20. Frame elements definition table

As shown in Figure 31 area labels are defined in a sequential manner, with lower numbers within each girder towards the start station of the bridge, and higher numbers within each girder towards the end station of the bridge.

For the purpose of this case study, the weight of splices and stiffeners have not been included in the analysis due to the lack of information available and objectives of this thesis. In a final stability analysis model, the stiffeners will provide additional transverse stiffness to the girder webs at the cross frame locations, and the splice weight will increase the stress and deformations at the cantilever sections of the bridge during the different construction stages.





Area	Joint1	Joint2	Joint3	Joint4
1111001	1111001	1111002	11111002	11111001
1111002	1111002	1111003	11111003	11111002
1111003	1111003	1120000	11120000	11111003
1120000	1120000	1120001	11120001	11120000
1120001	1120001	1120002	11120002	11120001
1120002	1120002	1130000	11130000	11120002
1130000	1130000	1130001	11130001	11130000
1130001	1130001	1130002	11130002	11130001
1130002	1130002	1140000	11140000	11130002
1140000	1140000	1140001	11140001	11140000
1140001	1140001	1140002	11140002	11140001
1140002	1140002	1140003	11140003	11140002
1140003	1140003	1150000	11150000	11140003
1150000	1150000	1150001	11150001	11150000
1150001	1150001	1150002	11150002	11150001
1150002	1150002	1160000	11160000	11150002
1160000	1160000	1160001	11160001	11160000
1160001	1160001	1160002	11160002	11160001
1160002	1160002	1200000	11200000	11160002
1200000	1200000	1210000	11210000	11200000
1210000	1210000	1210001	11210001	11210000
1210001	1210001	1210002	11210002	11210001
1210002	1210002	1220000	11220000	11210002
1220000	1220000	1221000	11221000	11220000
1221000	1221000	1221001	11221001	11221000
1221001	1221001	1221002	11221002	11221001
1221002	1221002	1221003	11221003	11221002
1221003	1221003	1230000	11230000	11221003

Table 21. Area elements definition





Alberto Arnedo Ruiz

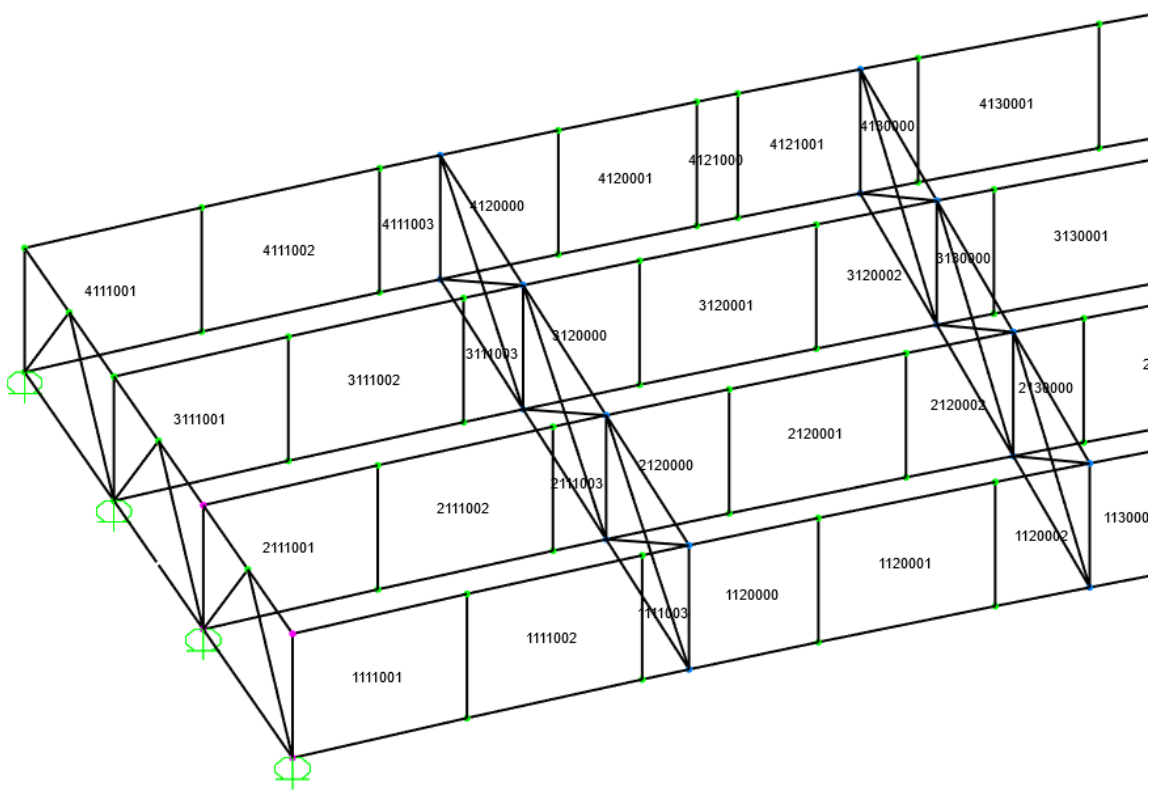


Figure 31. Zommed in model with area labels

4.2. Section properties assignment

The girder section properties are now assigned to the model. As discussed in section 3.5, this is done based on the plate elements second ID digit. A section type is then assigned to each girder section in which the plate falls under. Table 22 shows a portion of the web definitions with the table used to assign section properties based on the girder section.

Plate ID	Section	Girder Section
1111001	d	1
1111002	d	1
1111003	d	1
1120000	d	1
1120001	d	1
1120002	d	1
1130000	d	1
1130001	d	1
1130002	d	1

Girder	Assigned
Section	Section
1	d
2	k
3	n
4	k
5	d

Table 22. Web section definition





Alberto Arnedo Ruiz

In the case of the frame elements section properties are tabulated based on the dimensions given in Table 5 (see Table 23 and Table 24 for partial results). The frame elements are then tabulated (see Table 25) and, since they share their ID number with the first joint ID number, a section property is assigned based on the position of the ID number.

Joint	Flange Section Type	Flange Section	Girder number
1100000	а	a1	1
1200000	е	e1	1
1221000	f	f1	1
1231000	g	g1	1
1300000	I	l1	1
1400000	g	g1	1
1421000	f	f1	1
1431000	е	e1	1
1500000	а	a1	1
2100000	а	a2	2
2200000	е	e2	2
2221000	f	f2	2
2231000	g	g2	2

Table 23. Section properties at girder and section change work points (top flange)

Joint	Flange Section Type	Flange Section	Girder number
11100000	С	c1	1
11200000	h	h1	1
11221000	i	i1	1
11231000	j	j1	1
11300000	m	m1	1
11400000	j	j1	1
11421000	i	i1	1
11431000	h	h1	1
11500000	С	c1	1
12100000	С	c2	2
12200000	h	h2	2
12221000	i	i2	2
12231000	j	j2	2
12300000	m	m2	2

Table 24. Section properties at girder and section change work points (bottom flange)





Alberto Arnedo Ruiz

Frame	Section
1300002	l1
1310000	l1
1310001	l1
1310002	l1
1320000	l1
1320001	l1
1320002	l1
1330000	l1
1330001	l1
1330002	l1

Table 25. Frame section properties assignment

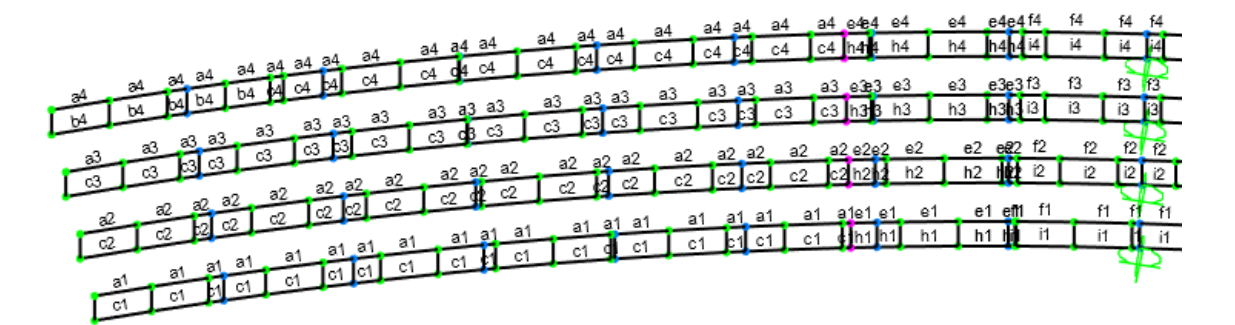


Figure 32. Frame section labels on 1st span

Lastly, an eccentricity needs to be given to the frame elements to adjust them in the real position. The joins in the model represent the top and bottom of the girder web, therefore, an eccentricity of half the flange thickness must be given in opposite directions to each flange. FEA software deals with this parameter in different ways and is out of the scope of this thesis. However, the selection of the top flange frames versus bottom flange frames is facilitated by the fact that the top flange plates have 7 digits, and the bottom flange 8, making it easier to select each flange members separately.

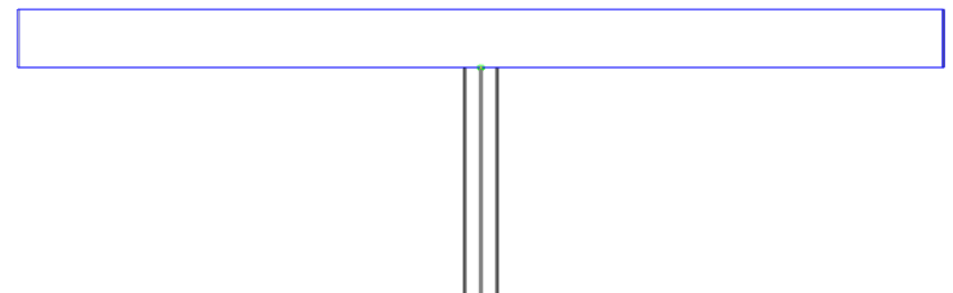


Figure 33. Extruded representation of girder web and top flange





Alberto Arnedo Ruiz

Alternatively, the joints could be defined at the centerline of the flanges. Although the additional dead located in the intersection between the model web plate and flanges is not significant, the elevation of the points along the length of the girder would vary and add one level of complexity to the modeling process.

4.3. Load assignment

In addition to the dead load, wind load is assigned to the girder webs. Since wind loads will vary depending on the governing local codes and is not the focus of this thesis, just the value and a summary of the load combinations is provided in this section. Wind load is per AASHTO Guide Specifications for Wind Lodas on Bridges During Construction [16]. The resulting design wind pressure for inactive work zone is 35 psf. A reduction factor of 0 is used for the second girder windward, and 0.25 is used for the third and fourth girder windward. Only load in one direction is considered for the purpose of the case study.

4.4. Construction stages

To define the construction stages, frame and plate elements of the model need to be assigned to specific groups. Groups are defined as using the elements ID numbers as explained in section 3.7.1. See Table 26 for group assignment partial table as example. Figure 34 shows the defined groups based on their color. Figure is for visual representation only since some colors repeat. See appendix for full group definition tables.

TABLE: Groups 2 - Assignments				
GroupName	ObjectType	ObjectLabel		
G11	Joint	1100000		
G11	Joint	11100000		
G11	Joint	1130000		
G12	Joint	1200000		
G12	Joint	11200000		
G12	Joint	1210000		
G12	Joint	1220000		
G13	Joint	1300000		
G13	Joint	1310000		
G13	Joint	1320000		
G14	Frame	1400000		
G14	Frame	1410000		
G14	Frame	1410001		
G14	Frame	1410002		
G21	Area	2111001		
G21	Area	2111003		
G21	Area	2120000		

Table 26. Group assignments





Alberto Arnedo Ruiz

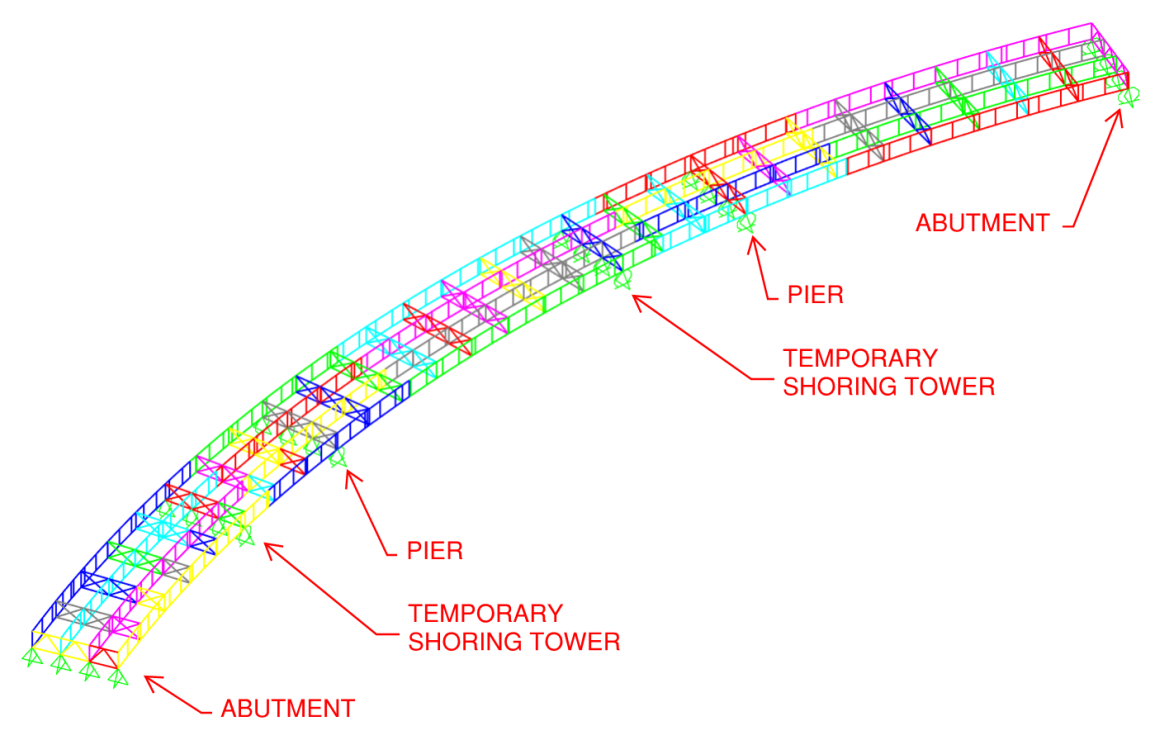


Figure 34. Model groups and support definitions

A set of two shoring towers are used for the proposed erection sequence. Figure 34 shows each vertical support. The first shoring tower is at the first span, to support the first girder section being erected. The second shoring tower is at the second span, to support the third girder section. The are located at the cross frame closer to the girder section end to minimize the temporary cantilever length.

For the purpose of this exercise, it is assumed that a keeper angle or other lateral restraining element is used at all the girders vertical supports. In addition, a longitudinal restrain is placed in bearings at the start abutment. Longitudinal restrain may also be achieved in the field with some keeper angles in the girder end, and are mostly for incidental loads only.

The general construction sequence selected goes as follows:

- Lift middle two girder for the first section as a girder pair with all cross frames in between.
- Lift girder 4 with the cross frames between girders 3 and 4.
- Lift girder 1 with the cross frames between girder 1 and 2.
- Repeat for the following sections in the same order.

Figure 35 through Figure 49 shows the graphical representation of the bridge at each proposed stage.





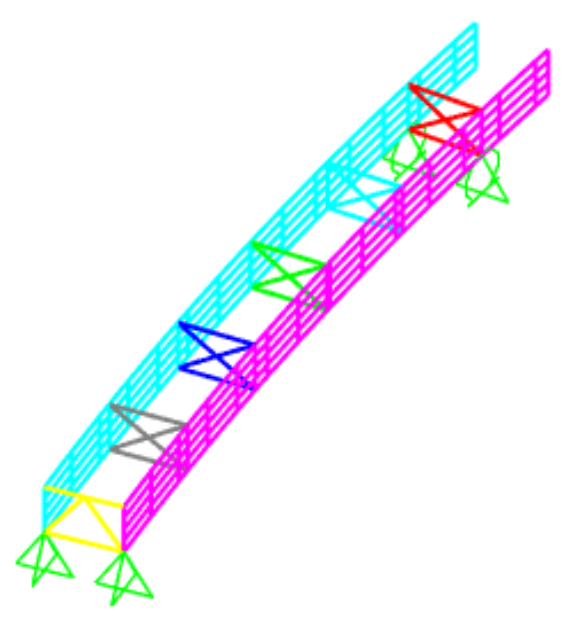


Figure 35. Stage 1.1 model

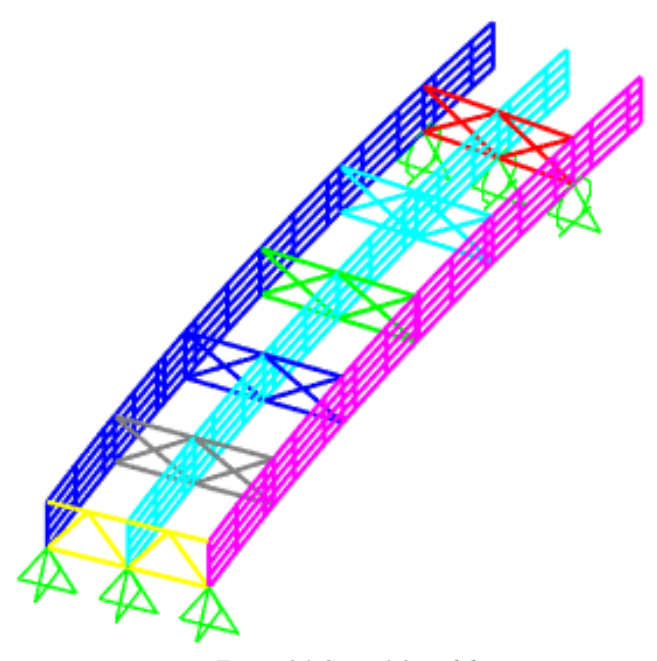


Figure 36. Stage 1.2 model





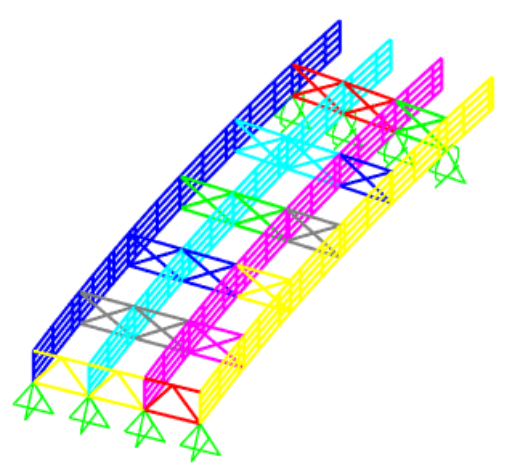


Figure 37. Stage 1.3 model

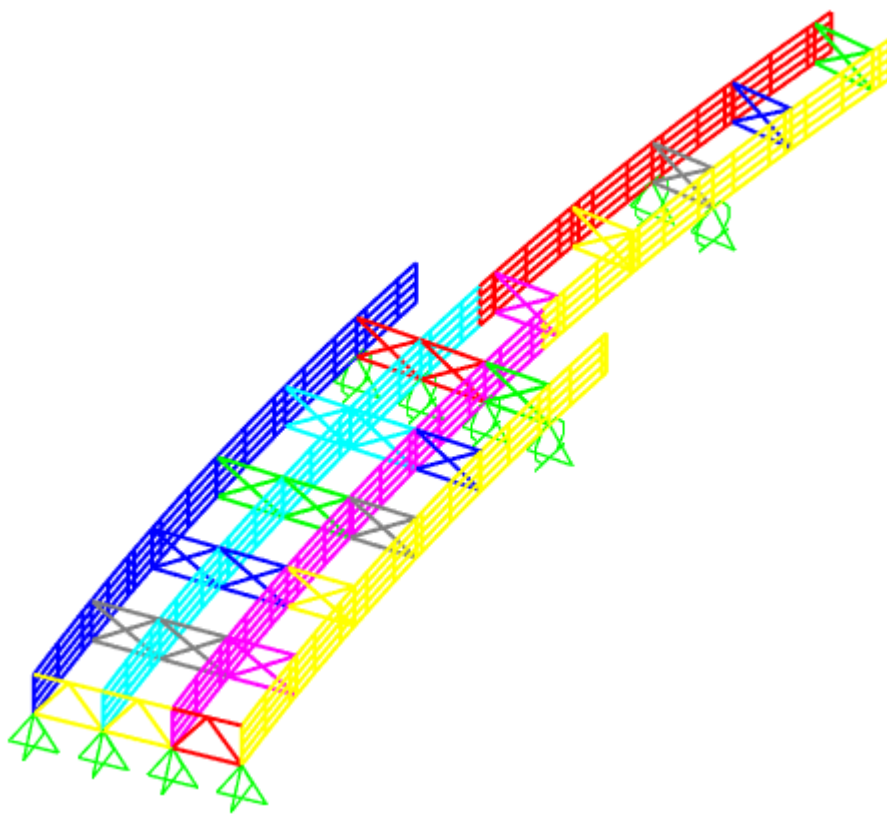


Figure 38. Stage 2.1 model





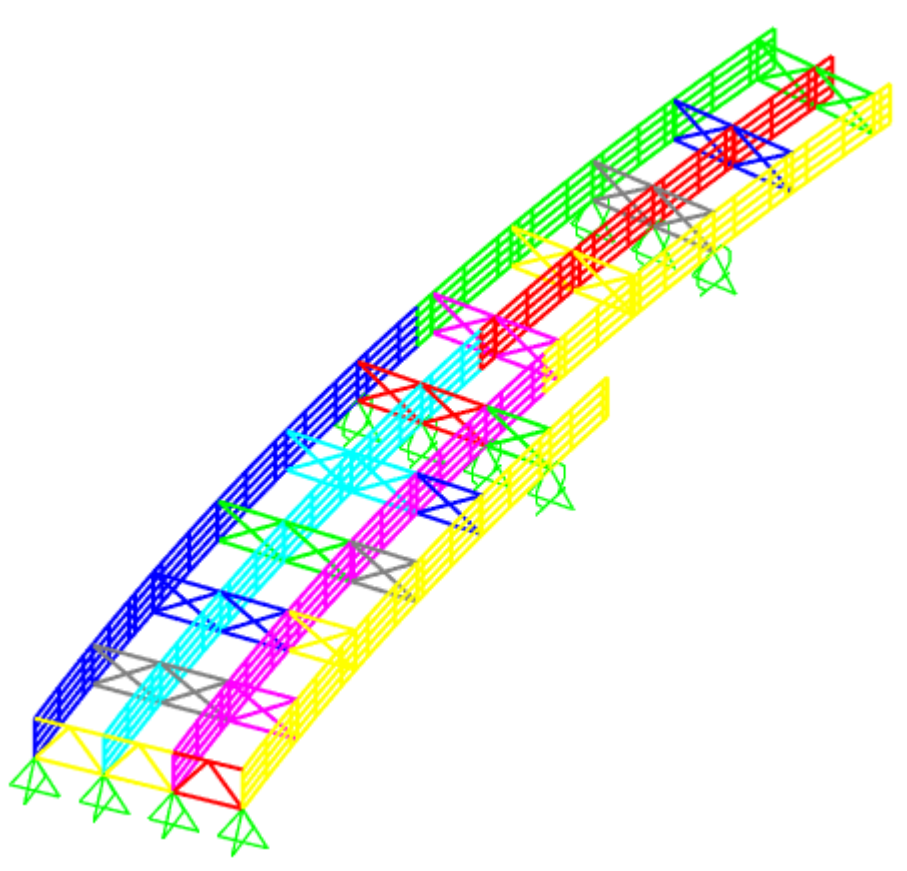


Figure 39. Stage 2.2 model

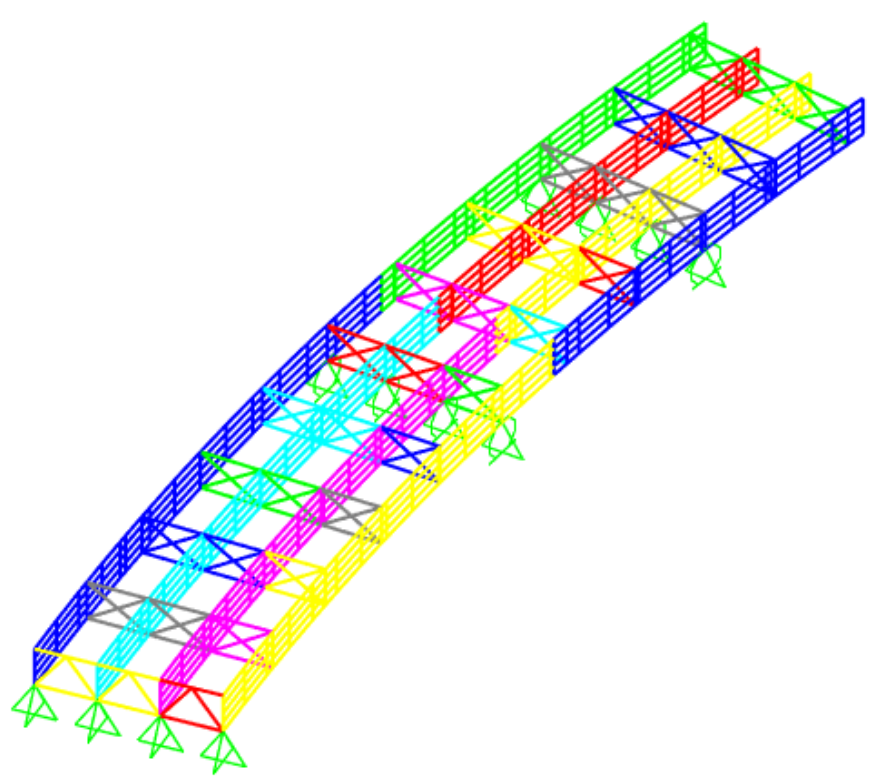


Figure 40. Stage 2.3 model





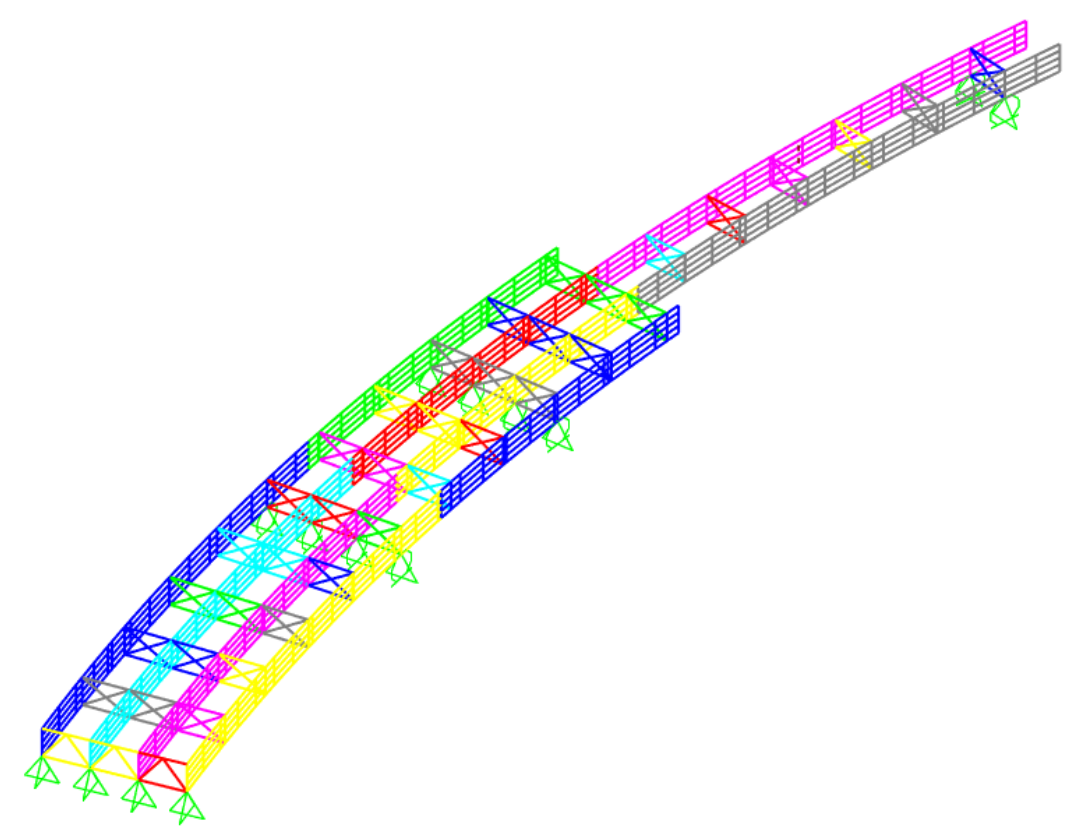


Figure 41. Stage 3.1 model

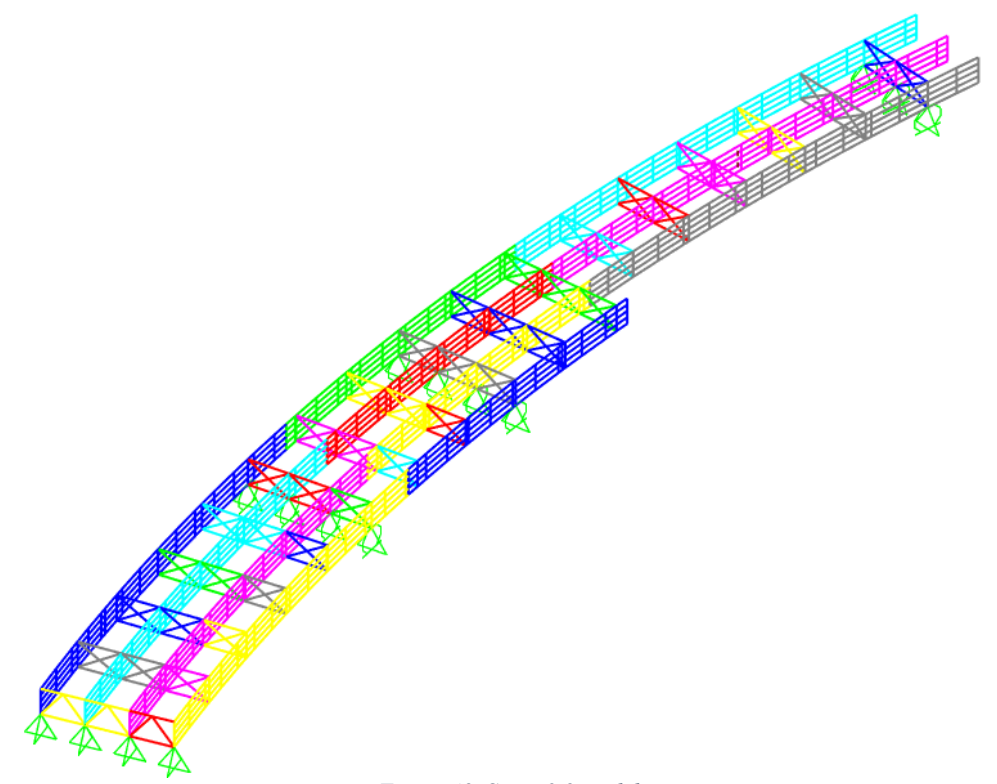


Figure 42. Stage 3.2 model





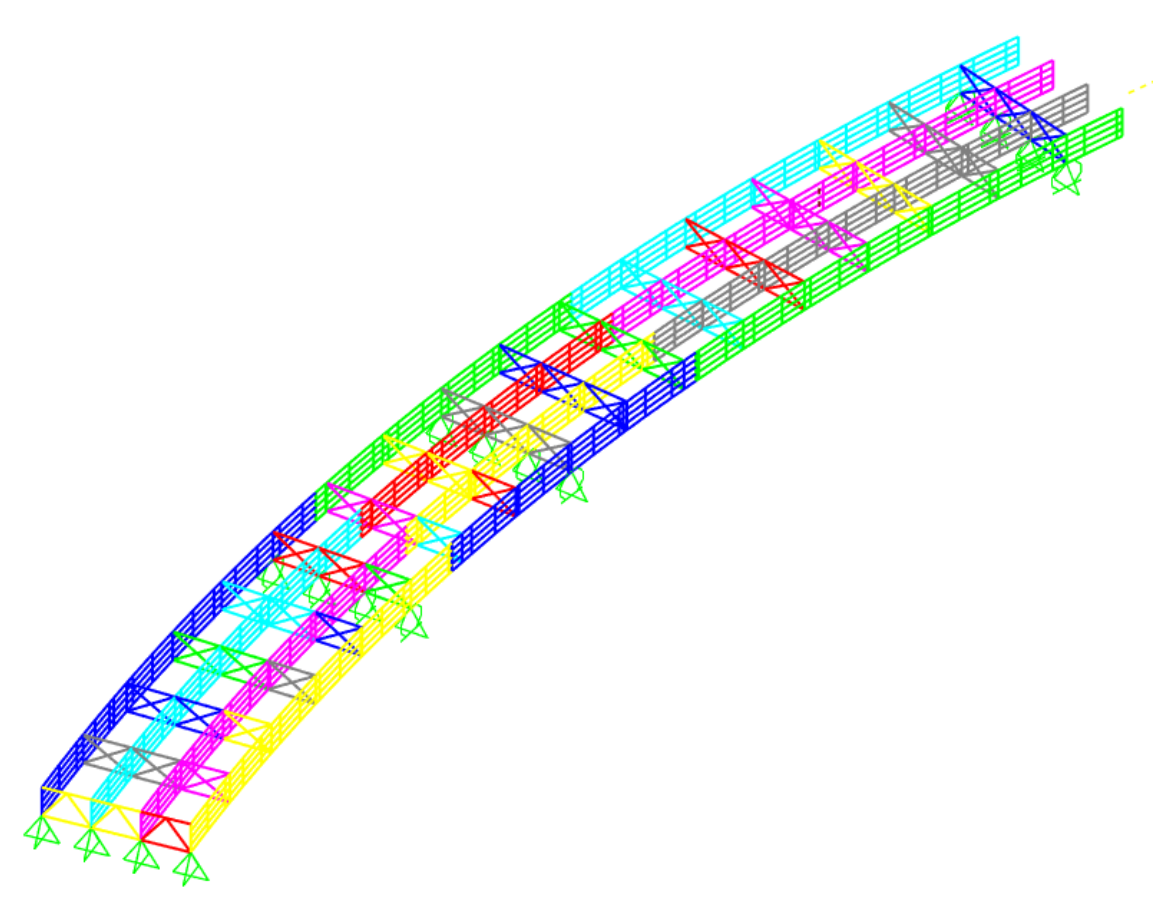


Figure 43. Stage 3.3 model

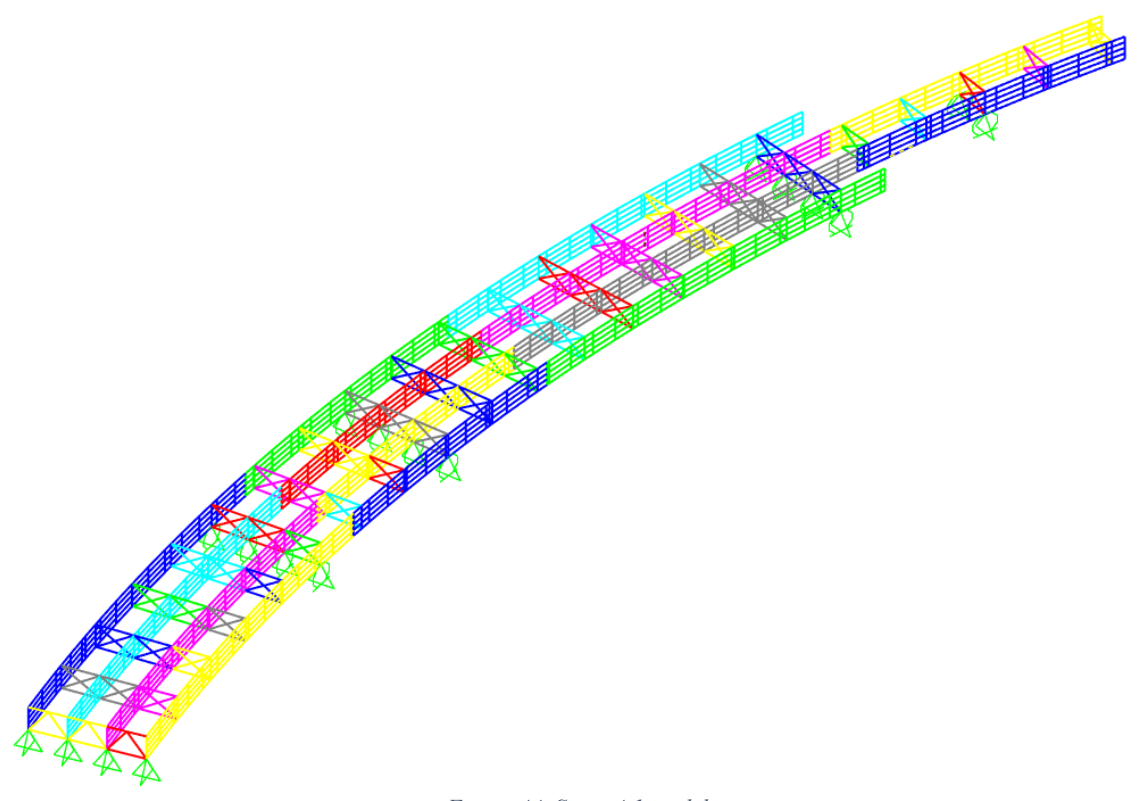


Figure 44. Stage 4.1 model





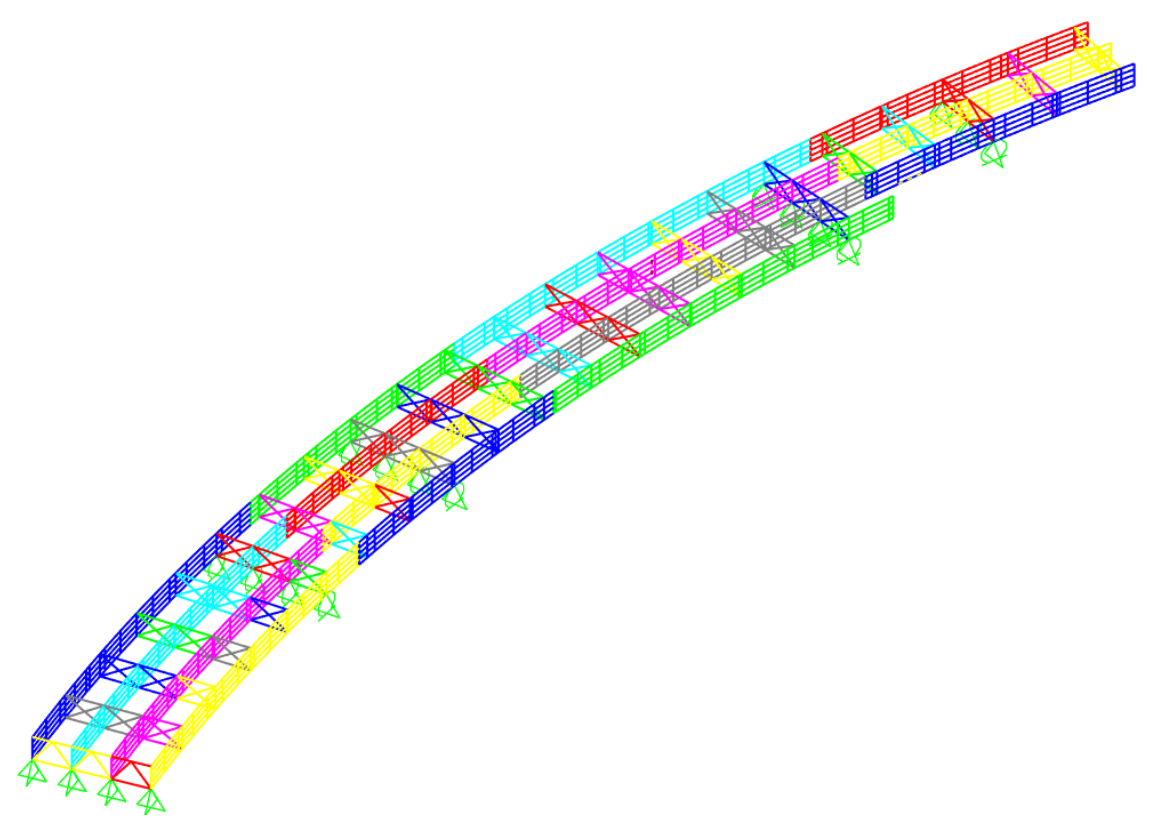


Figure 45. Stage 4.2 model

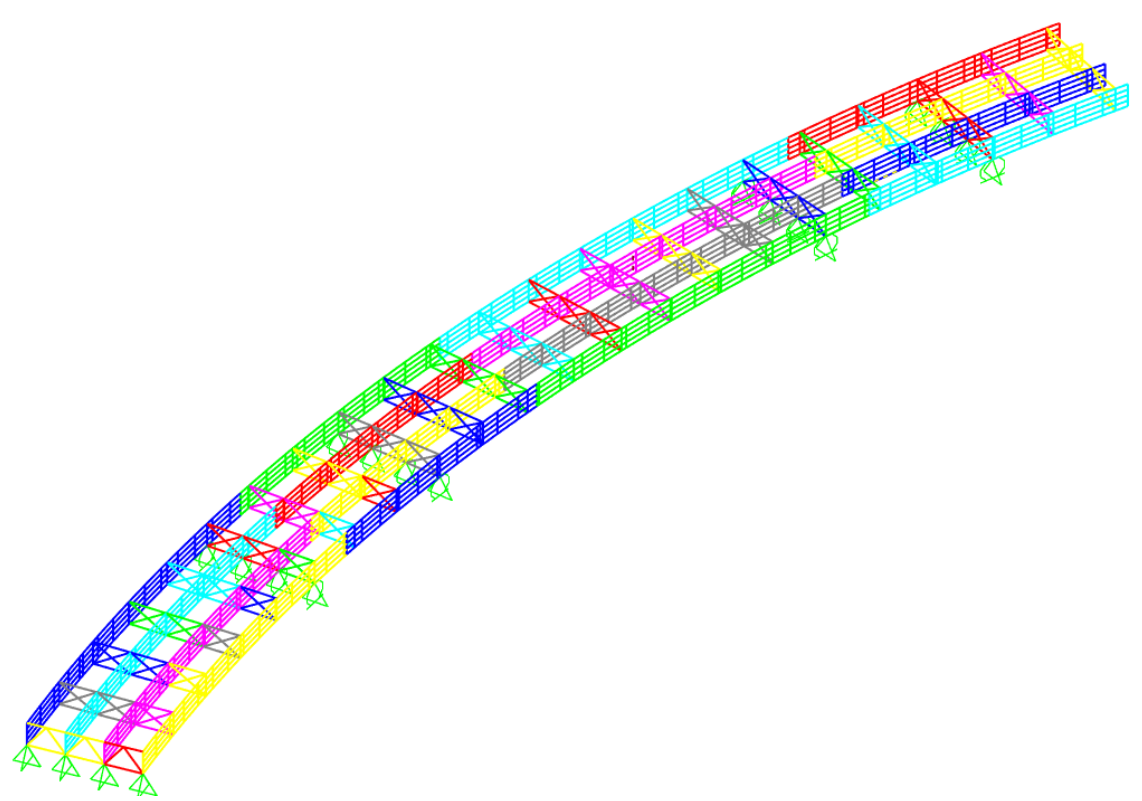


Figure 46. Stage 4.3 model





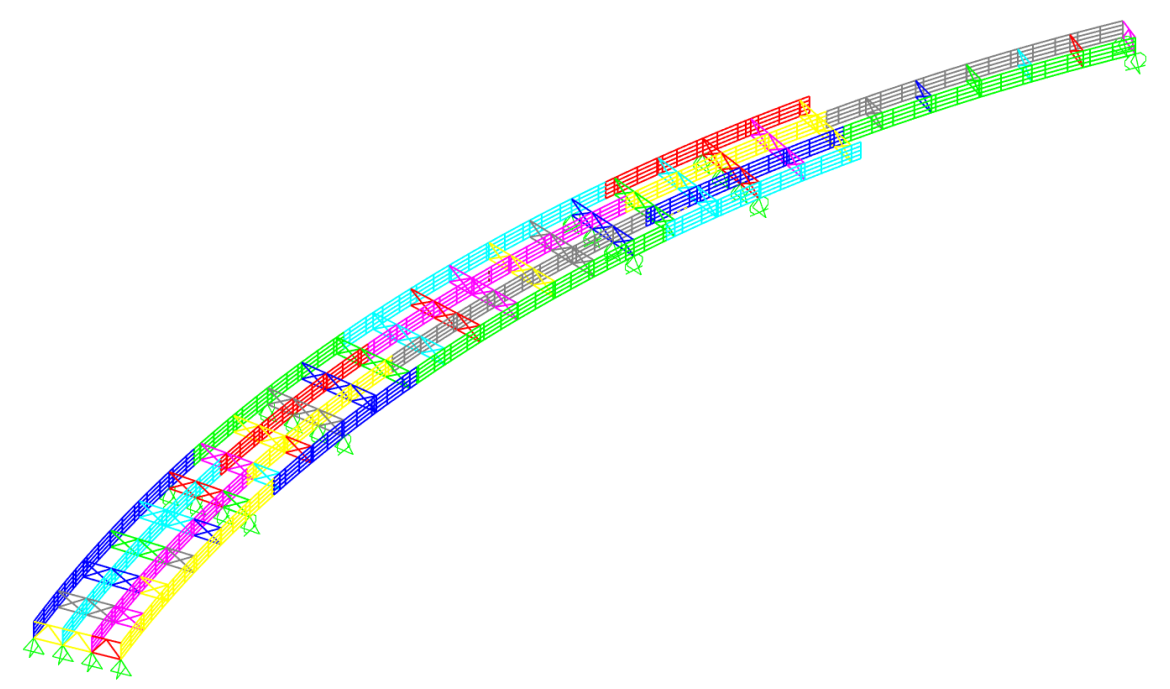


Figure 47. Stage 5.1 model

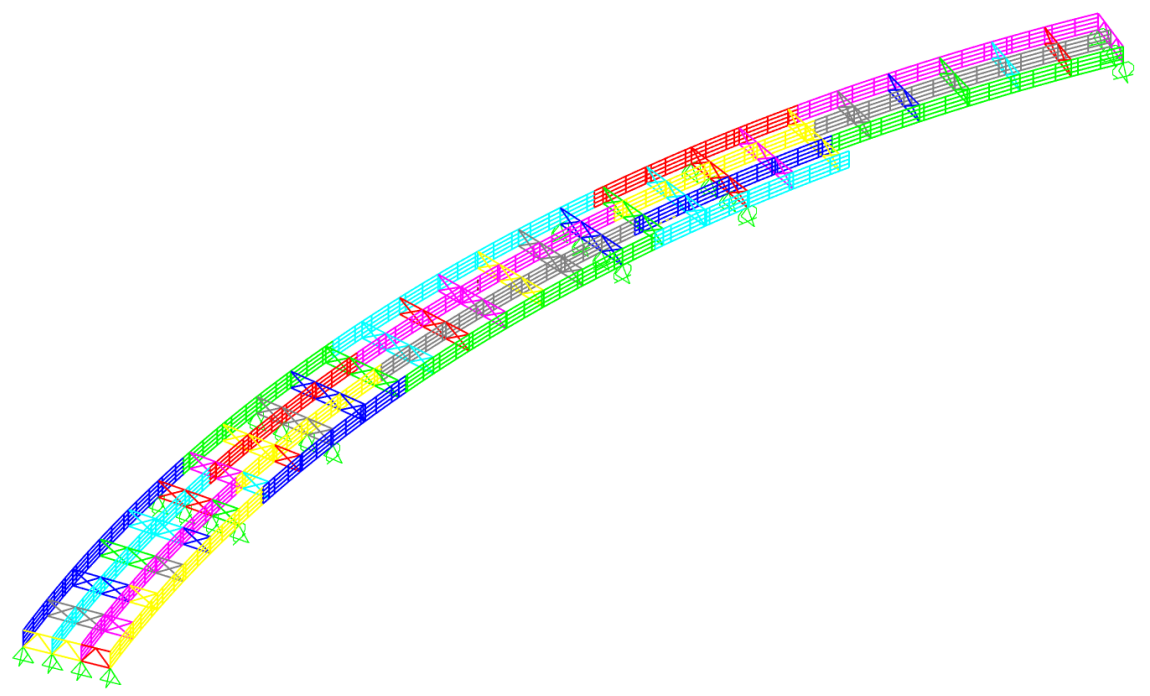


Figure 48. Stage 5.2 model





Alberto Arnedo Ruiz

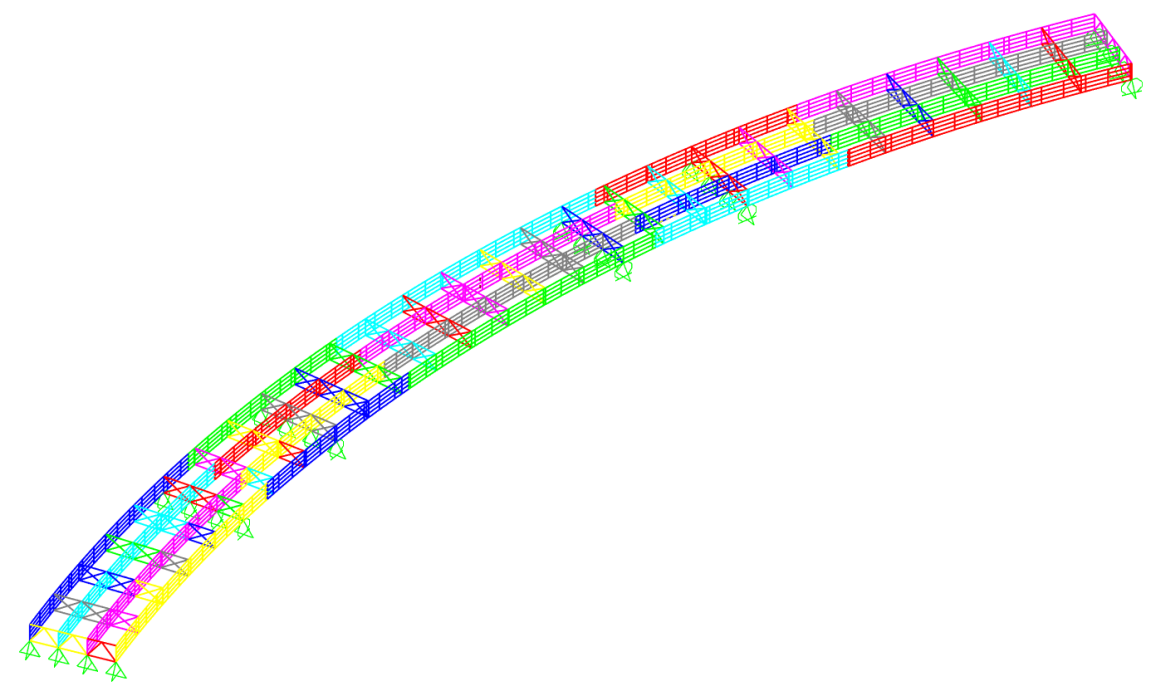


Figure 49. Stage 5.3 model

After the completion of each construction stage, the wind load as described in section 4.3 is added and the stresses in the bridge calculated. An envelope load combination is created to obtain the maximum deformations, forces, and stresses at each element throughout the whole staged analysis.

To perform a sensitivity study based on the meshed size, a second model using the previously created as a base is created. In the second model the web plate is subdivided in 12 vertical subdivisions, and the plate aspect ratio is kept as close as possible to 1. To do so the web and frame of the girders in the model are deleted. New mesh points are imported. Flange and web elements are created again. Section properties are assigned, and each element is assigned to one construction group. The base wind load is also assigned reassigned to the plate elements. See Figure 50 for fine mesh model.





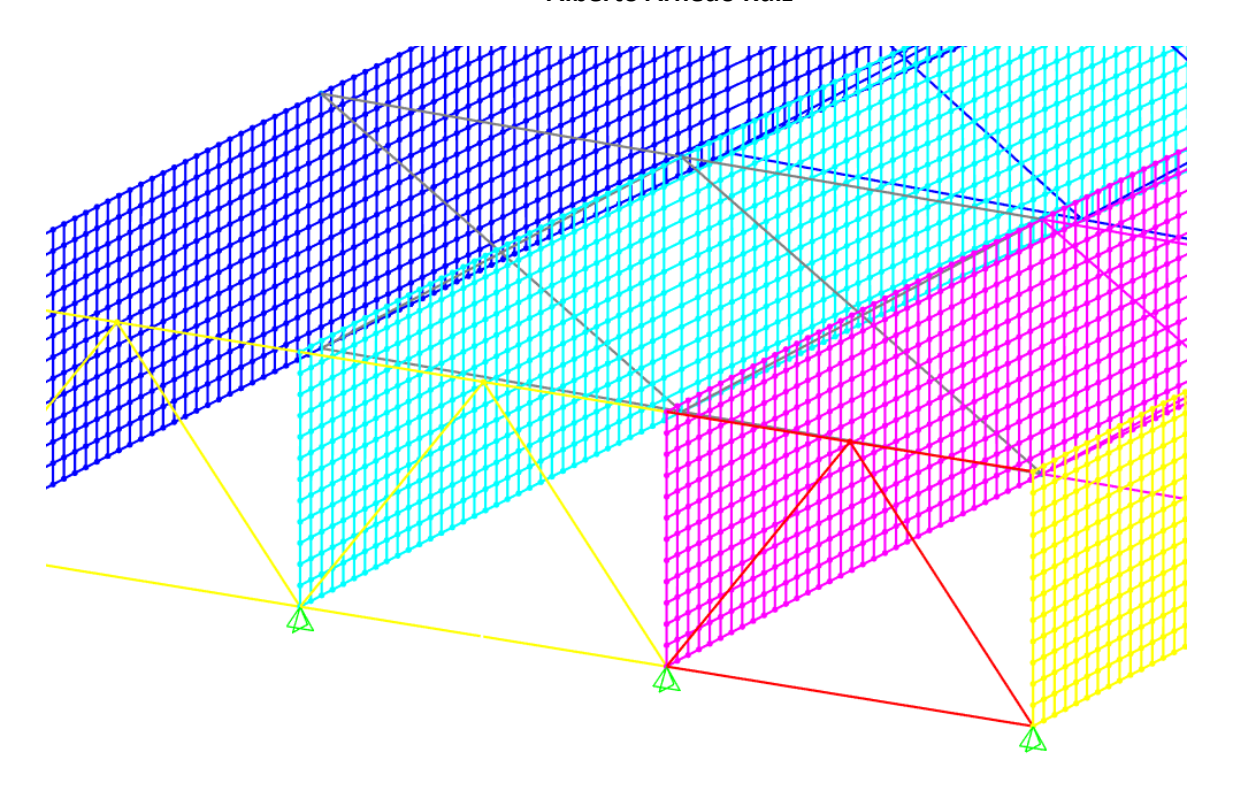


Figure 50. Mesh at finer model





Alberto Arnedo Ruiz

5. RESULTS

Results are obtained for two models:

- First model has the web divided in 4 sections along its depth, and plate aspect ratios are kept at a maximum of 1 to 5. Since the girder is 7ft deep, the maximum mesh size is 1.75ft x 8.75ft.
- Second model has the web divided in 12 sections along its depth, and a plate aspect ratio are kept at a maximum of 1 to 1. Since the girder is 7ft deep, the maximum mesh size is 0.583ft x 0.583ft.

To validate and compare the models, two results will be obtained:

- Total vertical reaction at final dead load stage. This value will be compared with an independent takeoff.
- Maximum deformation at flange joints in all directions

From the independent takeoff, the flanges weight a total of 476.44 kips, the web plates 353.05 kips, and the cross frames (assumed to be L6X6X1) a total of 58.50 kips, bringing the total weight of the steel superstructure to 884.99 kips.

5.1. Coarser mesh model

Joint reactions are shown in table format in Table 27 and graphically in Figure 51. Total sum of vertical reactions is 894.3 kips. The error between the weight takeoff of the bridge and the sum of vertical reaction is about 1%.

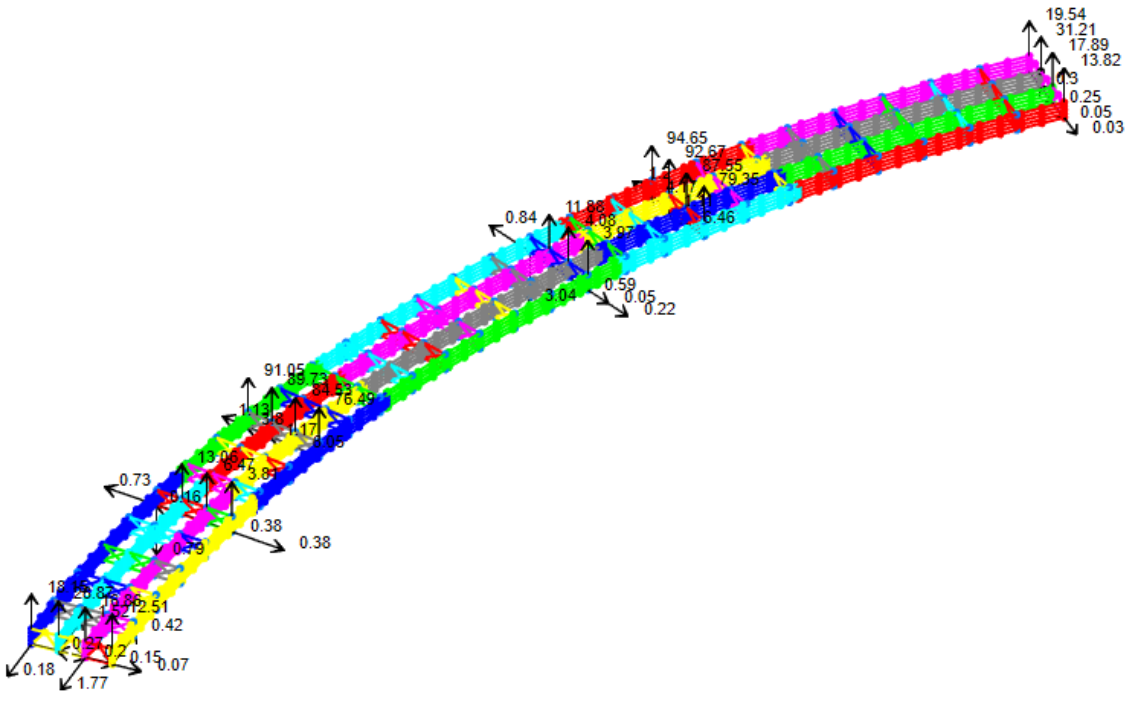


Figure 51. Joint reactions in final condition - coarser model





Alberto Arnedo Ruiz

Joint	OutputCase	F3
Text	Text	Kip
11100000	5.3	12.514
11160000	5.3	3.808
11230000	5.3	76.489
11360000	5.3	3.967
11430000	5.3	79.352
11600000	5.3	13.823
12100000	5.3	16.861
12160000	5.3	6.469
12230000	5.3	84.534
12360000	5.3	4.079
12430000	5.3	87.549
12600000	5.3	17.89
13100000	5.3	28.871
13160000	5.3	13.059
13230000	5.3	89.735
13360000	5.3	11.878
13430000	5.3	92.672
13600000	5.3	31.207
14100000	5.3	18.147
14160000	5.3	-0.793
14230000	5.3	91.05
14360000	5.3	-3.037
14430000	5.3	94.645
14600000	5.3	19.535

Table 27. Joint reactions table in final condition – coarser model

Joint	OutputCase	U1
Text	Text	in
12600000	Envelope	-1.215102

Table 28. Maximum longitudinal joint deflection (coarse model)

Joint	OutputCase	U2
Text	Text	in
2520003	Envelope	5.468125

Table 29. Maximum transverse joint deflection (coarse model)

Joint	OutputCase	U3
Text	Text	in
3530000	Envelope	-1.141053

Table 30. Maximum vertical joint deflection (coarse model)

The maximum deflection in each direction is also shown in Table 28, Table 29, and Table 30.





Alberto Arnedo Ruiz

5.2. Finer mesh model

Joint reactions are shown in table format in Table 31 and graphically in Figure 52. Total sum of vertical reactions is 894.01 kips. The error between the weight takeoff of the bridge and the sum of vertical reaction is about 1%.

TABLE: Joint Reactions			
Joint	OutputCase	F3	
Text	Text	Kip	
11100000	5.3	12.436	
11160000	5.3	4.823	
11230000	5.3	76.143	
11360000	5.3	3.554	
11430000	5.3	78.853	
11600000	5.3	13.774	
12100000	5.3	16.822	
12160000	5.3	5.172	
12230000	5.3	84.595	
12360000	5.3	4.802	
12430000	5.3	88.478	
12600000	5.3	17.89	
13100000	5.3	28.877	
13160000	5.3	13.184	
13230000	5.3	89.914	
13360000	5.3	11.772	
13430000	5.3	92.751	
13600000	5.3	31.253	
14100000	5.3	18.088	
14160000	5.3	-0.424	
14230000	5.3	90.839	
14360000	5.3	-3.279	
14430000	5.3	94.345	
14600000	5.3	19.435	

Table 31. Joint reactions table in final condition – finer model





Alberto Arnedo Ruiz

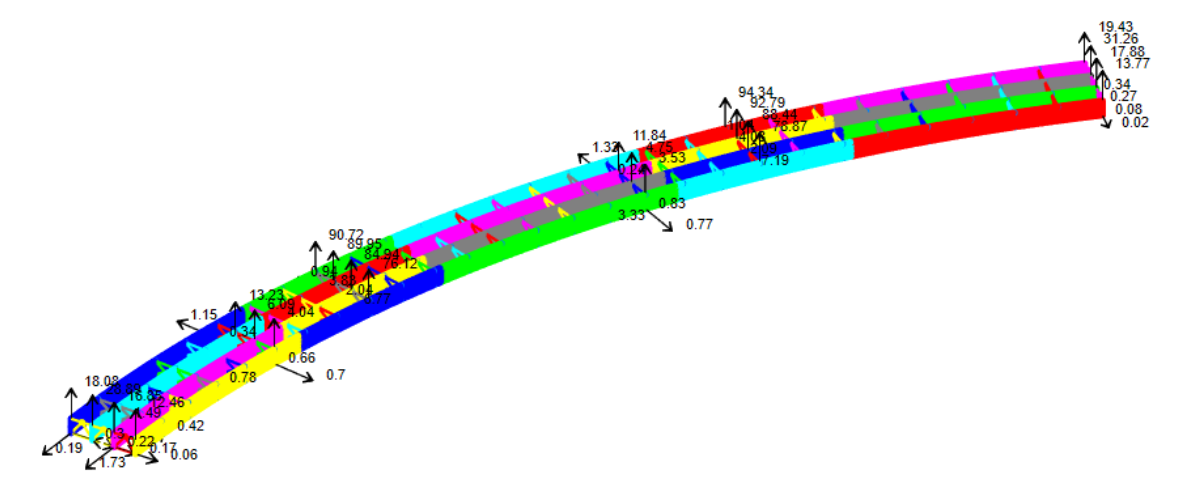


Figure 52. Joint reactions in final condition – finer model

Joint	OutputCase	U1
Text	Text	in
12600000	Envelope	-1.234466

Table 32. Maximum longitudinal joint deflection (fine model)

Join	t	OutputCase	U2
Text	t	Text	in
25200	30	Envelope	5.567792

Table 33. Maximum transverse joint deflection (fine model)

Joint	OutputCase	U3
Text	Text	in
3520029	Envelope	-1.154774

Table 34. Maximum vertical joint deflection (fine model)

The maximum deflection in each direction is also shown in Table 32, Table 33, and Table 34.

5.3. Comparison

As we can see from the comparison of the vertical reactions in both models, they are both well under 1% difference, which verifies the models are comparable. In terms of the deflection envelopes, the deflections in the finer mesh model are between 1% and 2% larger than in the coarser model.





Alberto Arnedo Ruiz

6. CONCLUSION AND FUTURE DEVELOPMENT

The purpose of this study is to provide a workflow methodology to model curved steel girder bridges in any 3D FEA software with the objective of performing a staged construction analysis, as well as the development of parallel models with different mesh sizes for sensitivity analysis purposes.

The two models analyzed of the same bridge give similar results, showing that the methodology used to model them, especially regarding the mesh generation for the frame and plate elements, is efficient and faster than the alternative methods discussed in section 1.1.

It is to be noted that the total running time of the coarse model was around 6 minutes, while the total running time of the finer model was closer to 125 minutes. Lacking more guidance with respect to the minimum mesh size in the analysis of curved steel girder bridges, it is recommended to perform most of the analysis in a coarser mesh that is believed to closely represent the behavior of the bridge. Once a final satisfactory construction sequence has been found with the required temporary shoring and bracing, a final, finer mesh model can be run to confirm the results found in the first place. The mesh used in the first model, with 4 vertical subdivisions along the depth of the girder and a plate aspect ratio of 1 to 5 seems to be a good starting point to get initial results at a reasonable time span.

Throughout the development of this thesis, several assumptions were used that limit the functionality of the methodology used. Among others, the following items can be included further developed to add functionality:

- Add functionality for steel girder bridges with variable spacing along the length of the bridge.
- Add option of cross frames parallel to abutments and piers rather than perpendicular to layout line.
- Automatic cross frame modeling based on configuration type.
- Macros development to automatize frame and plate elements tables





Alberto Arnedo Ruiz

7. BIBLIOGRAPHY

- [1] American Association of State Highway and Transportation Officials, "LRFD Bridge Design Specifications 9th Edition," American Association of State Highway and Transportation Officials, Washington, DC, 2020.
- [2] L. D. Benitez and M. A. Hass, "Placing curves overhead A simplified analysis of horizontally curved girder bridge erection," *Modern Steel Construction*, 2010.
- [3] G. M. J, T. H. Pechillo, J. M. Schneider, T. A. Helwig, M. A. O'Toole, S.-L. C. Kaderbek, M. Grubb and J. Ashton, "FHWA-NHI-15-044 Engineering for Structural Stability in Bridge Construction," Federal Highway Administration, U.S. Department of Transportation, Washington D.C., 2015.
- [4] U.S. Department of Transportation, "Manual for Refined Analysis in Bridge Design and Evaluation," Federal Highway Administration, U.S. Department of Transportation, Washington, D.C, 2019.
- [5] "Standard Specifications," New York State Department of Transportation, Albany, 2015.
- [6] "Guide Design Specifications for Bridge Temporary Works, 2nd Edition," American Association of State Hgihway and Transportation Officials, Washington D.C., 2017.
- [7] "Steel Bridge Erection Guide Specification," American Association of State Highway and Transportation Officials, Washington, D.C., 2023.
- [8] R. Lu, J. Judd and M. Barker, "Field Load Rating and Grillage Analysis Method for Skewed Steel Girder Hgihway Bridges," *Journal of Bridge Engineering*, vol. 26, no. 11, 2021.
- [9] "Acrow Bridge Support System Chosen as a Solution for a Challenging Conditions During Northwest Corridor Project in Atlanta," Acrow, [Online]. Available: https://acrow.com/case-studies/georgia-dot-case-study/. [Accessed 2025].
- [10] "Steel erection construction," Haydon Bridge Company, [Online]. Available: https://haydonbridgecompany.com/steel-erection-construction/. [Accessed 2025].
- [11] "Standard 1926 Safety and Health Regulations for Construction," Occupational Safety and Health Administration, 1970.
- [12] J. Stith, B. Petruzzi, T. Helwig, M. Engelhardt, K. Frank and E. Williamson, "Guidelines for Design and Safe Handling of Curved I-Shaped Steel Girders," The University of Texas at Austin, Center for Transportation Research, Austin, 2010.
- [13] J. F. Farris, "Behaviour of Horizontally Curved Steel I-Girders During Construction," The University of Texas at Austin, 2008.
- [14] T. A. Helwig, K. H. Frank, M. D. Engelhardt and E. B. Williamson, "UT Lift 1.2 Users Guide," The University of Texas at Austin, Texas, 2010.
- [15] J. Rivera and B. Chavel, "Steel Bridge Design Handbook Appendix. Design Example 3: Three-Span Continuous Horizontally Curved Composite Steel I-Girder Bridge," American Institute of Steel Construction, Chicago, 2022.
- [16] "Guide Specifications for Wind Loads on Bridges During Construction," American Association of State Highway and Transportation Officials, Washington, 2017.





- [17] "ASCE/SEI 37-14 Design Loads on Structures during Construction," American Society of Civil Engineers, Virginia, 2015.
- [18] "ASCE 7-22 Minimum Design Loads and Associated Criteria for Buildings and Other Structures," American Society of Civil Engineers, Virginia, 2022.
- [19] "Wire Rope Sling Handbook," Union A WireCo WorldGroup Brand, 2024.
- [20] "Catalog," LiftAll Products for better lifting, 2024.
- [21] D. Duerr, "Effectiv Bearing Length of Crane Mats," 2DM Associates, Inc., Consulting Engineers, Houston, 2010.
- [22] "Product catalog with application & warning information IMPERIAL," TheCrosbyGroup, Richardson, 2023.